Hochschule für Angewandte Wissenschaften Hamburg
Hamburg University of Applied Sciences

Hochschule für Angewandte Wissenschaften Hamburg

Fakultät für Life Sciences

Evaluation of scaling parameters towards an improved process development strategy for CHO cell perfusion cultures-step-wise scale-up from 15 mL to 5 L

Thesis zur Erlangung des Grades Master of Science

im Studiengang Pharmaceutical Biotechnology

vorgelegt von

Nicolas Marx

Matrikelnummer 2148247

Kopenhagen

am 25.01.2015

Erstgutachter: Professor Dr. Birger Anspach (HAW Hamburg)

Zweitgutachter: Dr. Martin Heitmann (Novo Nordisk A/S)

Für Gudrun Waller Marx

Preface

This project was initiated in April 2014 in collaboration with Novo Nordisk A/S in Måløv, Denmark. The experimental work was carried out in the laboratories of the Cell Culture Technology, the Mammalian Cell Technology and the Assay Technology Department at Novo Nordisk.

Acknowledgements

Many people helped, supported and advised me during this Master's project but also in the time before. It is hard to express the gratitude I feel for the people close to me be it work-related, personally or both.

Without the great help of Martin Heitmann I would not have been able to finish this thesis. During the long time I have been here, you invested countless hours to broaden my knowledge and understanding about mammalian cell culture. You were always there, patiently, to answer my countless questions around the project and the big (but now clearer) world of cell culture. Evenly fantastic was the way you supervised the project. I always felt welcome to approach you with theories and ideas about my experiments. Moreover, you motivated me to find the right decisions and created a perfect balance between guiding me and letting me find connections and correlations on my own. Additionally, I am very thankful for your engagement in helping to determine the future aspects of my career.

Besides the project work, I also greatly appreciated your invitations to informal get-togethers. The gaming evenings with family and friends helped a lot of keeping a clear head albeit getting into "RAGE".

I would like to thank Prof. Birger Anspach for accepting the role as my supervisor at the University of Applied Sciences Hamburg. Although during this Master's project, we did not collaborate in terms of the practical work, the organizational support around the Master's thesis was ideal. I greatly appreciated the advice prior to this project concerning the writing of a Master's thesis in the industry.

Furthermore, my thank goes to Ali Kazemi who was a co-mentor during this work. I was very happy to see that you were already interested in my academic career when I worked as an Intern at Novo Nordisk A/S. It seems to me that the mentoring was beginning back then. With hindsight, you had helped me to make the right decision concerning the consecutive study program. I highly appreciate your efforts to show me possibilities within bioprocess engineering and your advices how to use them.

Additionally I would like to thank the Cell Culture Technology Department at Novo Nordisk A/S for the patient and supportive help during this project. Concerning the execution of continuous DASGIP cultures, I want to express my gratitude to Carsten Leisted and Mette Riisager for sharing their knowledge within this system. Special thanks to Heidi Olsen, Monique Enevoldsen, Flemming Jørgensen and Kenneth Hanson for their support during the ATF-perfusion cultivations. Without the great commitment of Mustapha El Ayadi I would not have been able to run any cultivation. Thank you for the (extensive) medium preparation. Thanks to Pia Blume, Pia Zitthén and Joan Madsen who were always supportive and helped me to orientate in the lab environment.

Then, thank you, Peter Becker, for including me again in your department and your efforts concerning the organizational framework. Furthermore, I would like to thank Mats Åkesson for fruitful discussion in the ACA meetings and the initial insights to ATF-perfusion control. I am very thankful to Bjarne Poulsen who emphasized the pCO_2 problematic and invested his time to share his knowledge in up-scaling. Last but not least my thanks to Sebastian Scholz who acted as my source of knowledge for the Cedex and

ambr related issues when Martin was not available. Hopefully, we will be able to watch Germany beat Brazil again at the next World Cup (7:1!).

Thanks to Lotte Gottlieb Sørensen for performing the ELISA protein analysis.

Thanks to my office buddy Bjarke Schwalm Madsen for creating a relaxed atmosphere and being a good friend.

In this setting, I would also like to thank my former professors Dirk Lütkemeyer and Frank Gudermann from the University of Applied Sciences Bielefeld for introducing me to mammalian cell culture, establishing the contacts to Novo Nordisk A/S and being supportive even after I became an alumnus.

My biggest thanks, however, are directed to my friends and family. Everywhere I went in the last 6 years I was welcomed by new friends and visited by old ones. I could not have appreciated the new living conditions without you and would not have been able to get to the point where I am today. Thanks to my father Gerhard. You guided me and left me space when I needed it but most importantly you always fully supported me during my way. Thank you, Jan, for being an older brother to look up to but also a brother that reaches out for me. Danke an meinen Opa Emil: Deine stete Unterstützung ist bewundernswert und Deine unglaubliche, positive Lebenseinstellung sind ein wahres Vorbild.

The last lines are reserved for Nina. Thank you for your permanent support in different cities, cultures and living conditions. You built me up when I was down, motivated me when I was stuck and made me laugh when I was sad. But most all of you share your life with me. Thank you.

Abstract

Process development towards the production of difficult-to express proteins in perfusion cultivation necessitates the implementation of scale-down models to manage the high number of experiments which have to be conducted in Quality by Design (QbD) initiatives. Successive simplification of the process mode accompanied by the application of single-use equipment provides possibilities to mimic more complex processes in smaller scales in less time, with less work and less cost intensive conditions. The reverse up-scaling and transfer of process conditions and set-points from simple approximated cultivation systems to the final, more complex production method requires the application of appropriate scalable culture parameters.

In this work, scaling parameters were evaluated to systematically transfer culture criteria between three bioreactor systems and cultivation modes towards an improved process development strategy. The capability of simpler small-scale systems to approximate ATF-perfusion processes was assessed. Chinese Hamster Ovary (CHO) cells expressing a recombinant protein were cultured in 15 mL Advanced Microscale Bioreactor (ambr^{TM}) system in pseudo-continuous mode, 1 L DASGIP multiparallel bioreactor system in continuous mode, and 5 L Sartorius B-DCU system in Alternating Tangential Flow (ATF)-perfusion mode. Main critical process parameters (CPP) were analyzed, i.e. cell specific metabolic rates and productivity of the cell cultures, compared and transferred based on the evaluated scaling parameters. Different aspects of the particular processes and their impact on cell culture were assessed in order to build up an improved process understanding. Process parameters were found to be sufficiently transferable when scaled by the cell specific perfusion rate (CSPR). Bench-top bioreactors operated in continuous and perfusion culture modes showed coinciding metabolic rates but were distinct from ambr^{TM} pseudo-continuous cultures where a stable offset over a wide range of CSPR was characterized. Cell specific protein productivity (q_P) was similar between DASGIP and ambr^{TM} cultures but different from ATF-perfusion cultures. Aside from an imprecise measurement method, a partial retention of recombinant protein in the ATF-module was determined to have contributed to this observation. Moreover, deviating pCO_2 was identified as a possible impact factor on q_P. The differences were attributed to the physical characteristics, i.e. mass transfer, and different scales of the bioreactors rather than the different operation modes. Additionally, the biomass measure which is used for the calculation of cell specific rates was identified to play a crucial role when CPP should be transferred with the presented scaling-parameters. In general, transferability was feasible since similar trends were observed for metabolic rates and recombinant protein related data.

Publications

Parts of this thesis are intended for publication in *Biotechnology Progress* as follows:

Martin Heitmann, Nicolas Marx, Ali Kazemi Seresht, Bjarne Rask Poulsen. *Small scale (15 mL) continuous cultures for efficient investigation of CHO cell perfusion cultures.*

1 Introduction

After the first approval of a recombinant protein expressed in Chinese Hamster Ovary (CHO) cells in 1986 (Altamirano et al., 2013), mammalian cell cultures have extended the possibilities and prospects within the production of biopharmaceutical recombinant proteins. Mammalian cells, in contrast to bacteria and yeast, enable the expression of proteins with complex glycosylation patterns and posttranslational modifications, thereby paving the way for the production of more human-like proteins and thus the development of new therapies. Recombinant protein production with mammalian expression systems evolved from a niche existence to one of the leading forces for the biotechnological industry. In 2011, the annual sales for the top 30 proteins was estimated to be 112.93 billion USD (*www.pipelinereview.com*, accessed on 16 April 2013) and a total of 96 biopharmaceutical proteins expressed with mammalian cells have been approved between 1986 and 2011 (Lai et al., 2013). The development and importance of recombinant proteins expressed in mammalian cells for the biopharmaceutical industry is displayed by the latest approvals of the Food and Drug Administration (FDA) with more than 60% of the recombinant products originating from mammalian expression systems (Zhu, 2012).

One of the product categories represented in the top 30 protein sales are recombinant coagulation factors and related substances for the treatment and therapy of bleeding disorders with a sales volume of 6.83 billion USD in 2011 (*www.pipelinereview.com*). The first treatment with recombinant coagulation factors was executed in 1987 (White, 1989) and represented a milestone in diminishing life-threatening virus transmission and additionally overcoming the limited availability in contrast to the conventional use of plasma derived products (Franchini, 2010; Gringeri, 2011). Due to their highly glycosylated structure (Vehar, 1984) and their low half-life (Ludlam, 1995), recombinant coagulation factors are mainly expressed in mammalian cells, where CHO cells besides Baby Hamster Kidney (BHK) cells have been implemented as a reliable expression system based on their low proteolytic activity, the ability to secrete the target product into the medium, and the low risk of infection with human viruses (Kuplove, 1994; Adamson, 1994).

The expression of instable proteins such as coagulation factors necessitates an adapted cultivation mode considering the need of high volumetric productivity (VP) and rapid purification of the target product. A proposed method for the production of these difficult-to-express proteins is the application of perfusion cultures which are characterized by a continuous in- and outflow of fresh and spent medium, respectively. By introducing an appropriate cell retention device, which is coupled to an outflow stream, a recirculation of cells into the bioreactor is feasible, which results in high viable cell density (VCD). Thus, a higher product titer is possible compared to continuous culture (Kompala and Ozturk, 2006). Furthermore, the removal of metabolic by-products, such as lactate and ammonium, which can negatively affect the culture performance (Reuveny et al., 1986a; Reuveny et al., 1986 b), and a shorter residence time of the target product in the bioreactor, where it is exposed to degradative enzymes (Gramer et al., 1993), are advantageous effects of perfusion cultures.

For cell line and process development towards a perfusion process, the data acquisition following Process Analytical Technology (PAT) and QbD is facilitated when the targeted perfusion mode is mimicked

with continuous cultures so that the process is simplified and less cost intensive. A further simplification is achieved when continuous cultures are replaced with pseudo-continuous cultures. The simplification steps allow for a higher number of experiments at supposedly reproducible process conditions in smaller scales. Thus, with a successive scale-up strategy, the process development pathway can be aligned and optimized. But still, the transfer of the conditions and results from a simplified process in a smaller scale to the actually mimicked set-up is not trivial.

Within this framework, the question how closely ATF-perfusion processes are approximated by fully automated pseudo-continuous cultivations and continuous cultivations in smaller scale has not been answered yet. Therefore, in this work, cultivations of CHO cells in pseudo-continuous, continuous and perfusion mode with a stepwise increasing working volume from 15 mL to 5 L in different bioreactor systems were executed, in order to identify similarities and differences in cell culture performance. The used bioreactors included the 15 mL Advanced Microscale Bioreactor (ambr^{TM}) system (Sartorius Stedim Biotech S.A., France), the 1 L DASGIP Parallel Bioreactor System (Eppendorf, Germany) and the 5 L Sartorius BIOSTAT® B-DCU system (Sartorius Stedim Biotech S.A., France) with an ATF2-system (Repligen, USA).

To assess the question of transferability, several factors have to be considered and several experiments have to be executed. First, to compare cell culture performance between the systems, a suggested scaling parameter has to be chosen. Then, in order to understand the impact of the different scales, bioreactors and operation modes on cell culture performance, preliminary experiments have to be conducted. In this case, the variation of the defining operation mode conditions within one set of bioreactor system will provide the necessary information. Possible differences can then be attributed solely to the operation mode. Furthermore, the role of general process conditions that are influenced by the bioreactor system design will be examined in this work for the classification of their effect on cell culture performance. The preliminary experiments will provide additional resolution power to locate sources of possible differences.

To assess the question of how closely the simpler culture systems approximate ATF-perfusion processes, additional experiments are necessary. In order to generate a basis of comparison and to evaluate possible limitations of the proposed approach, mammalian cells will be cultured at different operating points in all three systems. The obtained critical process parameters (CPP) from these cultivations will be compared based on the proposed scaling-parameter. Moreover, the suitability of the scaling-parameter is to be critically questioned by comparison with other appropriate parameters. Furthermore, bioreactor system specific influences on the outcome of this study will be evaluated. This is especially relevant regarding the additional cell retention system in continuous perfusion cultures. Ultimately, the feasibility of simpler small-scale bioreactor systems to approximate CHO ATF-perfusion processes will be evaluated. Possible differences can then be attributed to the scale, bioreactor system, operation modes, or general process conditions.

2 Theory

In Global Research at Novo Nordisk A/S in Måløv, Denmark, one pillar of the research interest is the development of perfusion processes for the production of therapeutic proteins targeting bleeding disorders. A final production method for a target product at Novo Nordisk A/S is perfusion cultivation using the Alternating Tangential Flow (ATF) system. In general, large-scale perfusion processes have to be controlled at optimal set-points, which often form a reasonable compromise between optimal process parameters for the chosen cell line and the special characteristics of a large-scale cultivation, where diminishing economic risks, such as production downtime is essential (Werner, 1991). Thus, a choice has to be made in order to combine good volumetric productivity and stable process characteristics.
Recent initiatives, like QbD and PAT, aim for an improved process understanding by comparing as many culture parameters as possible, which leads to a consolidated knowledge about the cell line and its physical, chemical, and mechanical requirements at the very beginning of the process development chain. The comprehension of cell culture parameter interaction is particularly important for the actual production process, where CPP have to be defined. The quality initiatives that commence in the Research and Development (R&D) area result in a high number of experiments that have to be conducted even when using Design of Experiments (DoE) strategies. Due to economic reasons and time limitation, identifying and comparing these parameters is not possible by conducting experiments in production scale. Therefore, mimicry of large-scale cultivations is performed in simpler small-scale equipment. Often, these processes are already operated in continuous cultivation mode (Heath and Kiss, 2007; Fernandez et al., 2009). The method of using non-controlled small-scale systems provides a first approach for executing a high number of experiments since these systems are easier to handle and the set-up is less time-consuming. Routine experiments in process development are executed mostly in shake flasks (Buechs, 2001), which, as well as roller bottles or micro well plates, do not possess direct sparging or pH control. Eventually however, the tested process conditions have to be transferred to systems with active control systems, in order to simulate process conditions in industrial stirred tank bioreactors (STR). This transfer from uncontrolled, non-sparged shake flasks and micro plate wells to the conditions in a STR can often lead to changes in cell culture performance (Hewitt and Nienow, 2007). Newly developed controlled small-scale bioreactors could substitute uncontrolled culture systems. With a similar control capability as bench-top bioreactors, they may help to diminish the alterations during the transfer and could be used for fast and extensive data acquisition.

In Figure 2-1, the traditional and a newly proposed simplification of perfusion processes in lab- and small-scale and the application of these systems during process and cell line development are illustrated. Within the cultivation systems tested, the most accurate simulation of production-scale cultivation is achieved by using the Sartorius bioreactor system including a 5 L bioreactor with an ATF2-module for cell retention. The DASGIP bioreactor system, operated in continuous mode, allows an advanced investigation of culture conditions and screening operations in bench-top bioreactor scale. The multi-parallel arrangement and the compactness of the system enable the execution of a high number of experiments already in normal lab-scale dimensions. For a further simplification, bench-top bioreactors are replaced

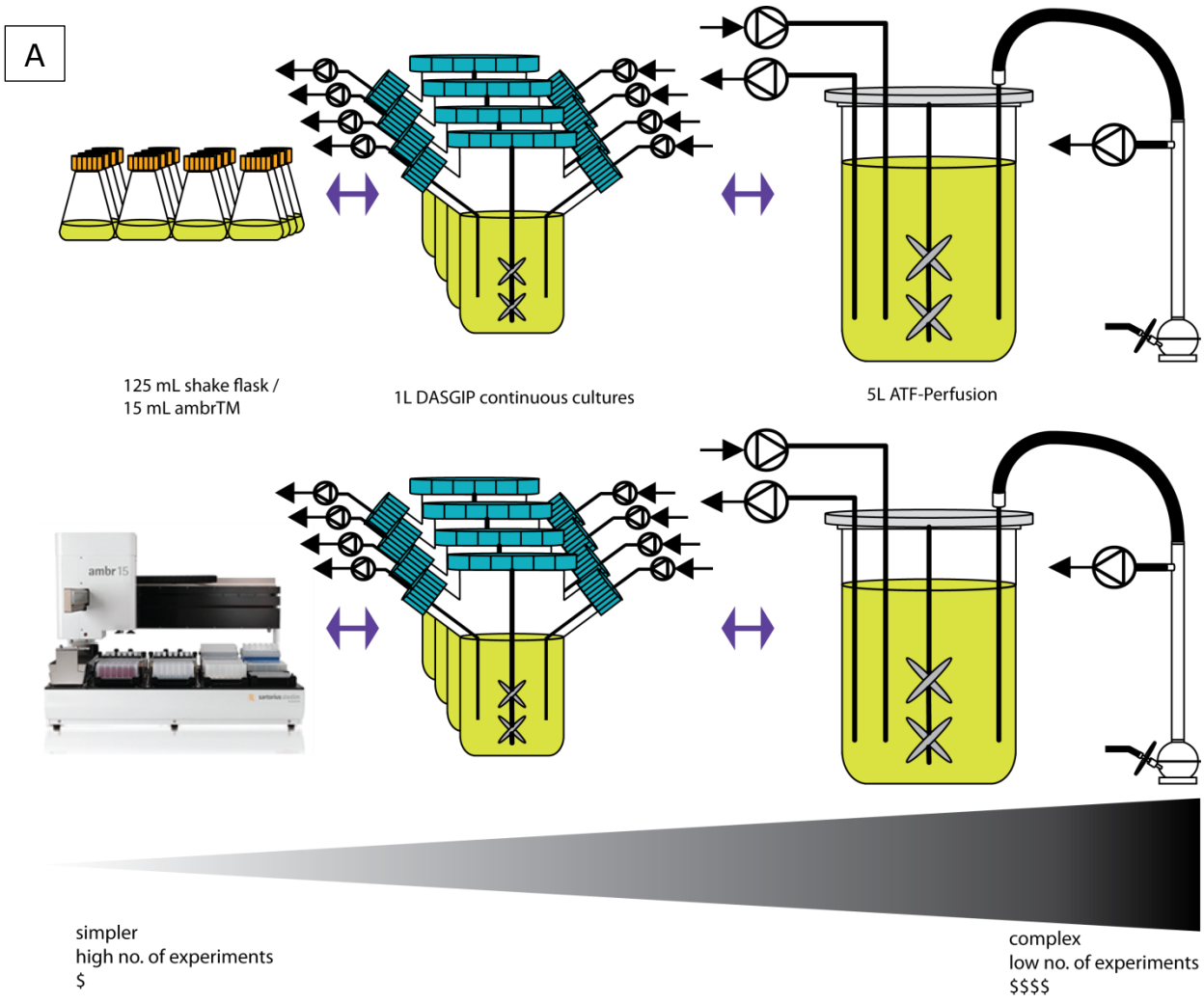

Figure 2-1: A: Simplification of a lab-scale ATF-perfusion process. Shake flasks are replaced with the ambr™ system for better process control possibilities. B: Exemplary cell line screening and process development stages with the use of the proposed simplification step. Clone selection is started in a pre-screen (284 well plates, 96 well-plates, DW= deep well plates, SF= shake flasks). The selected clones are subsequently tested for different CPP which are included in the process development strategy.

with the ambr™ bioreactor system which is a novel automated small-scale bioreactor system that can be operated in pseudo-continuous mode. Thereby, the potentials of convenient, disposable, easy-to-use equipment and controllable process conditions for a better understanding of mammalian cell cultures are combined.

Due to the different dynamic behaviors of the systems, a characterization based on a straightforward comparison via direct culture parameters, such as VCD and product concentration, might be imprecise, because the flow rates into and out of the system are not taken into account. These flow rates are not the same for perfusion and continuous cultivation. Cell specific rates, e.g. the cell specific growth rate, include these flow rates and therefore form a better basis of comparison. An approach to compare continuous and perfusion mode cultivation by specifically looking at the environmental conditions of every cell in the bioreactor is the use of the cell specific perfusion rate (CSPR) as proposed by Ozturk et al. (Ozturk et al., 1996). Few authors have been evaluating the effect of CSPR on the cell specific rates in perfusion cultures or even comparing different operation modes based on these parameters. Henry et al. compared pseudo-continuous, continuous and perfusion cultures and indicated a dependency of cell specific rates (whereas the dependency on the growth rate was not described) and the CSPR (Henry et al., 2008). However, for these experiments the same non-instrumented culture vessels were used, so that a generalization of the results to various instrumented bioreactor types with active process control is not guaranteed. Zeng et al. showed, by reviewing continuous and perfusion cultures from other researchers, that a correlation between CSPR and the cell specific growth rate was observable (Zeng et al., 1998). The obtained values for CSPR and the growth rate are not applicable for the transfer of CPP though, since different cell lines, media compositions, and bioreactors were used.

In order to elucidate the applicability of a transfer of process conditions between scales and operation modes, various interacting fields of biotechnology have to be considered when planning the experiments as well as describing and evaluating the results. In this chapter, an overview about technological and biological influences that were key tasks during this project are presented and introduced. In this framework, a balanced decision between the informative value and the significance of these influences for the processes has to be made. A central role for the outcome of a cell culture process is linked to bioprocess technology but also the cells' physiology. Thus, both the global and the local cellular level were included for the design and evaluation of the experiments. By focusing on the major determinants of a cell culture process, a basis was created that allowed to compare a high number of experiments with a sufficient resolution.

2.1 Pseudo-continuous processes with the Advanced Microscale Bioreactor (ambr™)

In small-scale cultivation systems, perfusion or even continuous cultivations are not feasible due to physical limitations. Therefore, a simplification of these process modes by implementing a pseudo-continuous mode can be conducted, which should presumably result in the same output since the definition of a continuous culture is maintained. Here, a constant flow and a constant volume are replaced

with an exponentially increasing flow and an exponentially increasing volume yielding in the same constant dilution rate. After a defined interval, a fraction of the cell suspension is discarded to prevent an overflow of the culture vessel. Figure 2-2 shows the concept of a pseudo-continuous process.
Beneath a critical interval length for the replacement of cell culture, VCD and specific rates are very well comparable to continuous processes (Westgate and Emmery, 1989; Leno et al., 1991). However, at high dilution rates and hence a large volume exchange pseudo-continuous culture is reported not to be a good approximation of continuous culture (Henry et al., 2008). Because of the simplicity in process control, pseudo-continuous processes provide an interesting model for cell culture processes in the early stage of process development in bioprocess engineering. By replacing highly instrumented and highly controlled processes, e.g. high cell density perfusion cultures with pseudo-continuous cultures, a basis for the understanding and optimization of the former can be constituted. Perfusion processes are moreover linked to higher operating expenses owing alone to the scale in which they can be executed or to additional equipment such as cell retention devices. This makes pseudo-continuous processes an appealing cost-effective alternative for researchers. Regarding the QbD and PAT initiatives, the demand for convenient pseudo-continuous systems is stimulated since this method of operation can be conducted in small scales. Scale-down for pseudo-continuous processes is easily performed, whereas perfusion and chemostat cultures are limited either by scale-down feasibility of the cell retention device or imprecise pumps. Small-scale pseudo-continuous systems with a working volume in the milliliter range could therefore be used for the first stage in process development. This system could be aligned towards a fully functional and robust continuous or perfusion process when there is a need for a high number of experiments due to e.g. cell line screening. Furthermore, the combination of pseudo-continuous and small-scale bioreactors bypasses the higher labor costs of lab or large scale processes and therefore offers a promising method towards a better process understanding.
Recently a new small-scale system was implemented as a useful research tool for multi-parallel and automated cultivation of mammalian cells. The Advanced Microscale Bioreactor (ambr^{TM}) system (Sartorius AG, Germany) consists of an automated workstation equipped with 15 mL single-use bioreactors with 9-15 mL working volume for mammalian cells. The micro-bioreactors contain an agitator shaft with impeller blades, pH and pO_2 sensors, a sparge tube and a removable vessel cap for liquid handling. For an automated determination of the cell concentration a CEDEX HiRes (Roche Diagnostics, Germany) can be connected. The withdrawal and addition of liquids is performed by an automated, programmable liquid handler (LH) which is able to pipette defined amounts of volume. The ambr^{TM} workstation is placed in a laminar downflow (LAF)-bench to ensure a sterile environment. The whole cultivation process can be programmed, including feeding profiles, in advance with the ambr^{TM} control software. Operational action during the cultivation is only needed to replace pipette tips, media and waste containers. In Figure 2-3, the ambr^{TM} workstation and the corresponding single-use ambr^{TM} vessel are displayed.

By using this system, gross errors by executing personnel are diminished, a faster workflow can be achieved and multi-parallel comparative cultivation processes can be performed. It has been shown that cultures run with the ambr^{TM} system show a similar outcome for cultivated mammalian cells to lab STRs with working volumes up to 200 L (Nienow et al., 2013; Rameez et al., 2014). It has to be highlighted that with this implementation up to 48 parallel cultivations are possible. Such a high number of experi-

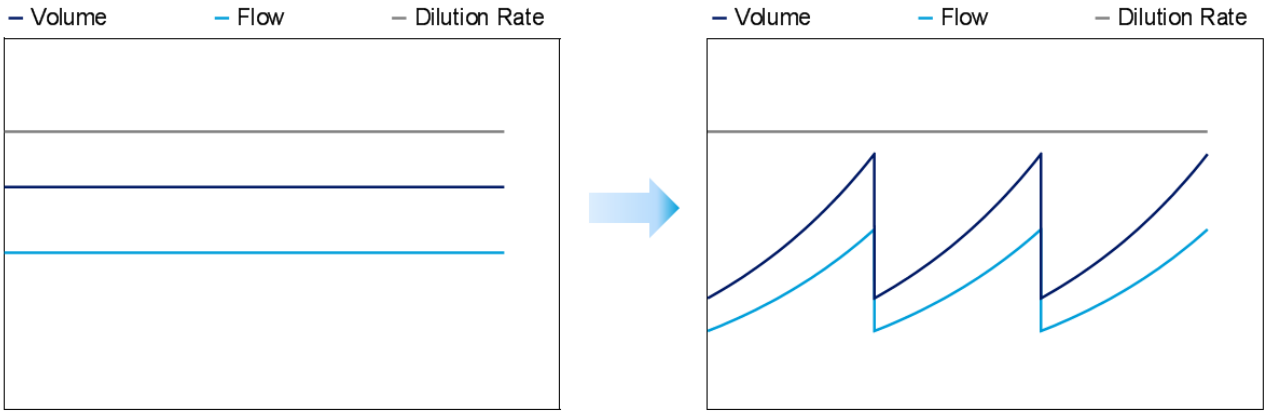

Figure 2-2: Definition and comparison of a classical continuous and a pseudo-continuous culture. Adapted from Heitmann (2013).

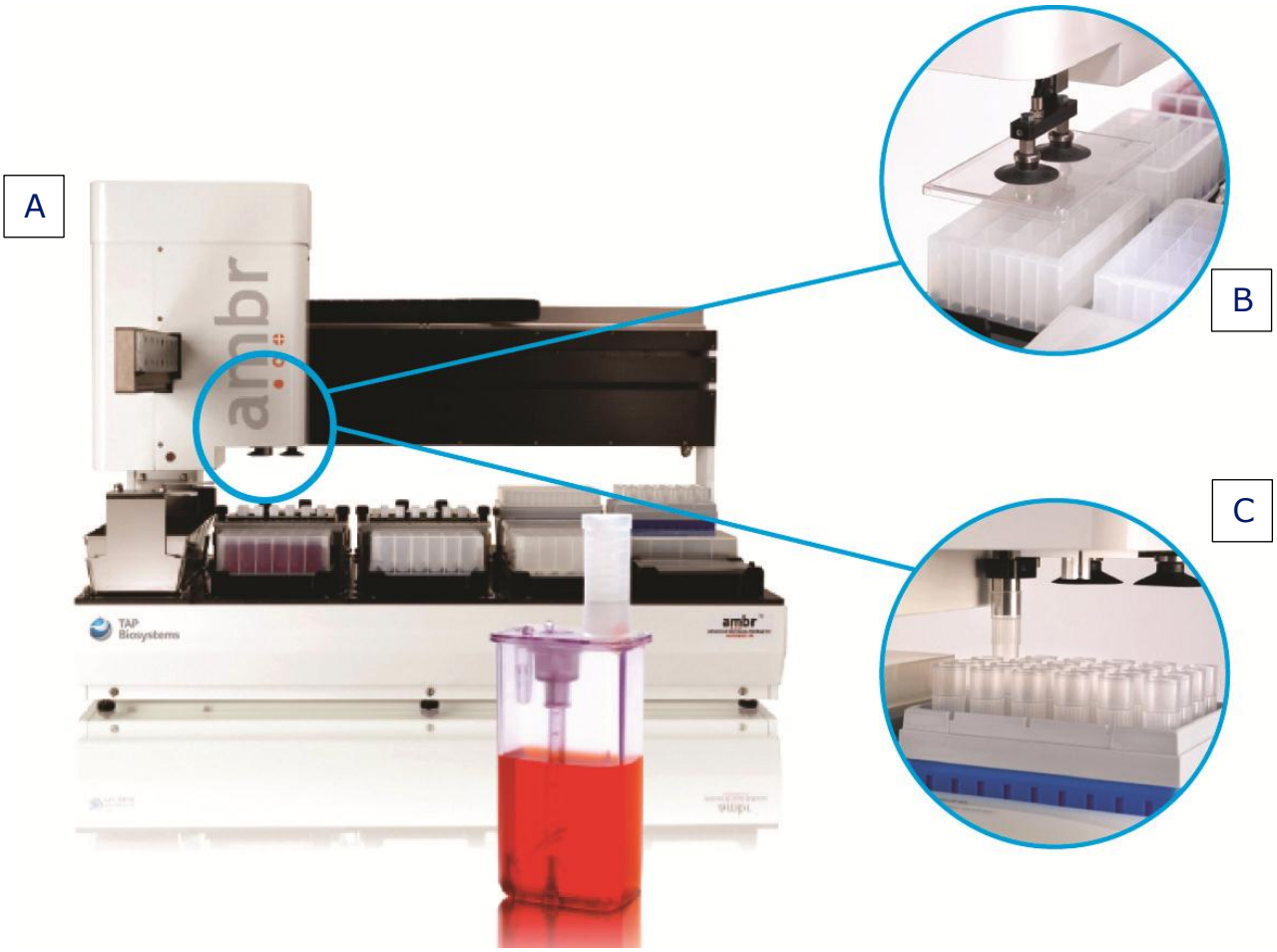

Figure 2-3: A: Fully equipped 15 mL ambr™ 24 workstation with bioreactor vessel (front). Plates for liquids are in front of the culture stations (CS) where the bioreactors are placed. The ambr™ 48 workstation is exhibiting space for 2 additional CS and 2 deep well plates. B: Liquid handler (LH) picking up a lid from a deep well plate. C: LH picking up a pipette. Images were retrieved from www.tap-biosystems.com and were adapted.

ments can be rarely executed by a single operator when conventional small-scale systems such as shake flasks are used. Moreover, the introduction of a small-scale system with controlled agitation and aeration conditions is avoiding further problems normally encountered when a transfer of process conditions between different operation modes is intended. Thus, the ambr™ represents an elegant tool for process development and an improvement compared to the conventional use of shake flasks (Zupke et al., 2012; Carpio et al., 2012; Casipit et al., 2012; Hsu et al., 2012; Nienow et al., 2013).

2.2 Continuous processes or chemostat with DASGIP bioreactors

Continuous or chemostat processes are characterized by a constant flow into and out of the bioreactor vessel at which the working volume does not change. Thereby, spent medium, cells, target protein and toxic byproducts are removed from the system and at the same time the culture is supplied with fresh nutrients. The chemostat is operated at certain dilution rates (D) which should be set below the critical dilution rate, D_{crit}, where a wash-out of cells occurs (Narang, 1998).

In research, continuous processes are widely used for the production and investigation of difficult-to-express proteins. These proteins require a certain mode of cultivation since either the used host system is producing low target protein titers, the protein is instable, or it exhibits an auto-inhibiting effect. Blood coagulation factor VIII serves as a paradigm and has been successfully licensed as one of the proteins produced with continuous cultivation (Bodeker, 2013). Alternative production methods like fed-batch processes, though exhibiting high product titer, are of relatively short duration and feature long residence times. With continuous processes, residence time can be altered by choosing an appropriate dilution rate and the process can be maintained long enough to produce a desired amount of protein. Additionally, continuous processes allow the use of smaller bioreactors compared to fed-batch cultures (Kadouri and Spier, 1996), thus saving space. However, addressing the question which process mode to choose solely based on product titer has become redundant. The matter should rather be considered based on the type of target protein and its special requirements for production (Konstantinov et al., 2006). The major advantage of continuous cultures over fed-batch cultures lies in the ability to provide a constant environment for the cells and thus a controllable process. Especially in the R&D environment, continuous processes have been used to study the cell culture behavior under defined conditions (Miller et al., 1988; Hiller et al., 1991; Berrios et al., 2011). The alteration of a variable in steady state conditions, where all parameters are static, allows for an easier evaluation than in dynamic systems such as fed-batch processes. Continuous processes, in contrast to pseudo-continuous processes, are limited by the availability of precise pump systems which determine the lowest possible flow rate and thus the scale of the used bioreactor. The DASGIP Vessel Type DS1000ODSS (Eppendorf AG, Germany) used during this project is a conventional glass bench-top bioreactors that can be operated in parallel with the DASBOX control unit allowing 8 cultivations at the same time. The unit is complemented by a peristaltic multi-pump system and apparatuses for gassing, agitation and temperature control. These units are connected to a computer with installed software for sensor calibration and for control of the cell culture process. The

1 L working volume of the DASGIP bioreactors should permit a sufficiently precise regulation of the dilution rate when using peristaltic pumps. The DASGIP continuous cultures were used in order to introduce a transition between the fully automated pseudo-continuous ambr™ cultures and the ATF-perfusion cultures with the Sartorius B-DCU system. In Figure 2-4, the DASGIP bioreactor system is shown.

Figure 2-4: DASGIP bioreactor system. On top, gassing, temperature, pH, stirring, and pump modules are displayed. These are controllable in remote mode with the DASGIP software on a linked PC. The bioreactors are placed in a container and are connected to PC (bottom) and modules. Images were retrieved from www.eppendorf.com and were adapted.

2.3 Perfusion processes with 5L-Sartorious BIOSTAT® B-DCU bioreactors and Alternating Tangential Flow (ATF) systems (ATF-perfusion)

A disadvantage of continuous processes that has often prevented its use for the production of pharmaceutical proteins is the low volumetric productivity combined with the necessity of higher instrumentation control compared to fed-batch processes. However, the advantageous features such as

low residence times for proteins and a theoretical long term consistent production are desired attributes for bioprocesses. The improvement of continuous processes by introducing cell retention devices in order to achieve high cell densities, and thus higher product titers, led to the implementation of perfusion processes as a promising cultivation mode for the production of biopharmaceuticals (Ozturk et al., 1994; Dowd et al., 2003; Konstantinov et al, 2006). In the case of the production of unstable proteins, perfusion cultivations are favored over other modes since they result in a better product quality (Choutteau et al., 2001). In R&D, perfusion cultivations can also be used to quickly establish a working cell bank or high cell density seed trains, thus reducing labor costs (Clincke et al., 2013). During perfusion processes a fraction of the cell suspension is led through a cell retention device which separates the cells from the medium. The cells are recirculated to the cultivation system whereas the cell-free medium is discarded as a harvest stream. Additionally, to assure high cell viability and preventing the accumulation of dead cells, a fraction of the cell suspension is discarded via a cell discard or bleed stream (Banik and Heath, 1995a, Banik and Heath, 1995 b; Castilho et al., 2002; Hiller et al., 1993; Ozturk et al., 1997; Mercille al., 2000; Dalm et al., 2004).The centerpiece of a perfusion system is the cell retention device which determines the performance of the perfusion process. Many different designs have been tested including external and internal cell separation. Spin filters and membrane systems are known to exhibit a low cell retention efficiency at high cell densities because of clogging and fouling, whereas gravitational and centrifugal systems show reduced efficiency at high volumetric flow rates (Ozturk et al., 1996).

The hollow-fiber membrane based ATF-system (Repligen, USA) supposedly minimizes the membrane associated clogging and can be operated at relatively high flow rates. The ATF-system consists of a metallic sphere that is divided into two chambers by a silicone diaphragm. The upper chamber is connected to a hollow-fiber cartridge which in turn is connected to the bioreactor. The lower chamber of the sphere is connected to the ATF-controller which alternately builds up overpressure and a vacuum by discharging or aspirating air, respectively, from the chamber. Because of the pressure change the diaphragm moves up and down, thus creating a flow from and to the metallic sphere. Hence, the cell suspension in the bioreactor is alternately drawn in the hollow fiber module and extruded again. The permeate site of the ATF-systems' hollow fiber module can be connected to a harvest pump. During the extrusion of the cell suspension, the applied harvest flow rate is the driving force for the separation of parts of the medium from the cells. The cells and the remaining medium within the hollow fibers are flushed back to the bioreactor. During the suction, cells that might be attached to the membrane are carried along with the incoming cell suspension, thus generating a cleansing effect. The frequency of the cycle can be individually chosen. The advantage of the ATF-system over other cell retention devices is linked to the cell-free harvest stream with long term operation ability. CHO cell densities of over $80 \cdot 10^6$ cells·mL^{-1} to over $100 \cdot 10^6$ cells·mL^{-1} can be achieved in ATF perfusion cultivation (Marx, 2012; Clincke et al., 2013), thus surpassing other membrane based retention systems (Castilho and Medronho, 2002). Additionally, the ATF-system can be purchased in different scales so that up-scaling of bioprocesses can be easily conducted. However, product binding to the hollow-fiber membrane at low cell viability has been observed (Robin, 2013). The ATF-system can be easily connected to conventional 5L-Sartorius bioreactors which in turn can be controlled by a BIOSTAT® B-DCU unit. Additional MFCS/win® software allows a more sophisticated perfusion process design. Processes operated with this set-up are

denominated ATF-perfusion in this work. The ATF-perfusion platform is the last step in the Cell Culture Technology department at Novo Nordisk A/S before the perfusion processes are transferred to bigger scales in other subsequent departments.

In Figure 2-5, the 5 L Sartorius bioreactor with the control unit and the ATF2-system are displayed. The principle of operation of the ATF-system is illustrated.

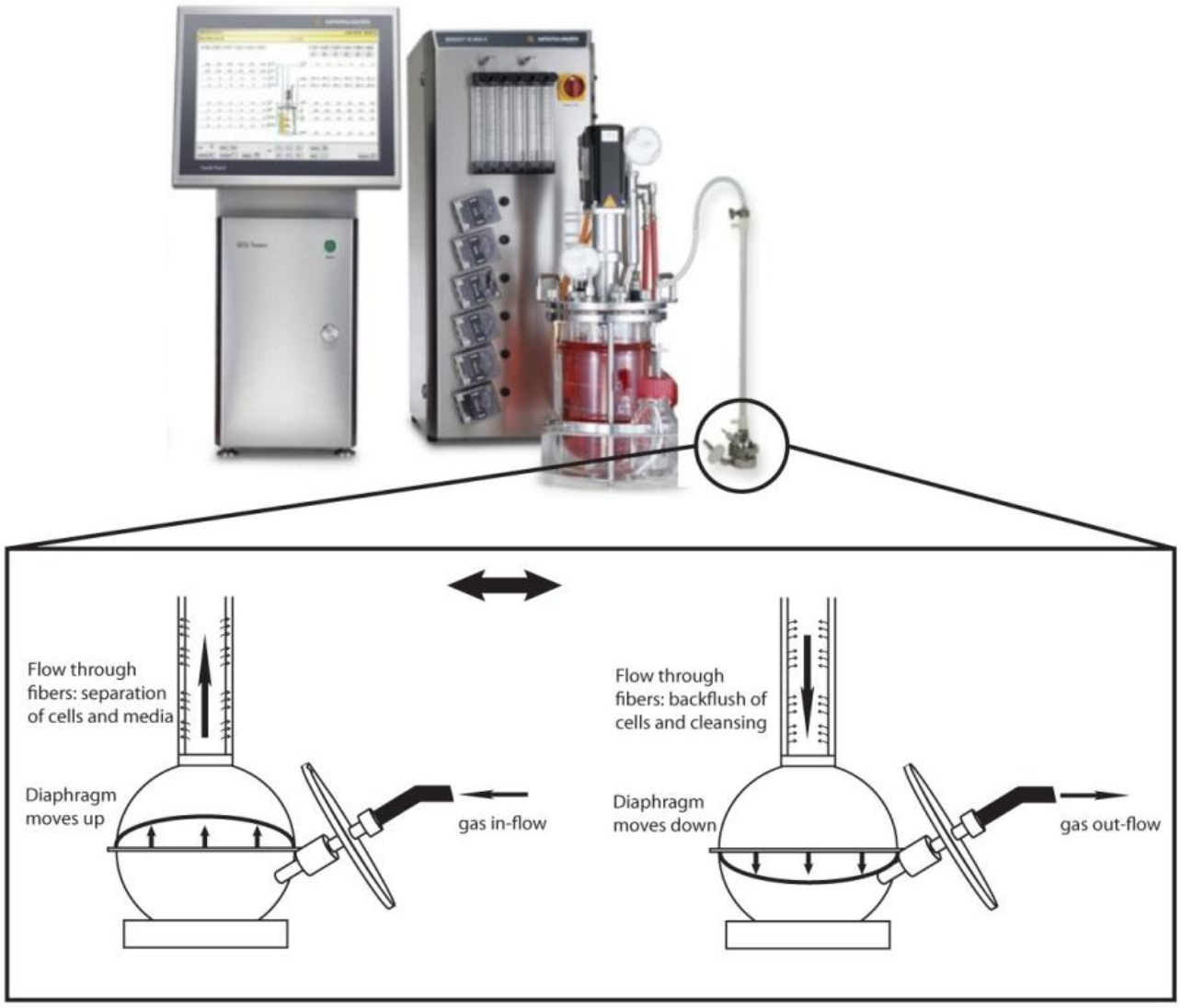

Figure 2-5: 5 L Sartorius bioreactor with B-DCU control tower and ATF2-system. The mechanism of cell retention of the ATF-module is depicted below. The two sequences, left and right, are repeated alternatingly. Images of the bioreactor and the DCU were retrieved from www.sartorius.com, the image of the ATF2 system was retrieved from www.refinetech.com. Both were altered.

2.4 Physiology of Chinese Hamster Ovary (CHO) cells in culture

Many factors influence the cell culture performance of CHO cells. These factors include, amongst others, physicochemical parameters of the ambient cell culture environment as well as nutrient and metabolite levels and composition in the cell suspension. In the following section factors that differed or have been actively changed between the different experiments are briefly described and their effects on CHO cell physiology are portrayed.

2.4.1 Effect of nutrients and metabolic byproducts

The main carbon sources in conventional mammalian cell culture media are glucose and glutamine. Glucose is metabolized via the glycolysis pathway in the cytosol and serves as an energy source for CHO cells. Glucose is transported into the cells with the help of membrane protein transporters and is subsequently phosphorylated by hexokinases in the cell cytoplasm to glucose 6-phopshate where it is further converted via several intermediates to pyruvate (Gódia and Cairó, 2006). Pyruvate can follow two different reaction pathways. One is the direct conversion to lactate by lactate-dehydrogenase, where nicotinamide adenine dinucleotide is oxidized from its reduced form NADH to NAD^+ which is reused for the glycolysis pathway. The other pathway requires the transport of pyruvate into the mitochondria where it is converted to acetyl coenzyme A (Acetyl CoA) and is afterwards introduced into the tricarboxylic acid cycle (TCA). Although less energy is generated during the first reaction pathway (Gódia and Cairó, 2006), the second reaction pathway is not preferably used by CHO cells and other immortalized cells or tumor cells (Zhou et al., 2011). This behavior is attributed to the deregulated metabolism of immortalized cells (Garber, 2006) which results in a faster glycolysis (Moreno-Sánchez et al., 2007). Thus, glucose is converted to a great extent to lactate and is not introduced via Acetyl CoA into the TCA. Therefore, CHO cell cultures also require glutamine as a second nutrient source which is essential for the TCA (Reitzer et al. 1979).

Glutamine is transported into the cytosol via unspecific amino acid transport systems (Gódia and Cairó, 2006). For the incorporation into the TCA, glutamine is converted to glutamate at the mitochondrial membrane by phosphate activated glutaminase (PAG). During this process ammonium is released. Glutamate is then transported into the mitochondria and interconnects with the TCA mainly at two points. It is converted by glutamate dehydrogenase to α-ketoglutarate which is part of the TCA. Here, another ammonium molecule is formed. This process is reversible, so that glutamate can also be formed from α-ketoglutarate. Glutamate is also generated during the translocation of electrons across the mitochondrial membrane with the malate-aspartate shuttle. In an intermediate step aspartate is converted to oxaloacetate, which is part of the TCA, by aspartate aminotransferase and, simultaneously, glutamate to α-ketoglutarate. Therefore, glutamate has to be regarded both as a substrate and a product. An important function of the malate-aspartate shuttle is the regeneration of NAD^+ which is

reused in glycolysis. A deregulated malate-aspartate shuttle results in a higher conversion of pyruvate to lactate in order to regenerate a sufficient amount of NAD^+ (Lu et al., 2008).

An efficient metabolism, i.e. feeding glucose via pyruvate into the TCA, can lead to energy in the form of 32 adenosine triphosphate (ATP) molecules in contrast to only 2 ATP when pyruvate is converted to lactate. However, not only the glucose metabolism but also the glutamine metabolism is deregulated (Gódia and Cairó, 2006). This inefficiency results in a high accumulation of lactate and ammonium which might have detrimental effects on cell culture performance. Effects on hybridoma and CHO cell growth have been observed at lactate concentrations above 40 mM and ammonium levels starting from 2-4 mM. (Ozturk et al., 1992; Lao and Toth, 1997; Altamirano et al. 2013). The adverse effect of lactate on cell growth is caused mainly by a reduction of pH of the medium and an increase in osmolality (Cruz et al., 2000; Altamirano et al. 2013), whereas the precise mechanism of ammonium toxicity is unclear (Altamirano et al, 2013).

2.4.2 Effect of pH

In cell culture, the pH has to be controlled in an optimal range since pH significantly affects cell growth, protein production and cell metabolism (Kurano et al. 1990; Borys et al. 1993; Miller et al., 1988; Link et al., 2004; Yoon et al., 2005). Normally, the pH is controlled within a dead-band around the set-point value. Due to the inaccuracy of the online and offline sensors for pH and the system's time response, a typical variation of ±0.1 pH units is considered acceptable. Bicarbonate and CO_2 are often used to control pH. pH excursions from this range can influence cell culture performance severely. Shifts of 0.2 pH units have been observed to increase transient apoptosis in mouse myeloma cells (Osman et al. 2001) and to alter the metabolism of CHO cells (Trummer et al. 2006).

2.4.3 Effect of carbon dioxide

Carbon (CO_2) dioxide is a catabolic product of the cell metabolism and as previously mentioned used for pH control. In solution, carbon dioxide is hydrated to carbonic acid which dissociates to bicarbonate and hydrogen ions

$$CO_2+H_2O \Leftrightarrow H_2CO_3 \Leftrightarrow HCO3^-+H^+. \qquad 2\text{-a}$$

Since CO_2 is in equilibrium with bicarbonate, an excess of CO_2 leads to an acidification of the cell culture. The addition of base for pH control would lead to a desired reduction in pH but at the same time to an increased osmolality since the equilibrium in reaction (2-a) is driven further to the right (de Zengotita et al., 1998). The high osmolality in turn can have negative effects on the cell culture performance (Kurano et al., 1990; Ozturk and Palsson, 1991). Sufficient ventilation of the culture system via the gas flow rate is therefore essential to remove excess CO_2 (Aunins and Henzler, 2008). The CO_2 partial pressure (pCO_2) has to be kept in a certain range, because cells also consume CO_2 for the

synthesis of pyrimidines, purines and fatty acids (deZengotita et al., 1998). The optimal level of pCO_2 is 40-50 mm Hg (Gódia and Cairó, 2006). Levels of more than 120 mmHg have been shown to inhibit cell growth of CHO cells (deZengotita et al., 1998).

2.4.4 Effect of osmolality

Osmolality describes a solution's osmotic pressure and is an important process parameter for mammalian cell culture. Osmolality has an effect on cell size, since water can easily pass the cell membrane via aquaporins and water channels (Verkman et al., 1996). A static description of the dependency of cell volume and osmolality is futile, because volume regulatory pathways are induced when CHO cells are cultured under osmotic stress (Sarkadi et al., 1984). The effect of osmolality on cell culture performance and morphology has been intensively studied under hypo- and hyperosmotic conditions (Ozturk and Palsson, 1990; Takagi et al., 1999; Lee and Lee, 2001; Kim and Lee, 2002; Kiehl et al., 2011). Therefore, media with a range of 270-330 $mOSm \cdot kg^{-1}$ are used which is acceptable for most cells (Zeng and Bi, 2006). Hyperosmotic conditions can be generated by base addition and CO_2 input which are linked by equation 2-a. The individual contribution of each factor on cell culture performance is therefore difficult to separate during cultivations. Studies specifically dedicated to elucidate particular effects of osmolality and pCO_2 by decoupling these parameters showed that pCO_2 and osmolality contributed to growth inhibition in a dose-dependent manner and had synergistic effects with osmolality (deZengotita et al., 1998).

2.5 Parameter for the comparison of different process modes, scales and bioreactor constructions

Commonly, cell culture performance is assessed by obtaining primary cell culture parameters, e.g. cell concentration and viability as well as metabolite and product concentrations. A comparison of different cell culture processes based on these values is possible as long as the employed mode of operation, the scale and equipment is identical or similar. The direct comparison of continuous and perfusion cultures based on VCD is not feasible since the perfusion set-up results in higher cell concentrations. Therefore, in this work, another set of parameters for comparison has to be applied. In this case specific metabolic rates provide a more uniform approach. Here, a relation between primary parameters, the set dilution rate and, most often, the viable cell concentration is established, thus regarding the time-dependent state of a single cell (see chapter 2.5.1). The utilization of specific rates permits the observation of individual cells and their environment rather than monitoring a cell population. This cell status is applicable for comparison across scales, process modes and bioreactor constructions (Ozturk, 1996; Konstantinov et al., 2006). However, problems can occur because of inaccurate and time-delayed measurements of metabolites and product concentrations which result in fluctuation of specific rate values.

For continuous or perfusion processes a relatively easy obtainable and sufficiently accurate specific rate is the CSPR. The CSPR is the quotient of the dilution rate D and VCD of the culture process and describes the fraction of supplied medium per cell and day, comprising all medium components in a single entity. The dilution rate can be easily controlled with adequate and precise pumps, whereas automated VCD measurement with a cell counter diminishes subjective errors. Thus, compared to metabolite specific rates, the instrumentation efforts to change and control the CSPR at certain set points are relatively low.

The CSPR has been suggested by several authors as a promising variable for the control and design of robust perfusion cultivation processes (Ozturk et al., 1996; Zeng et al., 1999; Konstantinov et al., 2006). Based on the assumption that the metabolic phenotype of the cells does not change over time and medium composition is sustained, consistent production of recombinant protein can be achieved, if the CSPR is maintained constant (Ozturk et al., 1996). The CSPR can also be used in order to optimize protein production, as proposed by Konstantinov et al. (Konstantinov et al., 2006). According to Konstantinov et al., the CSPR can be pushed towards the minimal CSPR ($CSPR_{min}$) which still allows a robust process. This is either achieved by keeping the cell density constant and lowering D, or by keeping D constant and increasing the cell density. With a bleed rate or cell discard rate the cell density can be varied, thus only the modulation of pumps is necessary. In both cases high fed-batch like protein titers should be achievable, whereas in the latter case also a higher volumetric productivity (VP) is predicted.

Finding the optimal CSPR for protein production in perfusion mode is time and cost intensive, so that simpler scale-down models which are mostly operated in continuous mode are preferable. By including two parameters, D and VCD, that directly affect substrate consumption and product formation, the CSPR offers the possibility to control a biological system across different process set-ups, so that a transfer of culture conditions can be performed with fixing the CSPR to certain set-points. As the CSPR of perfusion mode processes is linked to the bleed rate and harvest rate, whereas the CSPR of continuous mode is linked to the bleed rate alone, it is fundamental to determine whether the same effect on cell culture parameters can be observed. Few authors have been examining the correlation between CSPR and cell specific rates in different bioreactor set-ups. Their results demonstrate dependencies of various rates on CSPR. In connection with this thesis however, some questions were not addressed. In their work either the same, not fully controlled bioreactor systems (Henry et al., 2008) or processes with fundamentally different origins which resulted in large variations (Zeng et. al, 1998) have been evaluated and compared. Hence, the evaluation of the effect of CSPR on cell culture performance across scales, bioreactor systems and operation modes needed to be assessed.

2.5.1 Interconnection of dilution rate, cell specific rates and Cell Specific Perfusion Rate (CSPR)

The mathematical model for the calculation of the specific rates are substantially similar for pseudo-continuous, continuous and perfusion process cultivations. All models assume a constant reaction volume, V_L, over time or at fixed volume reduction time points,

$$\dot{V}_L(t) = F_{in}(t) - F_{out}(t) = 0, \quad \text{2-b}$$

where the variation over time, specified with in- and outflow rates, is 0.

The volumetric input flow rate F_{in},

$$F_{in}(t) = F_{feed}(t) + F_B(t) + F_{AF}(t), \quad \text{2-c}$$

includes the volumetric inflow rate of the medium, F_{feed}, the titration rate for base, F_B, and the addition of antifoam F_{AF}.

The volumetric output flow rate F_{out},

$$F_{out}(t) = F_{Bleed}(t) + F_{Harvest}(t), \quad \text{2-d}$$

is made up of the cell discard or bleed flow rate, F_{Bleed}, and the harvest rate, $F_{Harvest}$. The sampling flow rate, F_S, is included in F_{Bleed}. Due to the missing cell retention, F_H equals 0 in continuous and pseudo-continuous cultures. Here, only the bleed and sampling rate comprise the outflow rate.

Based on these assumptions, the dilution rate D,

$$D(t) = \frac{F_{out}(t)}{V_L(t)}, \quad \text{2-e}$$

can be defined as the quotient between the volumetric output flow and the liquid reaction volume.

These parameters are used to describe the mass balances in the bioreactor. The balance of the cell mass, m_{XL}, in the liquid reaction volume,

$$\dot{m}_{XL}(t) = -\frac{F_{Bleed}(t)}{V_L(t)} \cdot m_{XL}(t) + \mu \cdot m_{XL}(t), \quad \text{2-f}$$

comprises cell growth, μ, and the removal of cells with the bleed rate. The transformation to a concentration balance requires the consideration of

$$m_{XL}(t) = c_{XL}(t) \cdot V_L(t) \quad \text{2-g}$$

and its derivative

$$\dot{m}_{XL}(t) = \dot{c}_{XL}(t) \cdot V_L(t) + c_{XL}(t) \cdot \dot{V}_L(t). \quad \text{2-h}$$

Combined with equation 2-b the balance for the cell concentration, c_{XL} or VCD, can be denoted as

$$\dot{c}_{XL}(t) = -\frac{F_{Bleed}(t)}{V_L(t)} \cdot c_{XL}(t) + \mu(t) \cdot c_{XL}(t). \quad \text{2-i}$$

During steady state the balance can be solved to the cell specific growth rate, μ,

$$\mu(t) = \frac{F_{Bleed}(t)}{V_L(t)}, \qquad \text{2-j}$$

which is only dependent on the bleed rate, F_{Bleed}, at constant VL. Thus, when considering the continuous cultivation mode and equation 2-d and 2-e, a dilution rate that is higher than the achievable maximum specific growth rate leads to cell wash out. Similarly, a dilution rate below the minimum specific growth rate or maintenance growth rate does not allow a continuous cultivation.

The same method can be applied for the concentration balances of the substrate concentration in the liquid reaction volume c_{SL},

$$\dot{c}_{SL} = D(t) \cdot (c_{SR} - c_{SL}) - q_{S/X}(t) \cdot c_{XL}, \qquad \text{2-k}$$

which consists of the dilution rate, the substrate concentration of the medium reservoir, c_{SR}, the cell specific substrate uptake rate, $q_{S/X}$, and the cell concentration. In steady state, transposing the substrate concentration balance leads to $q_{S/X}$,

$$q_{S/X}(t) = \frac{D(t) \cdot (c_{SR} - c_{SL})}{c_{XL}(t)}. \qquad \text{2-l}$$

From equation 2-k it is apparent that a higher dilution rate leads to a higher cell concentration at steady state condition when the cell to substrate yield $y_{X/S}$,

$$y_{X/S}(t) = \frac{\mu(t)}{q_{S/X}(t)}, \qquad \text{2-m}$$

remains constant. However, as mentioned before, a dilution rate higher than the maximum growth rate would result in cell wash-out.

A similar approach provides the balance for the product concentrations c_{PL},

$$\dot{c}_{PL} = -D(t) \cdot c_{PL} + q_{P/X}(t) \cdot c_{XL}, \qquad \text{2-n}$$

and the cell specific production rate during steady state $q_{P/X}$,

$$q_{P/X}(t) = \frac{D(t) \cdot c_{PL}}{c_{XL}(t)}. \qquad \text{2-o}$$

Based on the equations above, the volumetric productivity VP,

$$VP(t) = D(t) \cdot c_{PL}(t) = q_{P/X}(t) \cdot c_{XL}(t), \qquad \text{2-p}$$

can be calculated.

The yields for the turnover of a substrate into a metabolite, $y_{S/P}$, can be easily derived from $q_{S/X}(t)$ and $q_{P/X}(t)$:

$$y_{S/P} = \frac{q_{S/X}(t)}{q_{P/X}(t)}. \qquad \text{2-q}$$

The calculation of the cell specific perfusion rate CSPR,

$$CSPR(t) = \frac{D(t)}{c_{XL}(t)}, \qquad \text{2-r}$$

illustrates the difference of continuous and perfusion process cultures, when equation 2-d is considered. For perfusion cultures, both the bleed and harvest flow rate have an effect on the CSPR, whereas for continuous cultures only the bleed flow rate has an impact.

The relationship of CSPR and growth rate during steady state can be represented when equation 2-j is transposed and inserted in equation 2-r:

$$CSPR(t) = \frac{\mu(t)}{c_{XL}(t)}. \qquad \text{2-s}$$

Thus, at steady state a linear relationship between CSPR and μ is to be expected. Furthermore, CSPR has an effect on specific rates such as substrate uptake rates,

$$CSPR(t) = \frac{\dot{c}_{SL}(t) + q_{S/X}(t) \cdot c_{XL}(t)}{[c_{SR}(t) - c_{SL}(t)] \cdot c_{XL}(t)}, \qquad \text{2-t}$$

and product formation rates,

$$CSPR(t) = \frac{-\dot{c}_{PL}(t) + q_{P/X}(t) \cdot c_{XL}(t)}{c_{PL}(t) \cdot c_{XL}(t)}, \qquad \text{2-u}$$

where also linear relationships at steady state can be assumed.

2.6 Scale-Up/Down parameters

The use of different bioreactor systems is usually an obstacle in process development towards industrial scale applications. Normally, due to the high number of experiments, systems that are easy to handle

and do not require process variable feedback control are used in the initial stages of screening for highly productive clones and optimization of process conditions. Successive scale-up is then carried out with the aim to transfer the identified optimized cell culture characteristics to large-scale industrial stirred tank bioreactors. Here, not only the applied working volume for cultivation changes but also geometrical and physical characteristics of the cultivation systems, so that a linear scale-up is not applicable (Marques, 2010). Parameters that have to be usually considered during scale-up for production purposes, such as pH and temperature, can be easily controlled and modulated in lab-scale. These factors have only a significant impact in ranges above lab-scale bioreactors where mixing is considered a major task (Lara, 2006). Since this thesis is only focusing on culture volumes below 5 L, scale-up methods towards industrial scales are not further discussed and can be found elsewhere (Nienow et al., 1996; Schmid, 2005). However, when focusing on the critical process parameters that have to be maintained throughout the scale-up to support a certain cell environment, much attention has been paid to oxygen supply. Assuring a sufficient oxygen supply by an adequate oxygen concentration in the liquid phase is of crucial importance for animal cell cultures (Trummer et al., 2006a). The oxygen transfer rate OTR, which describes the transfer of oxygen from the gas to the liquid phase, is proportional to the volumetric mass transfer coefficient k_La. This parameter in turn is dependent on geometrical characteristics of the used bioreactor as well as the modulation of e.g. stirrer speed (Van't Ried, 1979). Van't Ried proposed the following relation between the k_La value and characteristic vessel parameters:

$$k_L a = K \cdot \left(\frac{P}{V_L}\right)^{\alpha} \cdot (v_s)^{\beta}, \qquad \text{2-v}$$

with K, α, and β being constants. P is denoted as the gassed power input, V_L as the liquid volume, and v_s as the superficial gas velocity. Thus, it can be inferred that the k_La can be maintained in different bioreactor vessels to ensure sufficient oxygen supply by keeping the volumetric power input(VPI), $\frac{P}{V_L}$, and the superficial gas velocity v_s constant (Xing et al. 2009). These parameters are defined as

$$\frac{P}{V_L} = \frac{N_P \cdot N^3 \cdot {D_i}^5 \cdot \rho}{V_L} \qquad \text{2-w}$$

with the power number of the vessel configuration, N_P, the stirrer speed, N, the impeller diameter, D_i, and the density of liquid in the vessel, ρ, and

$$v_s = \frac{F_G}{A_V} \qquad \text{2-x}$$

with the volumetric gas flow, F_G, and the cross sectional area of the vessel, A_V.

Other potential scale-up parameters such as mixing time or impeller tip speed (both linked to agitation speed) are changed by VPI and superficial gas velocity based scaling.

An appropriate k_La value chosen by a scaled superficial gas velocity and VPI does not only determine defined oxygen concentrations in the cell culture liquid but at the same time the concentration of carbon

dioxide which is transported out of the liquid phase. This ventilation is affected by the chosen agitation speed and gas flow. As mentioned in chapter 2.4.3, pCO_2 has effects on cell proliferation and has to be taken into consideration when applying the chosen parameters for scale-up or scale-down.

Other parameters have been proposed and studied to determine applicable scale-up criteria (Hubbard, 1987; Chisti, 1993; Varley and Birch, 1999). A summary of cultivation process parameters is given by Schmidt (Schmidt, 2005). It has to be noted however, that no single scale-up criterion has been proven to be superior. Thus, the choice of scale-up parameter has to be evaluated for every individual case (Schmidt, 2005; Marques et al., 2010). In this work the VPI was used as a key parameter for scale-up. This method was already described for animal cells (Langheinrich and Nienow, 1999) and was recommended by the former Novo Nordisk consultant Alvin Nienow for a fed-batch cultivation strategy.

For the deployed bioreactors of this work the vessel related variables were obtained from literature or provided by the manufacturer. Table **2-1** provides an overview of the properties of the different vessels used during this work. Based on these parameters a scale-down approach was suggested. For the ambr™ system, the scaled airflow of 0.21 ccm was not applied, since pCO_2-stripping with a constant basic airflow of 0.1 ccm proved to be sufficient. Also, Nienow et al. (2013) reported in a thorough characterization of the physical characteristics of the ambr™ system that the k_La is lower at a reduced sample volume of 13 mL. Since a pseudo-continuous process was applied, the volume was increasing from as low as 9 mL to 15 mL and higher k_La had to be assumed during periods with lower actual volume.

The values for the ambr™ marked with an asterisk (*) were retrieved from Nienow et al. (Nienow et al., 2013). With these variables, the parameters for maintaining constant VPI and thus a constant k_La could be calculated. Since the same medium was used for all the experiments, the density of the medium was canceled out of equation (2-w). Combined with the fixed parameters determined by the type of bioreactor, only the stirrer speed and the airflow at constant VPI and superficial gas velocity, respectively, had to be changed for each bioreactor set-up. The initial values were assigned to the 5L-bioreactor. The calculated mutual power input was with 48 $W \cdot m^{-3}$ in the normal range routinely used in animal cell culture (Nienow et al., 2013).

Table 2-1: Important vessel related variables for the three different bioreactors used for successive scale-down calculations.

Variable	Type of bioreactor		
	5L-Sartorius	1L DASGIP	15 mL ambr™
Working volume V_L (L)	4.3	1.0	$15 \cdot 10^{-3}$
Impeller diameter d_i (cm)	7.50	5.20	1.14*
Power number N_P	1.2	1.2	2.1*
Cross sectional area of the tank A_v (cm^2)	201.10	83.32	4.155*
Stirrer speed (rpm)	250	283	727*
Airflow at constant v_s (ccm)	10.00	4.14	0.21*

3 Materials and Methods

3.1 Cell line, Medium and Seed-culture

The cells used for this work were derived from a CHO-K1 cell line that produced a recombinant protein with puromycin as a selection marker. The used medium was the chemically defined HyClone™ CDM4CHO™ medium (GE Healthcare, USA) which was adjusted to contain 6 mM L-glutamine. For the seed cultures which were propagated in shake-flasks (Corning, USA), 6 $\mu g \cdot mL^{-1}$ puromycin (Life Technologies, USA) was added. The medium used for the bioreactor cultures did not contain puromycin.

In order to establish a cell bank (CB), a vial with 10^7 cells was thawed. The cells from the research cell bank (RCB) had been stored in medium with 10% dimethyl sulfoxide (DMSO) at -196°C in liquid nitrogen. The thawed content of the vial from the RCB was transferred to a 15 mL Falcon® tube (VWR, USA) and centrifuged at 200 g for 5 minutes in a Centrifuge 5430R (Eppendorf, Germany). The supernatant was discarded and the cell pellet was re-suspended in 10 mL medium with a temperature of 36.5°C. 300 µL of cell suspension was removed for cell concentration measurement with a Cedex HiRes®. The cell suspension was then transferred to a 125 mL Erlenmeyer shake flask (Corning, USA) and diluted to $0.3 \cdot 10^6$ $cells \cdot mL^{-1}$ with fresh medium. The cell suspension was incubated in an Infors HT Multitron shake incubator (Infors AG, Switzerland) at 140 rpm and 36.5°C at a controlled 5% CO_2 atmosphere. After 72 hours, the cells were passaged to 500 mL shake flasks (Corning, USA) with an initial cell concentration of $0.3 \cdot 10^6$ $cells \cdot mL^{-1}$ and cultured in the shake incubator at 120 rpm while maintaining the other conditions. This procedure was repeated after 72 hours. Subsequently, $20 \cdot 10^7$ cells were transferred into a 50 mL Falcon® tube (VWR, USA) and centrifuged at 800 rpm for 5 min. Thereafter, the supernatant was removed and the cells were re-suspended with 20 mL medium containing 10% DMSO. 1 mL each was transferred to 20 1.8 mL Nunc™ cryogenic tubes (Thermo Scientific, USA). The tubes were stored at -80°C for 7 days in an in-house ice chest which ensured a temperature reduction of $-1°C \cdot h^{-1}$. Then, the cell containing tubes were transferred to a nitrogen freezer and stored for further use at -196°C.

The thawing procedure of cells from the CB was identical with the treatment described for the RCB. The cells were propagated in shake flasks with a step-wise up-scaling to up to 1 L working volume until the required cell number for inoculation of the bioreactor systems was reached.

3.2 Bioreactor experiments

This section describes the general set-points for process control and methods for each bioreactor experiment. As mentioned before, no puromycin was used in the medium for the bioreactor cultures. Temperature was controlled for all experiments at 36.5°C. pH was controlled, unless otherwise

mentioned, at 7.1±0.05 by addition of CO_2 and 1M sodium bicarbonate. The dissolved oxygen concentration (DO or pO_2) in the cultures was controlled at 40% air saturation. The values for agitation and basic gas flow can be found in chapter 2.6 or, if varying, are noted in the corresponding results section. Opposed to the experiments in bench-top bioreactors, the cultivations in the ambr™ system required the addition of 20 µL 3% Antifoam C (Sigma Aldrich, USA) each day. In other systems Antifoam was only added on demand.

Before inoculation, bench-top bioreactors were filled with phosphate buffered saline (PBS) and were autoclaved. Subsequently, the PBS was removed and replaced with medium. Vessels for the ambr™ system were supplied pre-sterilized. After polarization of the pO_2-electrodes, the medium was conditioned to the right temperature and pH set-points. Inoculation cell density for all cultures was $0.3 \cdot 10^6$ cells·mL^{-1}.

3.2.1 ambr™ bioreactor system

The used ambr™ system consisted of an ambr™ 48 workstation including 4 culture stations (CS) for up to 48 parallel cultivations. Cell counts were measured with an at-line Cedex HiRes® once per day. The feeding interval, e.g. the time length between two medium feeds, was programmed for 2 hours unless otherwise noted. Every 24 hours, the volume was reduced to the initial value. A simple algorithm was implemented to ensure a constant dilution rate at exponentially increasing inflows and culture volume:

$$V(t+1) = \frac{V(t) \cdot D}{n}. \qquad 3\text{-a}$$

The volume to be added at the next feeding time point, V(t+1), is the product of the volume determined before the feeding time-point, V(t), multiplied with the constant dilution rate, D. The product is divided by the number of feeds per 24 hours, n. The volume for each time point was recorded automatically by the ambr™ system and used for further calculations. The final working volume, just before the volume reduction, was set to 15 mL. Samples for substrate, metabolite, osmolality, and protein analysis were taken from the supernatant of the harvested cell suspension that was collected during the volume reduction step.

3.2.2 DASGIP bioreactor system

The DASGIP system was equipped with Type DS1000ODSS vessels. Electrodes for pH and pO_2 control were calibrated before the cultivation. The Bioreactors were connected via silicone tubing to medium reservoirs, bleed flasks and base reservoirs. Via the integrated DASGIP pump modules (MP4 and MP8) medium (F_{in}) and base (F_B) were pumped into and cell suspension (F_{bleed}) was pumped out of the bioreactor. The feed was controlled by a level sensor which acted as a switch for the feed pump controller. In order to mimic the ambr™ cultures more closely, a feed algorithm was implemented so that medium was supplied once every hour. The working volume was set to 1 L. Samples for cell count, pH

and pCO_2 were taken daily with a single use syringe that could be connected via a luer-lock mechanism to the bioreactor. Supernatant of the extracted sample was used for substrate, metabolite, osmolality, and protein measurements.

3.2.3 Sartorius-ATF perfusion bioreactor system

The Sartorius-ATF-perfusion system consisted of a 5 L double jacketed UniVessel® bioreactor vessel, a BIOSTAT® B-DCU control tower (both Sartorius Stedim Biotech S.A., France) and an ATF2-system (Repligen, USA) including a 0.2 µm hollow fiber module with 850 cm^2 surface area.

As can be inferred from chapter 2.5.1, the ATF-perfusion process differed from the classical continuous cultivation set-up of the DASGIP system. Inflow of medium (F_{in}) and base (F_B) was realized via integrated BIOSTAT® B-DCU pumps. The bleed (F_{Bleed}) was removed from the bioreactor with a Watson Marlow 120U peristaltic pump (Watson Marlow, USA). The harvest (F_H) was removed after filtration by the ATF-system. The working volume was 4.3 L. The same sampling technique was used as during the DASGIP cultivations.

In order to generate a higher VCD, the harvest rate was switched on after 72 hours of batch cultivation. Earlier experiments showed that by using a ramped harvest rate, i.e. increasing the harvest rate linearly, from an initially lower flow, F_{Hinit}, to the set-point, F_{Hset}, a smooth transition and minimal overshooting of VCD - as a consequence of the supply with fresh medium - to steady state VCD is achieved. Thus, the time between reaching steady state and the start of the culture was minimized so that the culture age of the cells for the three bioreactor systems was as comparable as possible. In this case, F_{Hinit} was 0.50 d^{-1} and F_{Hset} was 1.25 d^{-1}. After reaching F_{Hset} the bleed rate was initiated.

3.3 Analytics

3.3.1 Determination of cell concentration or biomass

For the determination of the viable cell concentration, samples were taken once daily and analyzed with an automatic Cedex HiRes® Cell Counter (Roche Diagnostics, Germany). The measurement is based on the trypan blue exclusion staining method. Trypan blue is excluded by intact cell membranes so that when mixing the dye with cell suspension only dead or dying cells exhibit a blue stained cytoplasm (Louis and Siegel, 2011). The Cedex HiRes® uses an image-based counting method to determine viable and dead cell counts. Based on the applied cell suspension volume, the cell concentration is calculated. Additional information such as average cell diameter, aggregation rate and cell size distribution is provided.

Given that the cell size changes over time in mammalian cell cultures, cell concentration might not be an adequate culture parameter for the description of the state of a cell culture. The growth rate, often

determined by the increase of cell number per volume unit, might be misinterpreted when using common cell measurement methods. Because of certain process conditions, cells can invest energy in augmenting the cell volume rather than in cell division. Then, the measurement of the biomass, as employed in microbial cultures, might be a more precise measurement for determining cell growth. The viable biomass volume VBV,

$$VBV(t) = c_{XL}(t) \cdot \frac{4}{3} \cdot \pi \cdot \left(\frac{AVC(t)}{2}\right)^3, \qquad \text{3-b}$$

including the viable cell concentration, VCD, and the average cell diameter, AVC, can be directly calculated from the given Cedex HiRes® data.

3.3.2 Determination of substrate and metabolic turnover products

Substrate concentrations were measured either enzymatically with a CuBiAn-HT270 system (Optocell, Germany) or with a BioProfile 100+ system (Nova Biomedical, USA). Usually the BioProfile system is used for providing a coarse overview of substrate and metabolite concentrations. The CuBiAn was considered to be a more sensitive analyzer so that the results of this system were primarily used for the comparison of cell culture performance in this project (Martin Heitmann, personal communication, 14.04.2014). The measurement principle of the BioProfile is based on the measurement of ions with ion selective electrodes (ISE) (see Durst, 2011). In the CuBiAn, a colorimetric reaction based on the interaction of the analyte and enzymes is measured and compared to a standard calibration curve. Unless otherwise mentioned, the substrate and metabolite derived data was measured with the CuBiAn-HT270.

3.3.3 Determination of target product concentration

The concentration of the recombinant protein in the supernatant of cell culture samples was analyzed with an in-house Sandwich Enzyme-Linked Immunosorbent Assay (ELISA). The measurement principle is based on the streptavidin-biotin-peroxidase complex (ABC). In this case, after coating the surface of a microtiter plate with a coating antibody, the sample containing the analyte (the recombinant protein) is added to the plates. The analyte functions as an antigen for the coating antibody. After an incubation step and washing step, a biotin-linked detection antibody is added and also binds the analyte. Subsequently another incubation and washing step, a streptavidin-peroxidase conjugate is added. Streptavidin has a very high affinity to biotin (Holmberg et al., 2005) and thus binds to the detection antibody. After incubation and washing, 3,3',5,5'-Tetramethylbenzidine (TMB) can be added that is converted by peroxidase to 3,3',5,5'-tetramethylbenzidine diimine which causes the solution to take on a blue color. The color intensity is concentration dependent. The reaction can be stopped by using phosphoric acid. The color intensity can be recorded and compared to a standard.

Previous results show wide variations for the protein of interest of this work when using this ELISA for analysis, but other instruments and techniques were not available.

3.3.4 Determination of offline-pH, pCO_2 and Osmolality

The measurements of offline pH and pCO_2 were executed with a RapidPoint® 500 Blood Gas System (Siemens Healthcare, USA). The measurement principle for pH determination is based on the potentiometric method using standard ISE. The partial pressure of CO_2, pCO_2, is measured with a modified Severinghaus electrode (Severinghaus, 2004).

Osmolality was determined with an Osmomat (Gonotec, Germany). The measurement principle is based on the comparison of the freezing point of H_2O and the sample. Pure H_2O, with an osmolality of 0 $mOsm \cdot kg^{-1}$, freezes at 0°C, whereas a solution with 1 $mOsm \cdot kg^{-1}$ exhibits a freezing point at -1.858°C. A linear calibration between 0 $mOsm \cdot kg^{-1}$ and 300 $mOsm \cdot kg^{-1}$ can be performed.

4 Results and Discussion

In total, 5 experiments with different bioreactors, operation modes and process conditions were conducted which resulted in 62 cell cultivations that were evaluated. The experiments were planned successively to include the findings of previous experiments into the design. An overview about the different experiments is presented in Table 4-1.

In the first experiment, a wide range of dilution rates was covered in DASGIP continuous cultures (chapter 4.1) in order to study the effects on cell culture performance and to establish a basis for comparison. In experiment 2, the observed results should be reproduced with data from cultivations in the ambr™ system (chapter 4.2.1). Additionally, the effect of varying feed intervals was studied. The third experiment was designed to investigate effects of adapting growth rates in the transition phase between batch phase and continuous cultivation phase by changing the initial dilution rate (chapter 4.2.3). A different start phase was also used in experiment 5 based on the expertise in perfusion process design in Novo Nordisk's Cell Culture Technology Department. The ATF-perfusion was executed for the scalability evaluation of the identified parameters in pseudo-continuous and continuous cultivation (chapter 4.3). The second cultivation in DASGIP bioreactors (experiment 4) should give information about effects of pH and pCO_2 variation on culture performance (chapter 4.2.4).

Table 4-1: List of experiments and corresponding bioreactor systems, operation modes, number of cultivations per experiment and the underlying purpose of the experiment. Chapters where the corresponding experiments are described and evaluated are listed on the right.

Experiment	Bioreactor system	Operation mode	No. of cultivations	Purpose	Corresponding chapter
1	DASGIP	Continuous	7	Screening of D	4.1 & 4.2.1 & 4.3
2	ambr™	Pseudo-continuous	24	Screening of D, Effect of feed intervals	4.2.1 & 4.2.3 & 4.3
3	ambr™	Pseudo-continuous	24	Reproducibility test, Effect of adaption to D	4.2.2
4	DASGIP	Continuous	6	Effect of pCO_2 and Osmolality	4.2.4
5	Sartorius-ATF	Perfusion	1	Comparison to ambr™ and DASGIP	4.3

4.1 Relationship of CSPR and various specific rates at different dilution rates of continuous cultures

The identification of scaling parameters towards a systematic process development strategy was first approached with 7 parallel continuous cultivations in DASGIP bioreactors. After an initial 3 days batch phase, the cultures were maintained for 61 days in continuous mode before terminating the processes. The processes can be divided into two experimental phases. In the first phase, each bioreactor was assigned one bleed flow rate and thus a dilution rate set-point. Therefore, a broad range of process conditions was covered in order to provide an overview of the effect of dilution rate on cell culture performance. However, the desired set-points of D differed from the actual achieved due to imprecise pumps which emphasizes the issue of continuous cultures in small scale. The actual set-points were maintained throughout the culture. In the second phase, a dilution rate set-point change was initiated to examine possible effects on cell culture performance. Since different dilution rates result in different metabolic states (Hiller et al., 1991), possible differences in cell culture data due to a set-point shift from low and high rates, respectively, to a mutual rate were investigated. It has been reported that cells cultured at the same dilution rate showed distinct steady states when the metabolic state was shifted beforehand (Europa et al., 2000). The shift of process parameters, e.g. the dilution rate, during process development is a common procedure for testing different set-ups in one experiment. Experiments with hybridoma cells in continuous cultivation indicate that physiological state multiplicity is achieved depending on the direction of the dilution rate shift (Follstad et al. 1998). Phase I comprises the cultivation from the start until day 35, whereas phase II includes day 35 until the end of the process. Table 4-2 shows the schematic experimental planning of phase I and phase II.

For a closer approximation of ambr™ pseudo-continuous processes, a level sensor controlled hourly feed was implemented, i.e. medium was pumped into the bioreactor once every hour if the level sensor was signaling a critical volume. The bleed rate was kept constant due to software restrictions. Besides the dilution rate, all other set-points were identical for the 7 cultures. The substrate and metabolite measurements during steady state were executed in the CuBiAn system, but the time range until day 11 was covered by Bioprofile measurements.

Table 4-2: Dilution rate set-points of 1 L DASGIP continuous cultivations

	Phase I:	Phase II:
	1st set-point (day 0-day 35)	2nd set-point (day 35-day 61)
culture 1	D_1=0.15 d^{-1}	D_2=0.25 d^{-1}
culture 2	D_1=0.24 d^{-1}	D_2=0.34 d^{-1}
culture 3	D_1=0.25 d^{-1}	D_2=0.35 d^{-1}
culture 4	D_1=0.28 d^{-1}	D_2=0.38 d^{-1}
culture 5	D_1=0.40 d^{-1}	D_2=0.35 d^{-1}
culture 6	D_1=0.44 d^{-1}	D_2=0.34 d^{-1}
culture 7	D_1=0.46 d^{-1}	D_2=0.35 d^{-1}

4.1.1 Phase I: Characterization of continuous cultures with different dilution rates

In phase I, processes that were run with a lower dilution rate exhibited lower VCD values than processes with higher dilution rate set-points. Figure 4-1 (A) shows the time course of VCD for exemplary cultures. VCD steady state condition for all cultures was reached after 14 days and, except for culture 1, was maintained until the end of cultivation phase I. The VCD for cultures 5, 6, and 7 was almost identical at $4.44 \cdot 10^6 \cdot cells \cdot mL^{-1}$ to $4.57 \cdot 10^6 \cdot cells \cdot mL^{-1}$ during steady state, although the dilution rate differed by up to 0.06 d^{-1}. This suggests that at around D=0.40 d^{-1} a critical dilution rate is reached, where higher medium supply rates do not support higher VCD. The steady state VCD of culture 4 (D=0.28 d^{-1}) with $3.95 \cdot 10^6$ $cells \cdot mL^{-1}$ was higher than the VCD of cultures 2 and 3 (D=0.24 d^{-1} and D=0.25 d^{-1}) with $3.66 \cdot 10^6$ $cells \cdot mL^{-1}$ and $3.74 \cdot 10^6$ $cells \cdot mL^{-1}$, respectively, albeit the small difference in D. This supports the assumption of an upper VCD limit at high dilution rates. Culture 1 showed the lowest VCD with an average of $3.13 \cdot 10^6$ $cells \cdot mL^{-1}$ during the assumed steady state.

Additionally, the processes with set-points increasing from D=0.15 d^{-1} to D=0.28 d^{-1} showed an initial damped oscillation phase until steady state was reached. The duration of the oscillation decreased with increasing dilution rate. In contrast, the processes with D≥0.40 d^{-1} showed none or only marginal fluctuations. A reason for this behavior is the adaptation process during the transition phase from batch to continuous cultivation. The cell specific growth rate, μ, was approximately 0.7 d^{-1} at the end of the batch phase. After the transition from batch to a continuous process, the substrate demand of the cells at this time point can only be satisfied with a high dilution rate close to the present growth rate. If a lower dilution rate was implemented, the growth rate and cell viability could not be maintained (Miller et al., 1988). The transition phase is characterized by an oscillating trend of VCD and thus μ. The oscillation originated mainly from the prevailing demand and supply of nutrients, since μ and the consumption rates of nutrients are interconnected. Higher μ is accompanied by an increase of substrate consumption. The supply with fresh nutrients, on the other hand, is fixed via D, so that a high demand at high μ cannot be satisfied permanently. Therefore, the high VCD at the beginning of the transition phase could not be supported and μ decreased which in turn led to lower substrate consumption rates. Thereafter, due to the fixed supply via D and the low substrate consumption rates, the available substrate amount was increasing in a time delayed manner. The higher substrate availability allowed again an increase in μ and VCD. The phases of high and low μ, VCD, and substrate consumption rates alternated until, in combination with the discharge of cells via the bleed flow, the parameters stabilized over time and leveled off. This procedure resembled a closed-loop control where the control deviation is adapted stepwise. This is also reflected by the fluctuating glucose and glutamine concentration in the beginning of the continuous cultivation phase (data not shown). Neither glucose nor glutamine was exhausted with a concentration over 2.0 mM and 0.7 mM, respectively, throughout process phase I. The oscillating behavior was also described by other authors (Martens et al., 1992; Banik et al., 1996). In this experiment, the tuning was more durable and provoked higher amplitudes the lower the dilution rate was set. Moreover, lower dilution rates resulted in lower glucose and glutamine concentrations and lower lactate concentrations. Ammonium concentrations were almost identical for all D (data not shown).

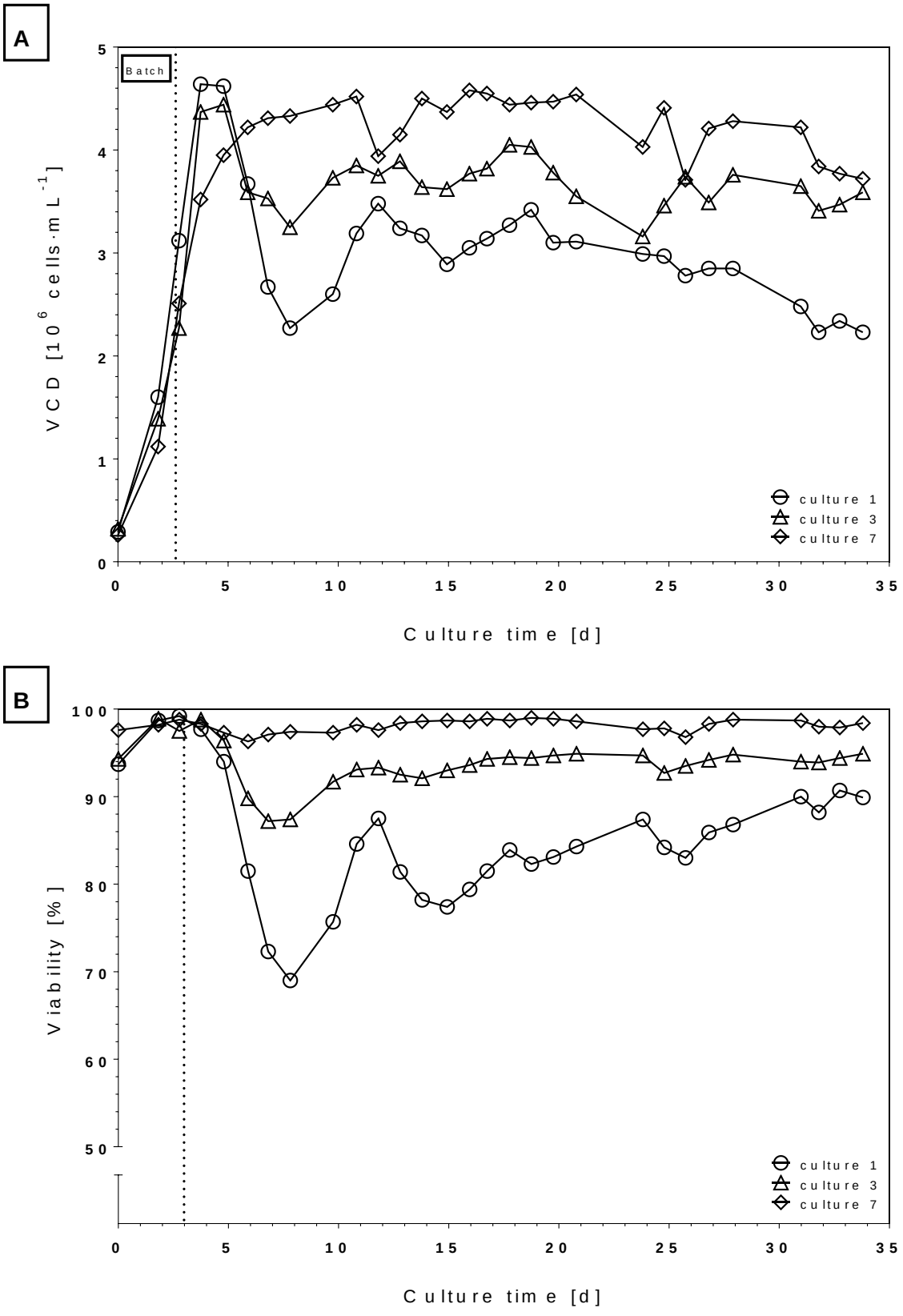

Figure 4-1: Course of VCD (A) and viability (B) over time for culture 1 (open circles), 2 (open triangles), and 7 (open diamonds) during phase I. The dotted line symbolizes the start of continuous cultivation.

However, ammonium measurements could not be evaluated further since samples had been stored for a longer period at -20°C so that evaporation effects were likely. Therefore, ammonium related data and calculations were only provided for a general overview of cell culture behavior.

Viability differences for cultures at different D set-points were also observed. Viability courses over time of cultures 1, 3, and 7 are displayed in Figure 4-1 (B). During the transition phase, the viability decreased for all cultures but to a different degree. At lower dilution rates a lower viability was recorded which, at least initially, correlated to the oscillating VCD. Viability stabilized over time, but distinct levels depending on D were kept. Culture 7 (D=0.46 d^{-1}) showed almost 99% viable cells, whereas for culture 3 (D=0.25 d^{-1}) a viability of only 94% was reached. This phenomenon is consistent with reports of hybridoma continuous cultures (Miller et al., 1988).In contrast to the other cultures, culture 1 demonstrated a noticeable different behavior. The VCD of culture 1 began to decline after an assumed steady state between day 14 and day 24 with ca. $3.13 \cdot 10^6$ cells·mL^{-1}. After a local minimum of $2.78 \cdot 10^6$ cells·mL^{-1} at day 26, the VCD seemed to stabilize but after day 28 the decreasing trend continued until the set-point change where $2.23 \cdot 10^6$ cells·mL^{-1} were recorded. Before the steady-state, strong oscillations of VCD and viability were recorded. The viability decreased until day 8, where it reached a vertex of 77%. From then onward, the viability showed an oscillating increase until day 31, where it stagnated at approximately 90%. The overall low viability can be ascribed to low nutrient and possible high toxin concentration that occur at low dilution rates (Miller et al., 1988). However, after the increase of viability after day 8, the VCD did not fully stabilize and decreased slowly, so that low viability due to a low dilution rate is not the sole explanation for the VCD trend after day 14. Additionally, metabolic byproducts such as ammonium and lactate, which could affect cell growth of mammalian cells (Ozturk et al., 1992, Lao and Toth, 1997), were either in a non-toxic range or at the same level as the other cultures. Therefore, other parameters might give more information.

Interestingly, the average cell diameter (AVC) of culture 1 showed an abnormal behavior compared to the other cultures. This relation can be observed when plotting viability and average cell size against the culture time (Figure 4-2).

After a decrease at the beginning until day 15 from 14.1 µm to 13.1 µm, the cell diameter increased to 14.9 µm until the start of phase II. The other cultures also exhibited an initial decrease in average cell diameter but after day 10 only increased slightly and remained constant in a range of 13.5 µm to 14.0 µm until the set-point change (data not shown). The decrease and increase in cell size of culture 1 can be partially explained by the viability time course. Small cell size is coherent with low viability since dead cells fully or partially disintegrate. The time courses of AVC and viability show similar oscillations until day 14 and thereafter run almost parallel until day 24. After day 24, the AVC increased faster than the viability which stabilized later at around 90%. At the beginning of this diverging trend, it was observed that the offline and online pH differed and a drift of the online-electrode was assumed. The offline pH increased until the end of phase I from 7.06 to 7.12 because of a lower lactate concentration (see Figure 4-4) and probably contributed to the increase in cell diameter of culture 1. Results of an experiment conducted subsequently, indicated that higher pH is associated with larger average cell diameter (see chapter 4.2.4). However, the effect of a slowly increasing culture pH was not investigated, so that the cell diameter could have been impacted by other factors.

Despite reflecting a morphological change, the decreasing average cell diameter also had implications on the evaluation of the measured biomass. In this case, biomass was expressed as cell density which was obtained by an image based system that counts the number of cells present in a defined volume and by that calculates a concentration. However, the changing cell volume is not taken into account with this method. Given the same concentration of cells – measured as cells per milliliter – larger cells take up more space within the cell culture liquid and thus reflect a higher volumetric biomass than smaller cells. When biomass is defined based on the fraction of cell volume per bioreactor volume (VBV), the measured biomass trend might differ from that of the VCD (see chapter 3.3.1).

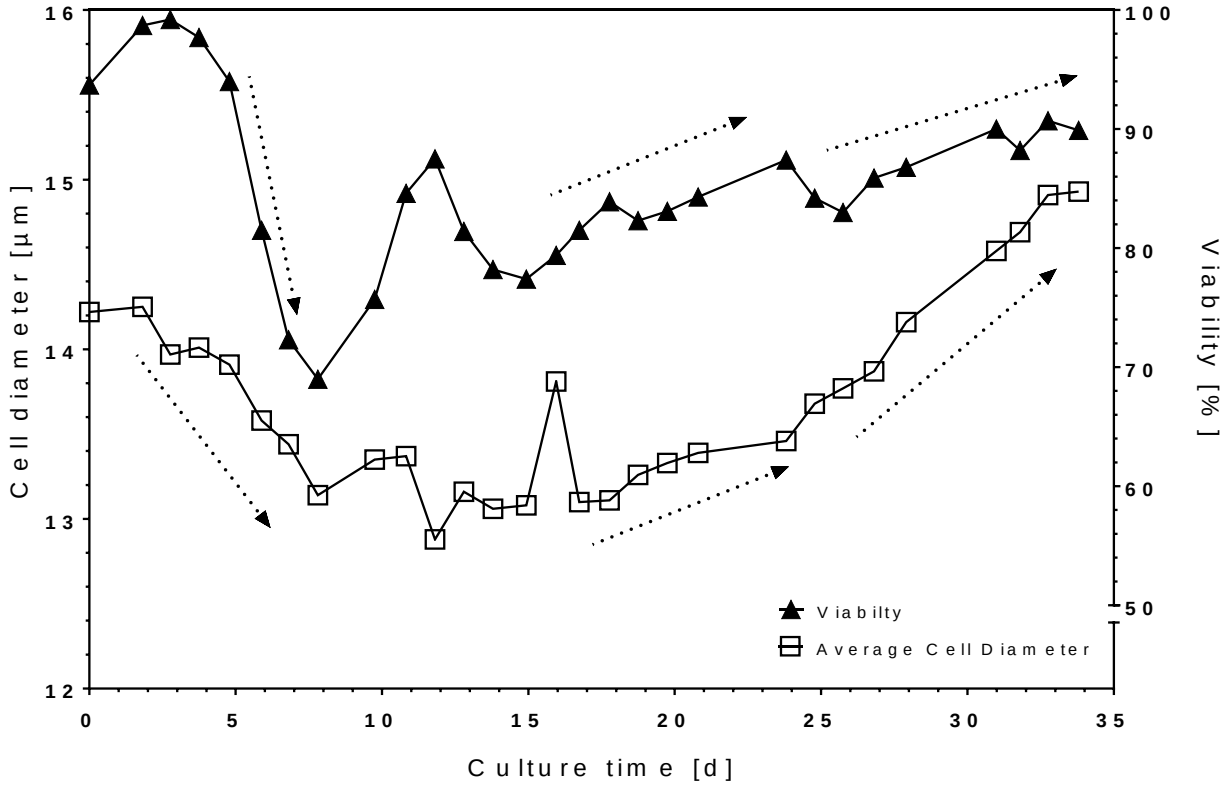

Figure 4-2: Course of average cell diameter (open squares) and viability (filled triangles) of culture 1 over time during phase I. Arrows emphasize the trend of the corresponding culture parameters.

When the VCD is replaced by the viable biomass volume (VBV) and plotted over time as shown in Figure 4-3, the initial fluctuations are reduced and a more robust steady state can be observed for most of the continuous cultures. The more stable steady state for culture 1 is prominent, since the cell diameter fluctuated more than in the other cultures. Consequently, VBV might be an additional tool for the description of cell culture performance when different cell sizes are monitored. The present example suggests that a dilution rate of D=0.15 d^{-1} supports a stable biomass concentration based on VBV. Yet, the VCD reflects a possible change in metabolism of the cells that accompanied the unusual time course of the cell diameter.

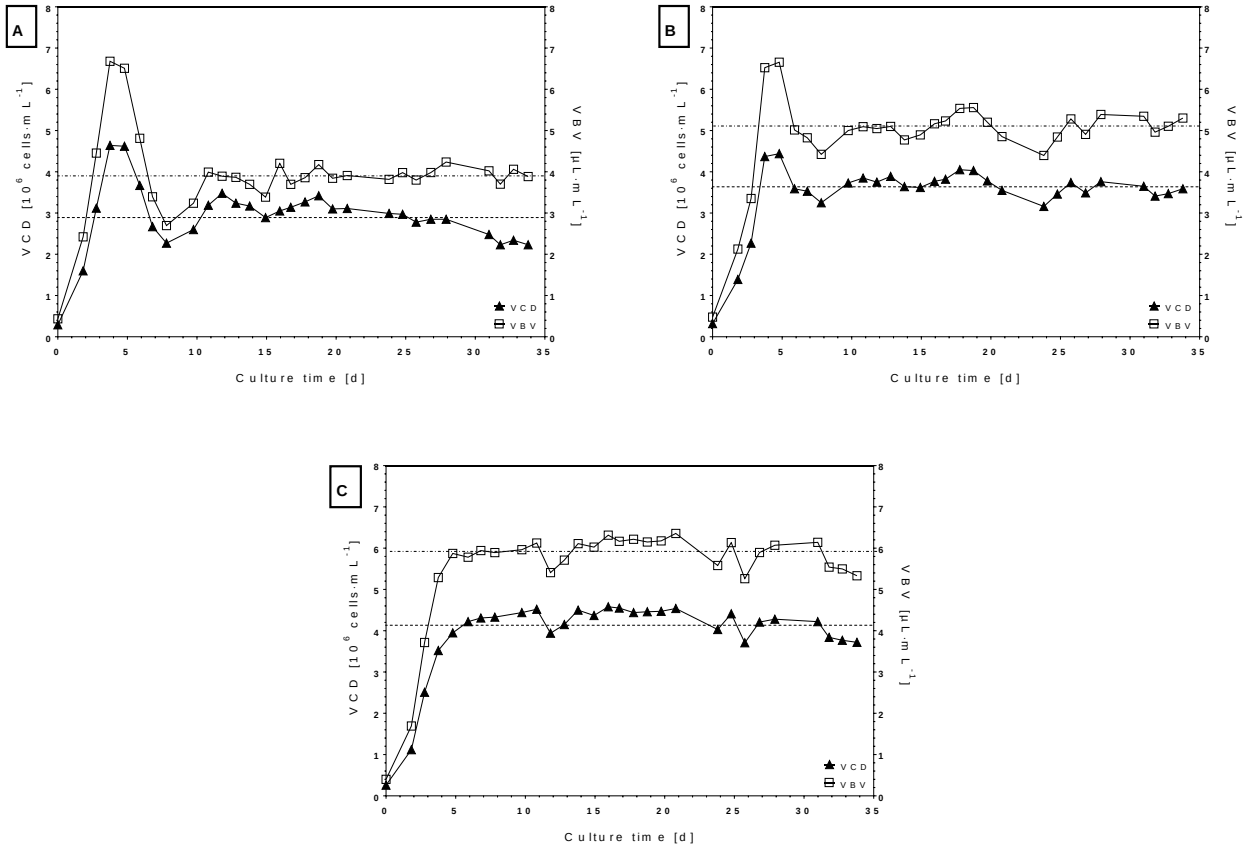

Figure 4-3: Course of VCD (filled triangles) and VBV (open squares) for culture 1 (A), culture 3 (B), culture 7 (C). The dotted lines represent the average of VCD and VBV, respectively, during steady state.

This peculiarity of culture 1 is represented by the trend of lactate and glucose shown in Figure 4-4.

At first, the lactate concentration was congruent with the VCD measurements and reflected the oscillating behavior in a staggered manner (see Appendix 1). From around day 14 until day 24, similar to the VCD course, the glucose concentration and the lactate concentration reached a more stable distribution of approximately 3 mM and 43 mM, respectively. After this time-point, the glucose concentration rose to 6 mM, whereas the lactate concentration declined to 30 mM just before the dilution rate set-point change. The lactate to glucose yield, $y_{Lac/Glc}$, decreased during this period from 1.36 mol·mol^{-1} to 0.66 mol·mol^{-1}. The glucose and lactate concentration of the other cultures did not vary to that extent and $y_{Lac/Glc}$ was almost stable. This change in metabolism, of course, is related to the decreasing VCD during this period. It also might indicate cell line instability since the process control, besides the transient increase in pH, was working normal. The cells cultured at a dilution rate of D=0.15 d^{-1} were stressed at a different level as cells from the other cultures which was reflected in viability and average cell diameter measurements. These results suggest that D=0.15 d^{-1} is close to the minimum growth rate for cell maintenance and might have, in combination with cell line instability, caused this abnormal behavior.

Prior experiments also showed unsteady performances of this cell line at low dilution rates. However, due to the limited data set, a final explanation for the observed behavior could not be proposed. Still, the data of culture 1 indicates that low dilution rates at around D=0.15 d^{-1} might lead to abnormal behavior and should be handled carefully for further evaluation. Only data between day 10 and day 24 was used for comparison between scales and process modes where a stable process was assumed and the steady state conditions were acceptable.

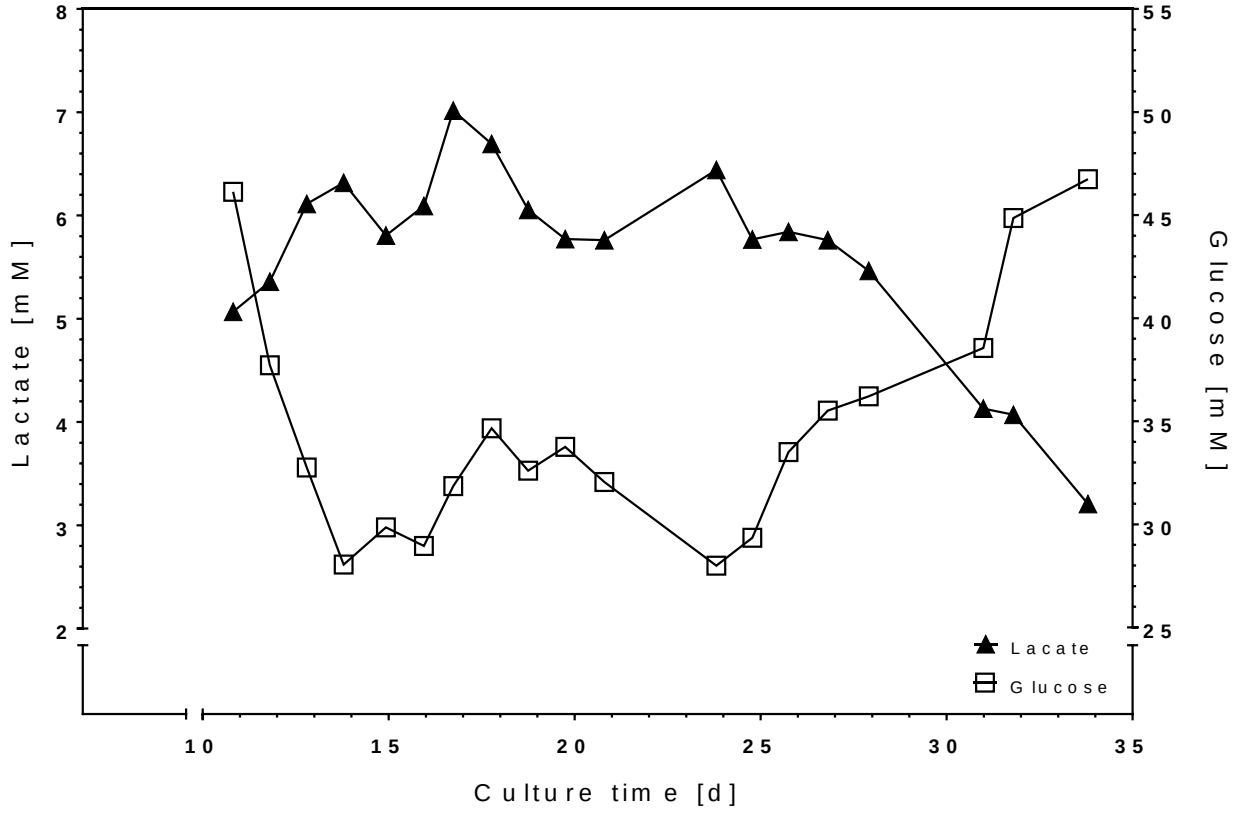

Figure 4-4: Course of lactate concentration (filled triangle) and glucose concentration (open square) of culture 1 over time.

Disregarding the special characteristic of culture 1, the trends of cultures 1-7 show exemplary the insufficiency of comparing continuous cultures with different dilution rates based on primary culture parameters. The sole review of VCD, substrate concentrations, and product concentrations only provides raw information about the effect of the set-point variable D on cell culture performance and thus just display the general output. A classification whether cells exhibit a distinct metabolism is difficult, since not only D but also VCD determines the metabolic state and productivity of a culture. The inclusion of the dilution rate into the parameter data set by calculating cell specific rates enables a better resolution of its effect on cell culture performance and thus the efficiency of a process. As described earlier, the CSPR, which includes D, can be used for process control and provides the advantage of linking VCD, product titer, cell specific production rate, and VP.

As mentioned in chapter 2.5.1, higher dilution rates theoretically lead to higher VCD. Figure 4-5 reflects this trend. VCD values between $3.13 \cdot 10^6$ cells·mL^{-1}and $4.57 \cdot 10^6$ cells·mL^{-1} were achieved for dilution rates between 0.15 d^{-1} and 0.46 d^{-1}, respectively. The marginal plateau of the VCD values at dilution rates D≥0.4 d^{-1} illustrates the achievable upper VCD limit at high dilution rates as mentioned in the section before. The calculated coefficient of determination of R^2=0.9484 underlines the dependency of D and VCD but does not show a very high linear relation. When only cultures with $D_1 \leq 0.4$ d^{-1} are regarded, a R^2 of 0.9952 is obtained which further emphasizes the achievable VCD limit at higher dilution rates. Although culture 1 showed a distinct metabolism, the steady state VCD seemed to fit to the dilution rate set-point.

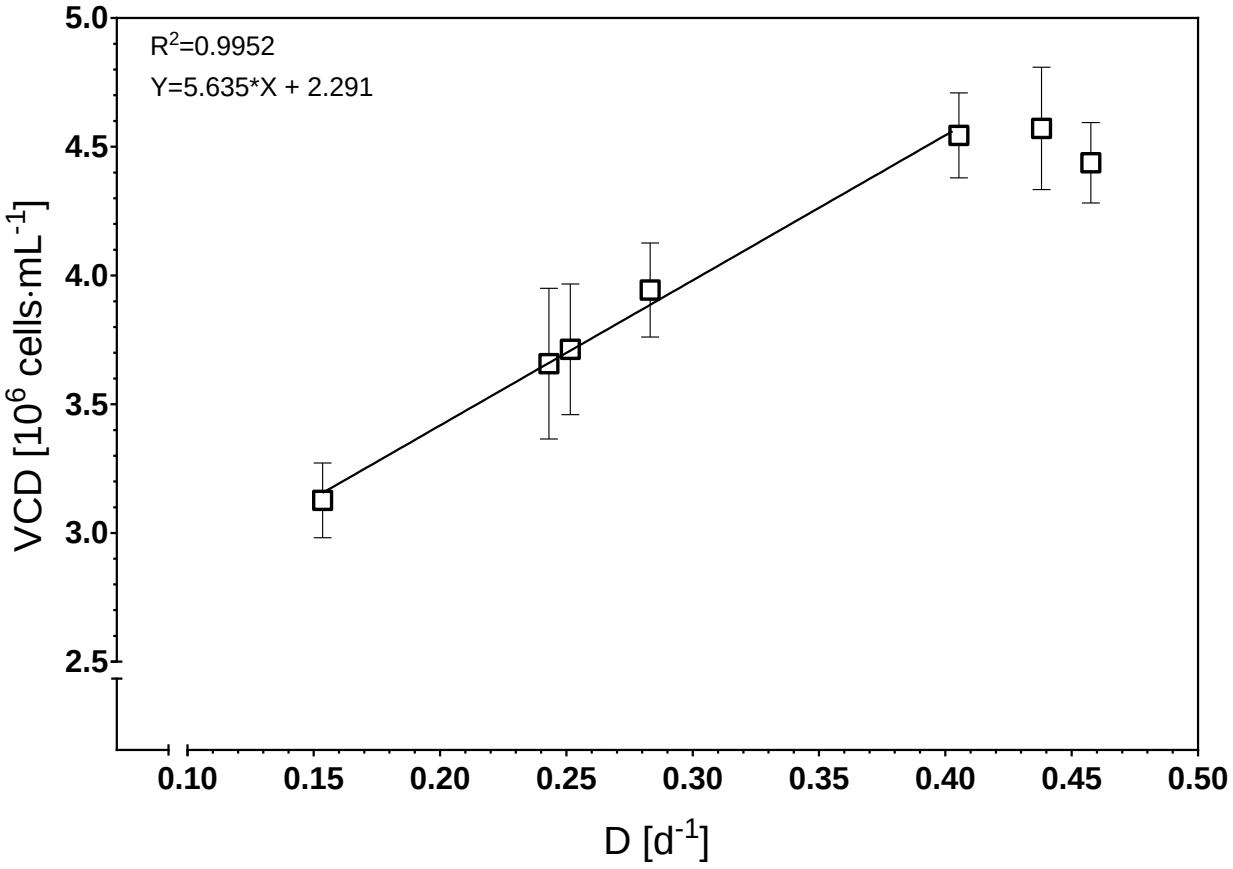

Figure 4-5: VCD arithmetic mean (open squares) during steady state condition for different dilution rate set-points. R^2 is the coefficient of determination of the linear regression analysis. The equation for the regression line is shown in the top left corner. The error bars show the standard deviation of the data points used to calculate the arithmetic mean for steady state between day 14 and 24 (N=9).

Theoretically, in steady state condition, the dilution rate equals the cell specific growth rate μ if VCD measurements are constant. Thus, a similar trend as in Figure 4-5 can be expected when plotting μ over CSPR. Indeed, when regarding Figure 4-6, the same trend is observable. A slight saturation-like trend of μ at high CSPR can be identified. Since the calculation of μ is dominated by the dilution rate at almost linearly increasing VCD, this trend is not as prominent as in the D-VCD diagram so that a highly linear CSPR to μ relationship with a R^2 value of 0.9937 can be found. Growth rates ranged between 0.15 d^{-1} and 0.46 d^{-1} for CSPR between 0.049 nL·cell^{-1}·d^{-1} and 0.103 nL·cell^{-1}·d^{-1}, respectively. This is concordant with

the report of Zeng et al. where also a linear dependency was proposed (Zeng et al., 1998). Altogether, choosing a certain growth rate set-point via the dilution rate also allows targeting a defined CSPR operating point and vice versa.

Besides the growth rate as a critical process parameter, a process is also defined by its substrate and metabolite production rates. The effects of CSPR on these rates are displayed in Figure 4-7. A linear dependency of the glucose consumption rate, q_{Glc}, the lactate production rate, q_{Lac}, the glutamine consumption rate, q_{Gln}, and partially the ammonium production rate, q_{Amm}, on CSPR is observable. For q_{Glc}, q_{Lac}, and q_{Gln} very high coefficient of determinations with $R^2>0.97$ were calculated. The non-linear correlation of q_{Glu} and CSPR ($R^2=0.2683$) was a result of the generally low glutamate concentrations

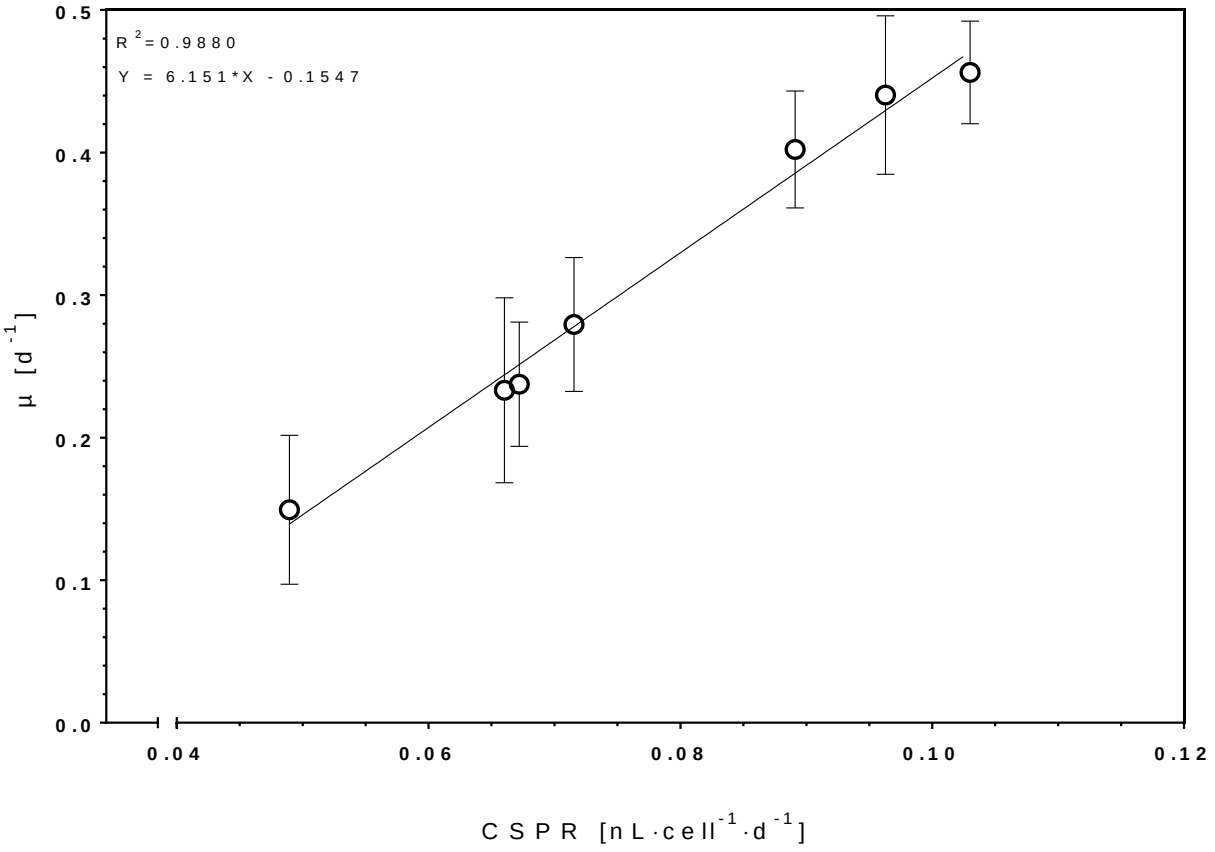

Figure 4-6: Averaged growth rate μ (open squares) during steady state for various CSPR values. R^2 is the coefficient of determination of the linear regression analysis. The equation for the regression line is shown in the top left corner. The error bars show the standard deviation of the data points used to calculate the arithmetic mean (N=9).

which resulted in large fluctuations for the calculated rate. Hence, a reliable analysis of the cell specific glutamate rate was impaired. The measurement for ammonium might not be reflecting the true values since the samples had been stored for more than a month at -20°C before analysis (Martin Heitmann, personal communication, 10.09.2014). Nonetheless, the underlying trend of higher q_{Amm} at higher CSPR is noticeable.

The diverging trends of q_{Glc} and q_{Lac} show that more lactate per glucose was produced at higher CSPR. This phenomenon is widely described in literature and is related to glucose concentrations in the medium.

Higher glucose concentrations in the reaction space resulted in an increased uptake of glucose of hybridoma cells (Miller et al., 1989) which is mainly converted into lactate via pyruvate due to an inefficient metabolism (see chapter 2.4.1). Since CSPR is representing the available volume of medium per cell and day, higher glucose concentrations are present at higher CSPR (Konstantinov et al., 2006), thus higher glucose consumption rates are achieved. An increase in q_{Glc}, however, is not associated with a comparable increase in lactate production which results in a higher lactate to glucose yield, $y_{Lac/Glc}$, for different cell lines (Sanfeliu et al., 1997; Yang et al., 2000). Consequently, at a CSPR of 0.103 nL·cell^{-1}·d^{-1} the lactate to glucose yield was calculated with 1.53 mol·mol^{-1} whereas only 1.18 mol lactate per mol

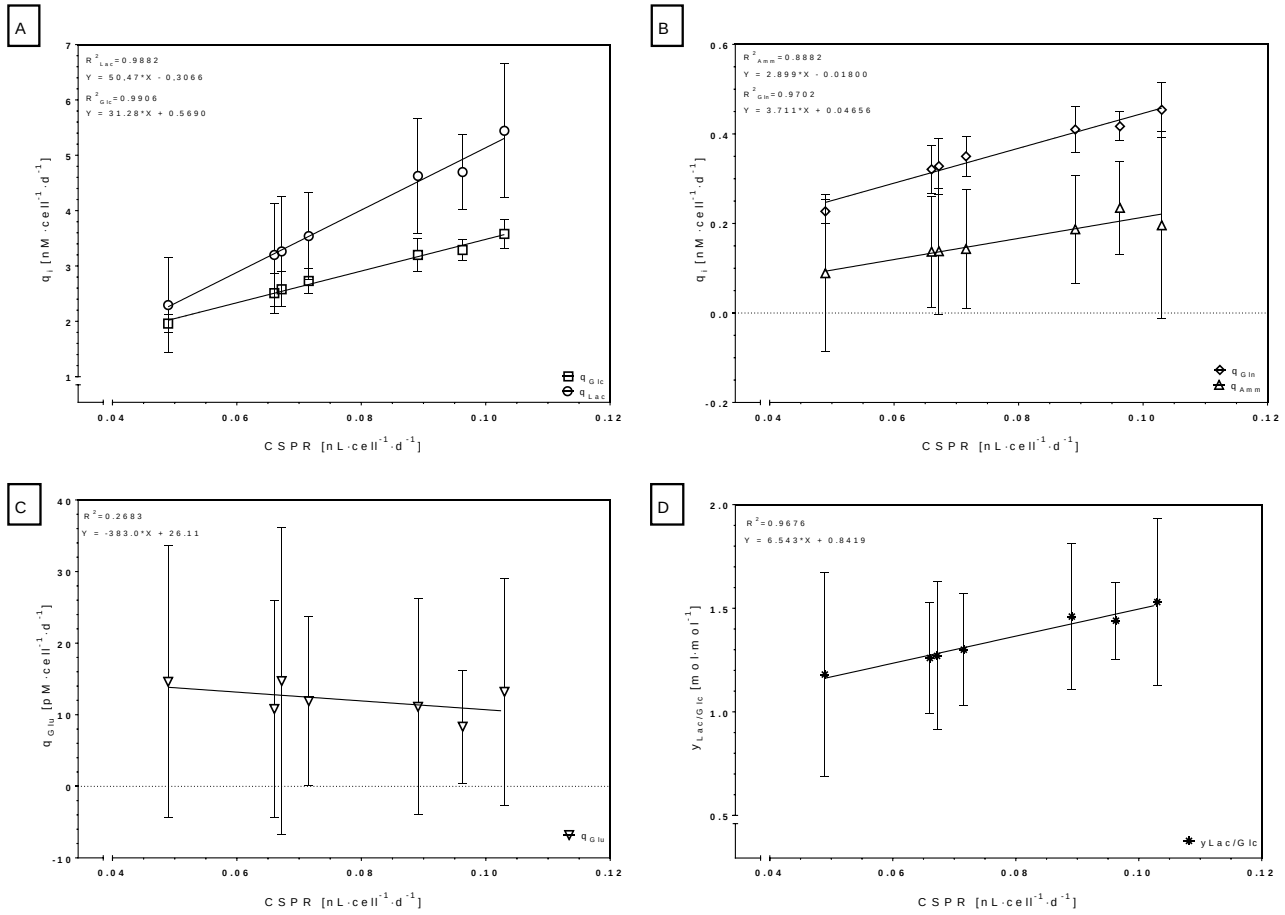

Figure 4-7: Cell specific consumption and production rates of glucose (open squares) and lactate (open circles) (A), glutamine (open diamonds) and ammonium (open triangles) (B), and glutamate (open inverse triangles) (C) over CSPR. In (D), the lactate to glucose yield, $y_{Lac/Glc}$ (asterisk), is shown over CSPR. The equations for the regression analysis are shown in the top left corner. The error bars show the standard deviation of the data points used to calculate the arithmetic mean (N=9).

glucose was formed at a cell specific perfusion rate of 0.049 nL·cell^{-1}·d^{-1}. Theoretically, 2 mol of lactate can be generated from 1 mol of glucose when no other metabolic pathway is used (Lodish, 2000). Thus, a yield of 1.53 mol·mol^{-1} at a relatively high CSPR compared to $y_{Lac/Glc}$ at lower CSPRs reflects a more inefficient metabolism, where less than 25% of the glucose could be used for energy generation in the TCA.

Glutamine consumption rates also showed higher values at higher CSPR. At a cell specific perfusion rate of 0.049 nL·cell^{-1}·d^{-1} q_{Gln} was 0.23 nM·cell^{-1}·d^{-1}, whereas at CSPR=0.103 nL·cell^{-1}·d^{-1} a q_{Gln} of

0.45 nM·cell^{-1}·d^{-1} was measured. Despite the issues of ammonium analysis, it seemed that, just as for the glucose to lactate turnover, the increasing glutamine consumption was accompanied by a non-parallel increase in ammonium production. This is also in accordance with literature (Sanfeliu et al., 1997; Yang et al., 2000).

In the case of q_{Glu}, the decreasing trend could indicate a more efficient utilization of glutamate at high CSPR. Since glutamate is a side product of glutaminolysis, a positive q_{Glu} suggests that glutamate, after the conversion from glutamine, is not fed into the TCA. Negative q_{Glu}, which could occur as indicated by the error bars, would show on the other hand that glutamate of the feed medium and of the glutaminolysis reaction is converted into compounds used in the TCA. Glutamate consumption values in the picomol range, however, indicated a more or less direct turnover and incorporation of glutamate into the TCA. This is supported by the extreme linear dependency of lactate and glucose to CSPR. An inefficient glutamate utilization could affect the regeneration of NAD^+ via the malate-aspartate shuttle, thus provoking a higher pyruvate to lactate turnover (Altamirano et al.,2001) to satisfy the NAD^+ demand of the cell in the cytosol (Altamirano et al., 2013).

The limited measurement capacity did not allow concentration determination of other substrates, so that a full balance analysis of the TCA flux was not executed. Albeit a possible measurement inaccuracy for ammonium and glutamate, the dependencies emphasize the role of CSPR as a tool for process control where substrate consumption and metabolite production can be regulated via a CSPR open loop control. The linear potential between CSPR and substrate consumption and metabolite production rates was also reported in literature (Henry et al., 2008).

Besides the metabolic rates, one of the most important CPP is the product concentration which in turn determines VP and the cell specific protein production rate, q_P, at a given dilution rate. A high volumetric output at stable cell specific productivity is desired. When plotting q_P against the CSPR (Figure 4-8 (A)), it is obvious that no linear relationship is observable. At higher CSPR the values for q_P exhibited fluctuations that could be misread as a gradually increasing trend with higher CSPR leading to higher q_P. The large error bars, however, reflect noisy ELISA results and put the slightly higher mean values into perspective. The physiological properties of this cell line were not evaluated so that detailed data on metabolism associated protein production was not available but protein production seemed to be non-growth associated. This is in accordance with results from other experiments where this cell line was used. Higher substrate consumption rates therefore do not lead to higher protein production rates and indicate inefficient utilization of energy sources.

If an underlying non-growth associated protein production is assumed, the volumetric productivities of cultures 3 and 6 were showing notably different behavior. This is emphasized when plotting VCD against VP (Figure 4-8 (C)) for which a proportional relationship should be expected. Especially culture 6 at VCD=4.57·10^6 cells·mL^{-1} was considerably lower as e.g. culture 7 at the same VCD. The VP for culture 6 was only 58% of the latter. Culture 3 on the other hand was around 18% higher than culture 2 which exhibited a comparable VCD. When these two cultures (3 and 6) are excluded from the linear regression, a linear relationship can be observed (R^2=0.9513), whereas a R^2 of 0.3144 is calculated when all data points are included. Thus, culture 3 and 6 were regarded as outliers concerning VP. Due to the almost constant cell specific productivity and the linear dependency of VP on VCD, a similar function of VP against CSPR as in Figure 4-5 can be observed in Figure 4-8 (B). In between CSPR values of

0.049 nL·cell^{-1}·d^{-1} and 0.089 nL·cell^{-1}·d^{-1}, the volumetric productivity increased, whereas a CSPR higher than 0.089 nL·cell^{-1}·d^{-1} did not result in higher VP.

However, the results were not satisfying. Large error bars were calculated for most of the cultures. The used ELISA analysis produced large variations within triplicate measurements (data not shown), so that the informative value of the generated recombinant protein related data was lowered. General trends could be determined, but the resolution power could not provide a clear basis for comparison. Both, the actual protein measurement with the available indirect ELISA and the storage and transfer of protein samples exhibited various error sources (Martin Heitmann and Ali Kazemi Seresht, personal communication, 07.07.2014) that contributed via error propagation to these noisy protein measurement results. Other detection methods were unfortunately unavailable during this project. Therefore, the relationship between CSPR and protein concentration derived rates and parameters for this continuous cultivation could only be evaluated conditionally.

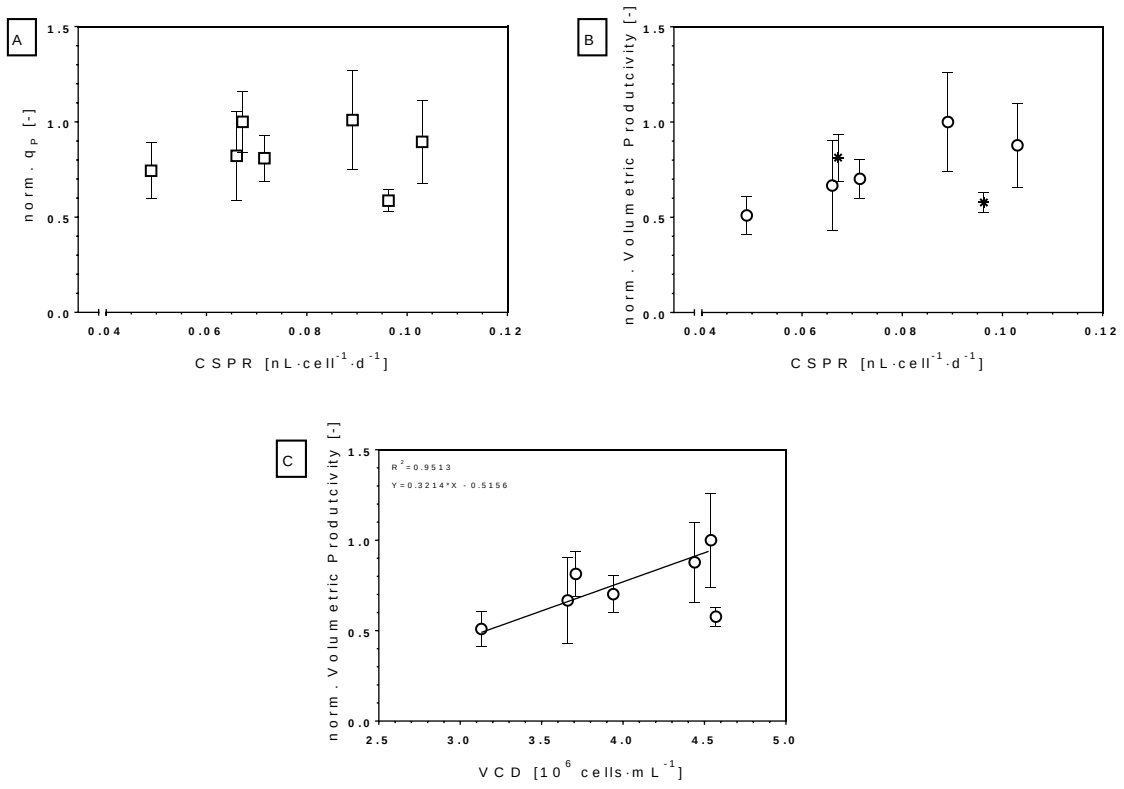

Figure 4-8: Normalized cell specific production rate, q_P (open squares), (A) and normalized VP (open circles) (B) over CSPR. In (B), the assumed outliers are depicted with an asterisk. Below, the normalized VP is plotted against the VCD. The linear regression was calculated without the assumed outliers(C). The error bars show the standard deviation of the data points used to calculate the arithmetic mean (N=9).

4.1.2 Phase II: Effects of a dilution rate shift on cell culture performance

After day 35, a dilution rate set-point change was initiated in order to elucidate possible effects on cell culture performance. It has been reported in literature that cells can adopt a different metabolism in continuous cultivation depending on the environmental conditions they experienced before in the propagation phase (Follstad et al., 1998; Europa et al., 2000). A set-point shift during cultivation is often executed to test different process conditions within one experiment which reduces time and labor costs, amongst others. The reported different metabolic states or steady state multiplicity would in turn impact the applicability of transferring process conditions when a set-point change was performed. To avoid sudden extreme nutrient excess or limitation, the new dilution rate set-points (D_2) were chosen to be shifted by $\Delta D \leq 0.1\ d^{-1}$. The corresponding cultures for an up- or down-shift were chosen in a manner for most cultures to achieve a similar set-point of circa $D_2=0.35\ d^{-1}$. Thus, the dilution rates of cultures 1 ($D_2=0.25\ d^{-1}$), 2 ($D_2=0.34\ d^{-1}$), 3 ($D_2=0.35\ d^{-1}$), and 4 ($D_2=0.38\ d^{-1}$) were increased with $0.1\ d^{-1}$. The dilution rates of cultures 6 ($D_2=0.34\ d^{-1}$), and 7 ($D_2=0.35\ d^{-1}$) were decreased by $0.1\ d^{-1}$. Culture 5 was only shifted by $0.06\ d^{-1}$ in order to reach $D_2=0.35\ d^{-1}$. The same conditions in terms of dilution rate change and effective D_2 were therefore applied for cultures 2 and 3 (group 1) representing the up-shift in dilution rate and cultures 6 and 7 (group 2) representing the down-shift in dilution rate as can be seen in Table 4-3.

Table 4-3: Culture parameters of DASGIP continuous cultures before ($_1$) and after ($_2$) a dilution rate shift.

	Culture	D_1 [d^{-1}]	D_2 [d^{-1}]	ΔD [d^{-1}]	Diff. [%]	$CSPR_1$ [$nL \cdot cell^{-1} \cdot d^{-1}$]	$CSPR_2$ [$nL \cdot cell^{-1} \cdot d^{-1}$]	Diff.[%]
Group 1	1	0.15	0.25	-0.097	63	0.049	0.082	67
	2	0.24	0.34	-0.101	41	0.066	0.101	52
	3	0.25	0.35	-0.095	38	0.067	0.095	41
	4	0.28	0.38	-0.095	34	0.072	0.101	41
Group 2	5	0.41	0.35	0.060	-15	0.089	0.083	-7
	6	0.44	0.34	0.099	-23	0.096	0.095	-2
	7	0.46	0.35	0.109	-24	0.103	0.097	-6

Culture	$y_{Lac/Glc1}$ [$mol \cdot mol^{-1}$]	$y_{Lac/Glc2}$ [$mol \cdot mol^{-1}$]	Diff. [%]	Norm. VP_1 [-]	Norm. VP_2 [-]	Diff. [%]	VCD_1 [10^6 $cells \cdot mL^{-1}$]	VCD_2 [10^6 $cells \cdot mL^{-1}$]	Diff. [%]
1	1.18	1.24	5	0.51	0.26	-50	3.13	3.19	2
2	1.26	1.65	18	0.67	0.36	-46	3.66	3.39	-7
3	1.27	1.56	22	0.81	0.28	-66	3.71	3.58	-4
4	1.30	1.58	22	0.70	0.38	-46	3.94	3.77	-4
5	1.46	1.40	-4	1.00	0.65	-35	4.54	4.01	-12
6	1.44	1.42	-2	0.58	0.85	47	4.57	3.65	-20
7	1.53	1.43	-7	0.88	0.65	-26	4.44	3.74	-16

With this design, the effects of shifting up or down the dilution rate to a mutual dilution rate on cell metabolism and possible differences regarding ΔD could be investigated. The different acquired metabolic

states at D_1 were expected to change after the set-point shift (Hiller et al., 1991). An up-shift in dilution rate would theoretically result in a higher VCD, whereas a down-shift in dilution rate would lead to lower VCDs (see chapter 2.5.1), which has also been reported by Hiller et al. (Hiller et al., 1991). A proof or evidence of the contrary would be valuable for the further experimental design.

Interestingly, all cultures that were shifted to $D_2 \approx 0.35\ d^{-1}$ showed a reduction in VCD (Figure 4-9). Only culture 1 exhibited slightly higher VCD_2 values after a shift from $0.15\ d^{-1}$ to $0.25\ d^{-1}$. The percentage reduction differed between the cultures where D was reduced to the cultures were D was increased. Cultures at $D_2 \approx 0.35\ d^{-1}$ with $D_2 > D_1$ showed a decrease of 4% to 7% in VCD, whereas cultures with $D_2 < D_1$ showed a decrease of 12% to 20%. The smaller decrease for culture 5 (12%) in comparison to group 2 might be due to the lower ΔD. At $D_2 \approx 0.35\ d^{-1}$, VCD_2 was ranging between $3.39 \cdot 10^6 \cdot cells \cdot mL^{-1}$ and $3.77 \cdot 10^6 \cdot cells \cdot mL^{-1}$ for the cultures with up-shifted D and between $3.65 \cdot 10^6 \cdot cells \cdot mL^{-1}$ and $4.01 \cdot 10^6 \cdot cells \cdot mL^{-1}$ for cultures with down-shifted D. Thus, different VCD_2 have to be expected when changing D. A clear trend for this behavior could not be determined. Nonetheless, the decrease for all cultures with $D_2 \approx 0.35\ d^{-1}$ was not expected since the corresponding D_2 should support even higher VCD as could be derived from Figure 4-5 in chapter 4.1.1.

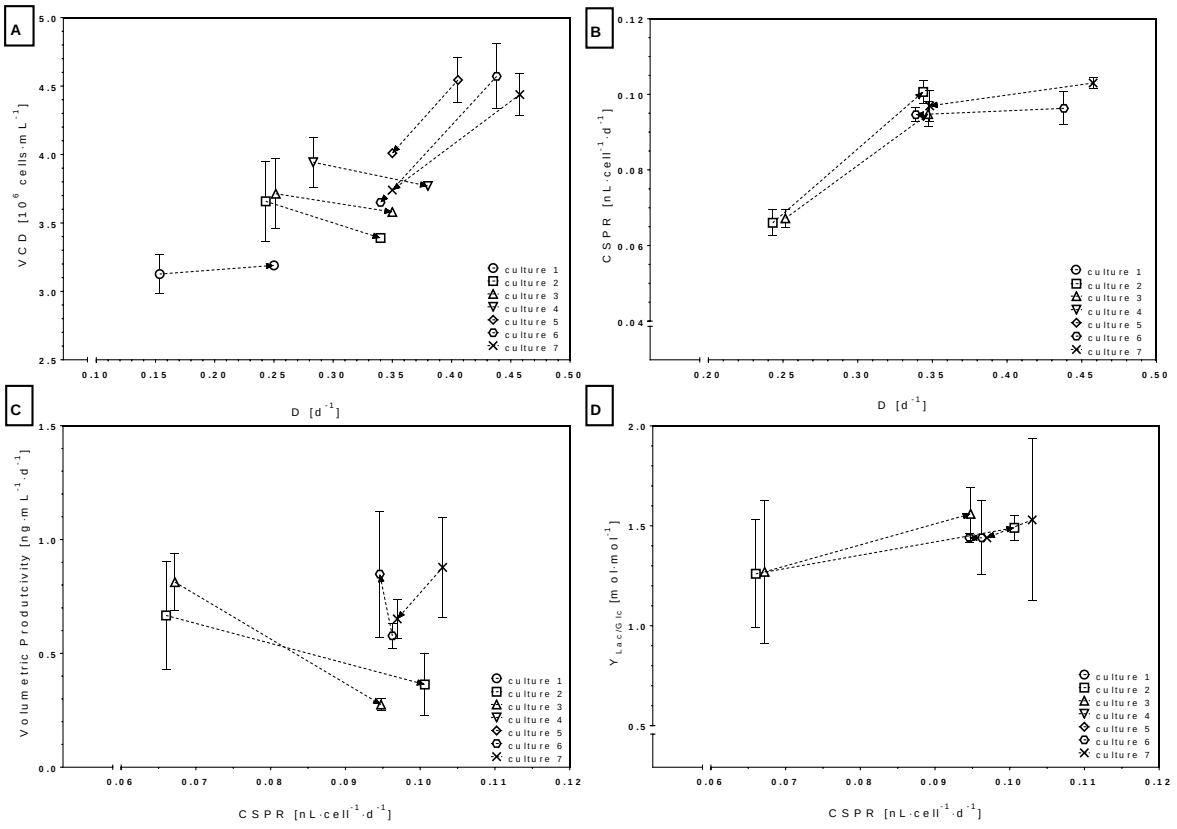

Figure 4-9: Comparison of key process parameters before and after a dilution rate change. The arithmetic means of the corresponding steady states are depicted; error bars show the standard deviations (D_1: n=9; D_2: n=4). The dotted arrows originate from the values during the first D set-point. A: VCD over D for all cultures. B: CSPR over D for cultures 2, 3, 6, and 7 which form group 1 and group 2. C: $y_{Lac/Glc}$ over CSPR of the same cultures as in (B). D: VP over CSPR of the same cultures as in (B). Cultures 1-7 are depicted as: 1=open circle, 2= open square, 3=open triangle, 4=open inverse triangle, 5=open diamond, 6=open pentagon, 7= cross. Substrate and metabolite measurement was conducted with the Bioprofile 100+ system.

Following the set-point change, group 1 and group 2 exhibited almost the same $CSPR_2$ with a mean of 0.097 $nL \cdot cell^{-1} \cdot d^{-1}$ and a maximum deviation of 0.004 $nL \cdot cell^{-1} \cdot d^{-1}$. Compared to $CSPR_1$, group 2 showed only slightly lower $CSPR_2$, whereas group 1 exhibited drastically higher $CSPR_2$ values after the set-point change. Percentage differences for the latter between +41% and +52% and the former between -2% and -6% were calculated. Cultures 1 and 4 showed the same high increase in CSPR as group 1 with +52% and +67% respectively, whereas the $CSPR_2$ of culture 5 was slightly decreased by -7%. Thus, the CSPR was adapted to values similar to high dilution rates in phase I.

The lactate to glucose yield of group 1 and group 2 after the dilution rate change showed almost no difference between the cultures within each group. In general, the yield increased up to 22% for cultures with $D_2 > D_1$ except for culture 1 where $y_{Lac/Glc}$ did not change substantially. This more inefficient utilization of glucose after an up-shift of D is also described by Hiller et al. (Hiller et al., 1991) and has also been mentioned in chapter 4.1.1. Cultures with $D_2 < D_1$ showed only a slight decrease with 4% to 7% in $y_{Lac/Glc}$ which is in the same range as the decrease in CSPR. This is in agreement with the beforehand proposed dependence of $y_{Lac/Glc}$ on CSPR. The differences in magnitude between the two groups seem not to be affected by the percentage change in dilution rate (for group 1: A 38% to 41% increase in D; for group 2: A23% to 24% decrease in D). Similar percentage dilution rate changes of up- and down-shifted cultures with an increase in dilution rate of 34% for culture 4 and a decrease of 24% for culture 7 did result in a $y_{Lac/Glc}$ change of +18% and -7%, respectively. However, considering the rather large error bars, a definite change in $y_{Lac/Glc}$ could not be determined.

The differences between group 1 and group 2 were also noticeable when observing the change in VP at the old and new corresponding CSPR. The VP of group 1 was lower after the set-point change and lower than the VP_2 of group 2. In group 2, culture 6 with an increased VP showed an opposed behavior than culture 7. However, as assumed in chapter 4.1.1, VP_1 of culture 6 was an outlier. Therefore, only culture 7 was considered for VP comparison. VP_2 of group 1 were between 41% and 58% lower than for culture 7. The percentage decrease of VP_2 in comparison to VP_1 was 26% for culture 7 and 46% to 66% for group 1. The values obtained are considerably lower than for similar $CSPR_1$ values without a set-point change. Since no unusual metabolism - as is indicated by $y_{Lac/Glc2}$ - regarding the beforehand calculated yields at $CSPR_1$ was observed, the reduction in VP must be found elsewhere.

An explanation for the decreased VP might be the age of the culture. For long term CHO cultures it has been reported that recombinant protein expression decreased up to 50% compared to initial values after 38 days of cultivation due to molecular stress (Kaufman et al., 1985). Transcription factors of the enhancer binding protein family might be up-regulated under stress conditions which contribute to long term culture instability (Bailey et al., 2012). A change in dilution rate contributes to cell stress, so that the unexpected behavior might be a combination of both. It was not the intention to investigate changes in dilution rate in detail. Therefore, the observations made were sufficient for the continuation of this project.

In conclusion, it can be denoted that a change in dilution rate will result in different VCD and VP compared to the original set-up at corresponding CSPR values. Therefore, without further cause and effect analysis, a change in dilution rate during the experiments of this work was ruled out. However, this additional experiment might prove to be valuable in order to understand results of other experiments were set-point shifts were initiated.

4.2 Evaluation of CSPR as a scaling factor between 15 mL pseudo-continuous and 1 L continuous cultures

The observed interdependencies in 1 L continuous cultures point out that CSPR is a promising parameter for controlling various cell specific rates and VP within one type of cultivation mode and bioreactor system. The transfer of process conditions to other bioreactor scales and operation modes, i.e. the ambr™ system in pseudo-continuous mode, with CSPR as a scaling factor should be – in theory (see chapter 2.5.1) – also possible. Other challenges for this transfer of process conditions, however, were numerous. Besides the use of CSPR as a scaling parameter for CPP, other factors had to be included for the physical scale-up or scale-down respectively from the ambr™ system to the DASGIP system or vice versa.

As already mentioned in chapter 2.6, a classical scale-up between systems of different culture volumes is often performed based on the k_La. The k_La based scaling, e.g. keeping VPI and superficial gas velocity constant, concomitantly alters other factors which might have implications for scale-up. An extensive study to characterize the physical properties of the ambr™ system showed that, although a similar outcome in terms of VCD and VP was reported, this bioreactor system exhibits different characteristics than bioreactors in larger scale. Reynolds numbers were found to be in the transition region rather than being turbulent, which is owed to the small scale. Moreover, the VPI is not evenly distributed in the vessel, but regions with very low dissipation exist. Thus, mass transfer might be a problem in this system. The authors conclude that very high VPI is required to keep k_La constant which in turn exposes the cells to higher shear stress. The fact that, despite the different physical characteristics between the ambr™ and other bioreactor systems, a similar process performance was possible was ascribed to the cell's response to similar stresses. In the ambr™ system and larger bioreactors, this stress is generated in the same manner, i.e. stirring and sparging whereas in the ambr™ the fluid mechanical stresses are higher and the environmental stresses are lower than in bench-top scale. It was proposed that cells react on these strains in an integrated way (Nienow et al., 2013).

In this case, the change in process mode added another factor that could influence the outcome of this scaling study. For the continuous DASGIP and pseudo-continuous ambr™ cultivations, basic process conditions were equalized. Both cultivations were started with an initial batch phase that was ended after 72h. Thereafter, the continuous operation mode was started at the set dilution rate. Differences in the bioreactor system design influenced the process operation. The aeration system of the ambr™ allowed the implementation of a constant basic gas flow. When the pO_2 could not be maintained anymore at its set-point by the employed constant flow, additional O_2 was supplied by a separate flow. Thus, the final gas flow rate was higher than the initially set constant flow rate. With the used DASGIP set-up, only a fixed gas flow rate could be realized where a gas mixture of air, oxygen and carbon dioxide was controlled by the DASGIP software to control pH and pO_2. Thus, different overall gas flows were applied during the two cultivations.

In this chapter a general comparison between ambr™ pseudo-continuous cultures and DASGIP continuous cultures is presented where differences and similarities are highlighted and discussed. Based

on these findings, subsequent experiments, which were conducted in order to identify causes for possible differences, are introduced and discussed.

4.2.1 Comparison of ambr™ pseudo-continuous and DASGIP continuous cultures

In order to compare the process parameters from cultures cultivated in ambr™ and DASGIP bioreactors, a 90% confidence interval (CI) was used. Two different CIs were calculated. The first CI was derived from the arithmetic mean (CIM) of the corresponding values during steady state. The second comprised all data points (CID) that were used to calculate the arithmetic mean of the corresponding parameter group. Thereby, the CID from all the data points depicts the expectable distribution of single data points for other experiments when using the same measuring devices and comprises a wide range of values. The CIM of the arithmetic mean indicates where anticipated values could reside if more sensitive and reproducible measurements were available or a more stable steady state was achievable. Since the ambr™ is the first process technology tool towards up-scaling, the CIs were calculated for the ambr™ system. Values that were within the 90% CIM were considered to be significantly similar (Rita and Ekholm, 2006).

Since pseudo-continuous and continuous cultivation should eventually result in the same measurable cell culture parameters, a comparison of primary culture parameters can provide a first overview of the reproducibility between the two operation modes and bioreactor systems. In Figure 4-10, the VCD and viability over time of an ambr™ and DASGIP culture are displayed.

Interestingly, the cultures showed differences during the transition phase between batch and continuous cultivation. Both, VCD and viability were comparable for the two cultures during the first 72 hours of the batch phase. After the switch to continuous cultivation, the VCD of the DASGIP culture exhibited drastically higher VCD values than the ambr™ culture with a peak at day 5 with $4.79 \cdot 10^6$ cells·mL^{-1}. In contrast, the VCD of the ambr™ culture was only $3.66 \cdot 10^6$ cells·mL^{-1} at day 5. Thereafter, the VCD of the DASGIP culture dropped until day 8 to $3.25 \cdot 10^6$ cells·mL^{-1} and commenced with a damped oscillatory behavior. During the same time range, the VCD of the ambr™ culture showed a maximum of $4.19 \cdot 10^6$ cells·mL^{-1} at day 7. Subsequently, also the ambr™ culture switched over to the oscillatory characteristic. The cause for the oscillation was already explained in chapter 4.1.1. The staggered peaks and the higher maximum VCD for the DASGIP culture can be explained by the different growth rates after the batch phase (data not shown). Here, higher growth rates were observed in the DASGIP culture compared to the ambr™ culture with 0.90 d^{-1} and 0.58 d^{-1}, respectively. The higher growth rate of the DASGIP culture led to a higher increase in VCD which could not be supported by the set D, which in turn eventually resulted in a more drastic decrease in VCD. The lower growth rate of the ambr™ culture in the beginning caused a lower increase in VCD so that the impact of the implemented D was not so prominent and resulted in a smoother transition. This deduction also explains the drop and the subsequent stabilization of the viability of the DASGIP culture which was simultaneous with the peak and stabilization of the VCD. Higher growth rates and a drop in viability after the batch phase as well as a

stronger oscillatory characteristic of the VCD over time were all observed for DASGIP cultures compared to ambr™ cultures at different D. Cultures at higher dilution rates showed smaller differences between the systems, which is congruent with the observations in chapter 4.1.1, since the high growth rates in the transition phase are better supported by the high Ds. The observed differences resulted in an additional experiment in order to investigate the effect of different transition phases on cell culture performance (chapter 4.2.2).

In general, the two cultures show a consistent trend for both VCD and viability. After initial differences in both VCD and viability the cultures stabilized and a relatively constant steady state was observed after day 14 with a VCD of approximately $3.59 \cdot 10^6$ cells·mL^{-1} for the ambr™ culture and $3.71 \cdot 10^6$ cells·mL^{-1} for the DASGIP culture. The viability was 96% and 94%, respectively. The data after day 24 was not considered since ambr™ process conditions were changed and because of the considerations in chapter 4.1.1.

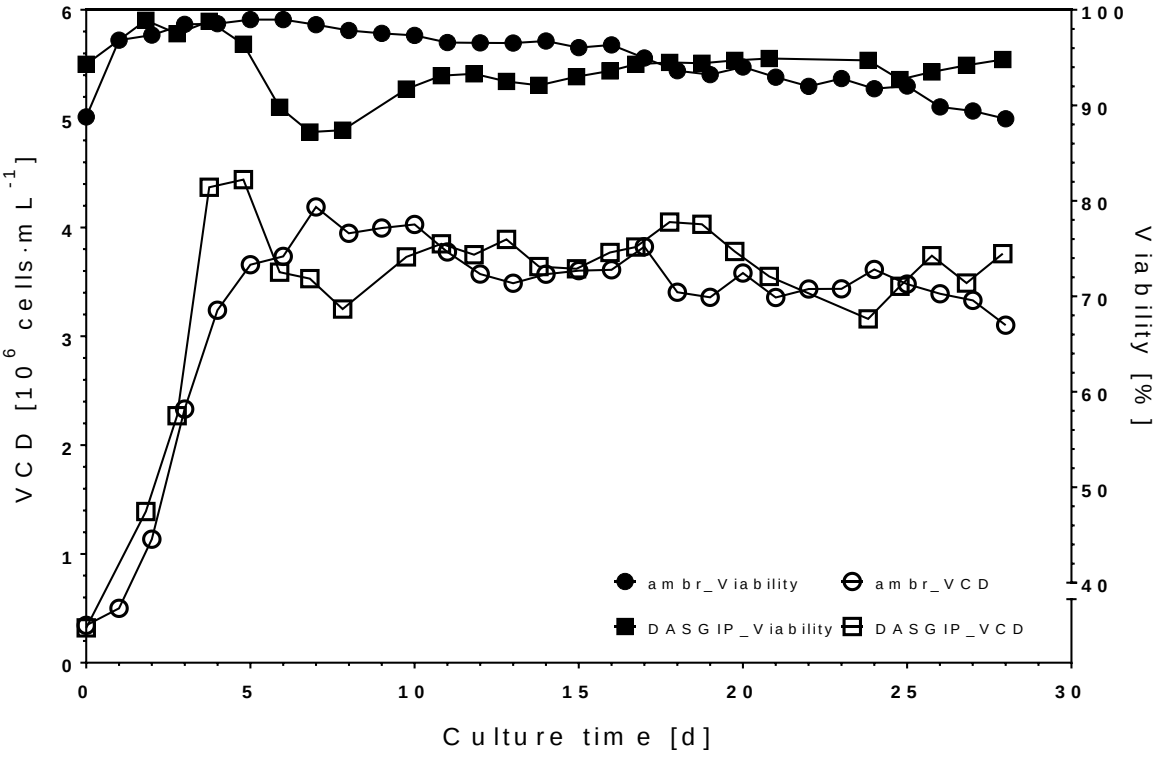

Figure 4-10: Time course of VCD and viability for ambr™ pseudo-continuous and DASGIP continuous culture both operated at D=0.25 d^{-1}. Symbols: VCD: clear; viability: filled; ambr™ data points: circles; DASGIP data points: squares.

In contrast to similar VCD and viability values, the measured AVCs were considerably different between ambr™ and DASGIP cultures. Figure 4-11 (A) depicts the time trend of AVC for all D combined of the corresponding bioreactor systems. Interestingly, the ambr™ cultures showed a significantly higher cell diameter throughout the cultivation. Both culture systems reached a stable AVC between day 14 and 24 with approximately 14.3 µm for ambr™ cultures and 13.8 µm for the DASGIP cultures. The offset between the two culture systems might originate from different aggregation rates which were also

observed (Figure 4-11 (B)). Apparently, lower aggregation rates concomitantly lead to lower measured cell sizes. Presumably, the aggregates distort the calculation of the average cell diameter since the cell sizes of aggregated cells are included in the AVC (Ronni Bertelsen, Roche, Switzerland, e-mail communication, 15.01.2015). The more unstable aggregation rate of the ambr™ system might not be reflected properly because of technical problems around day 17 which probably have affected cell related measurements. Thus, a more stable trend could be expected when no technical difficulties would occur. A lower aggregation rate is typically achieved by higher VPI. Since calculated VPI for ambr™ and DASGIP were similar, the heterogeneous distribution of VPI in the ambr™ vessel (Nienow et al., 2013) might have led to higher aggregation and thus higher recorded cell diameters.

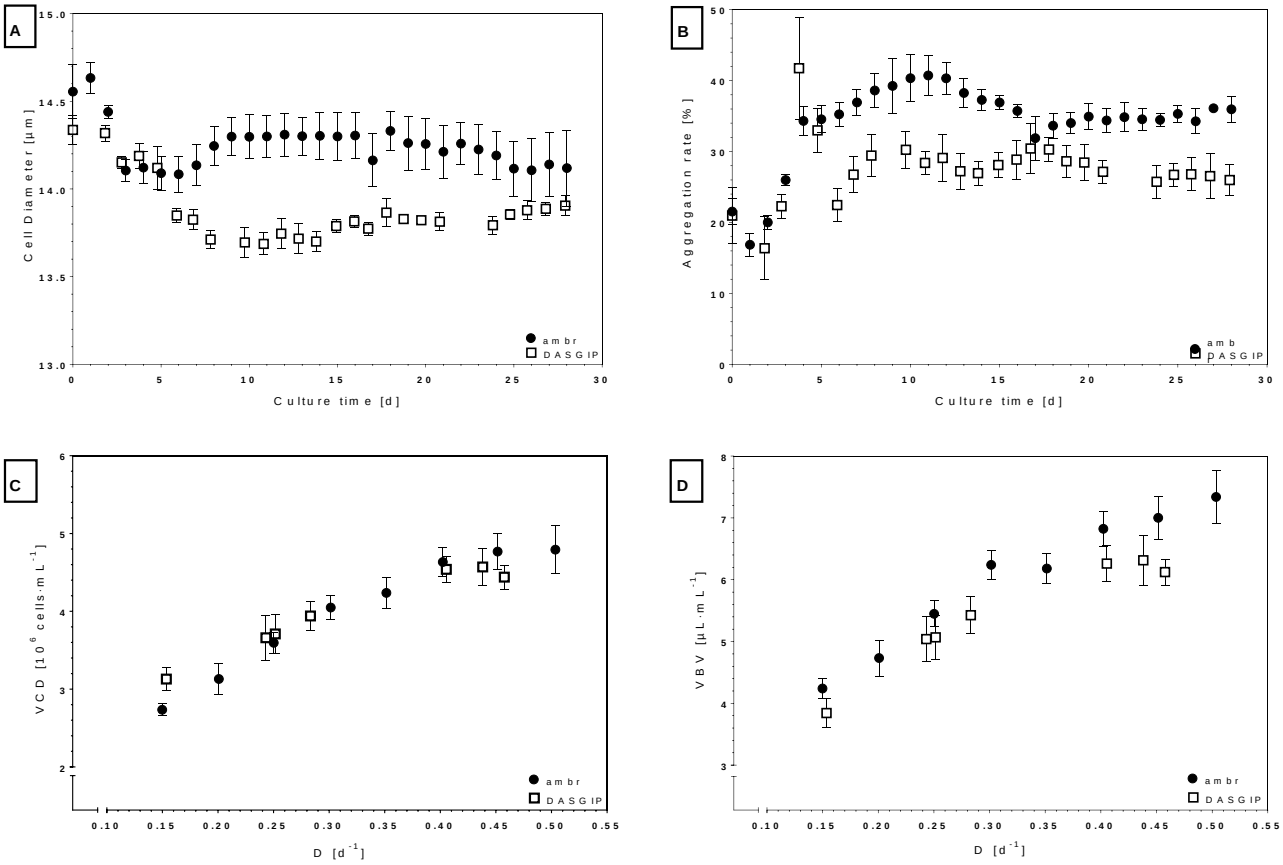

Figure 4-11: Top: Average of the AVC (A) and the aggregation rate (B) of all cultures of ambr™ (filled circles) and DASGIP cultures (open squares). The DASGIP and ambr™ cultures operated at D=0.15 d^{-1} were excluded due to the peculiar trend described in chapter 4.1.1. The error bars indicate the standard deviation calculated from all data points of the corresponding cultures (ambr™: N=7; DASGIP: N=6). Bottom: Arithmetic means of VCD (C) and VBV (D) of ambr™ pseudo-continuous cultures (filled circle) and DASGIP continuous cultures (clear squares) over dilution rate D during steady state condition. The error bars represent the standard deviation calculated from the VCD values of both cultures during steady state condition (ambr™: N=10; DASGIP: N=9).

The VCD values of the ambr™ cultures at different dilution rates showed almost the same trend as the corresponding DASGIP cultures (Figure 4-11 (C)). At lower D, the VCD measurements for the DASGIP cultures were slightly higher than the corresponding ambr™ cultures, e.g. 3.71 cells·mL^{-1} and 3.59 cells·mL^{-1}, respectively, at D=0.25 d^{-1}. In turn, the ambr™ cultures exhibited slightly higher VCD values than DASGIP cultures at higher dilution rates with 4.76 cells·mL^{-1} and 4.44 cells·mL^{-1}, respectively,

at D=0.45 d^{-1}. The achievable upper VCD limit at higher dilution rates described in chapter 4.1.1 is also observable for the ambr™ cultures. The small difference in VCD between the cultures, however, is negligible as indicated by the error bars. A 90% CI was not included due to the non-linear correlation. In terms of VCD, it can be concluded that ambr™ cultures run in pseudo-continuous mode are very well suited to reproduce data of continuous DASGIP cultures.

Yet, when it is assumed that the cell diameter was in fact lower in the DASGIP culture and was not a distorted function of the measurement system, then a lower biomass, expressed as VBV, was observable for DASGIP compared to ambr™ cultures (Figure 4-11 (B)). The trend of VBV was similar for ambr™ and DASGIP cultures up to D=0.3 d^{-1}, whereas ambr™ cultures showed slightly higher VBV. This is not surprising since almost identical VCD but lower cell diameters were measured for DASGIP cultures. At D≥0.4 d^{-1}, the ambr™ cultures showed, in contrast to DASGIP cultures, a further increase in VBV. DASGIP cultures exhibited the same behavior as in Figure 4-11 (C). When comparing two biomass measures, these different outcomes illustrate the necessity of highly accurate determination methods. Since all CPP and specific perfusion rates are calculated with a measure for biomass, it is highly important which biomass unit is chosen. However, the method of determining the VBV is erroneous due to error propagation and the utilization of AVC. Moreover, references for VBV and derived rates in literature are spare, so that for further calculation VCD was used. It illustrates, however, that the choice of biomass determination is crucial for the evaluation on basis of specific perfusion rates.

The comparison of growth rates of the two systems shows the ability of pseudo-continuous cultures to reflect continuous cultures. In Figure 4-12, the cultures' growth rates are compared as a function of CSPR.

Regarding the 90% CIM, the DASGIP cultures lay within the limits which showed that the cultures of both systems were significantly similar. The determination of the 90% CIM was not possible at CSPR=0.149 $nL \cdot cell^{-1} \cdot d^{-1}$. However, the error bars of the ambr™ cultures and the trend of the 90% CIM suggest that even the culture with this CSPR might be statistically not different from ambr™ cultures. The large standard deviation of both cultivation systems originated from the oscillatory behavior of the VCD described earlier, which affected the calculation of μ. The error bars of the ambr™ cultures were higher than the ones from the DASGIP cultures due to a technical malfunction which acted as a disturbance variable on VCD measurements and thus on μ for all ambr™ cultures. Since μ is a calculated variable, error propagation also contributed in general to high standard deviations. Nonetheless, the oscillatory behavior of VCD played a central role for the spread of μ which is indicated by the wide-ranging 90% CID.

Still, the transfer of μ as a process set-point parameter between pseudo-continuous and continuous culture and different scales resulted in a significantly similar CSPR. Thus, CSPR was proven to be a suitable scaling parameter when averaged μ is considered. However, the wide CID indicates that μ is not reproducible on a day to day basis. The different daily fluctuations of μ in ambr™ and DASGIP cultures could in turn have an effect on the cell's metabolism and the performance of the cell culture. The generation of a more stable process, and thus a stable μ, is part of process optimization which, especially for the pseudo-continuous process in the ambr™ system, still has to be thoroughly performed. Starting points for optimizing the process might be the screening of the transition phase of ambr™ cultures, which

showed differences compared to the classical continuous set-up, and an investigation of the effect of different feeding intervals on cell culture performance.

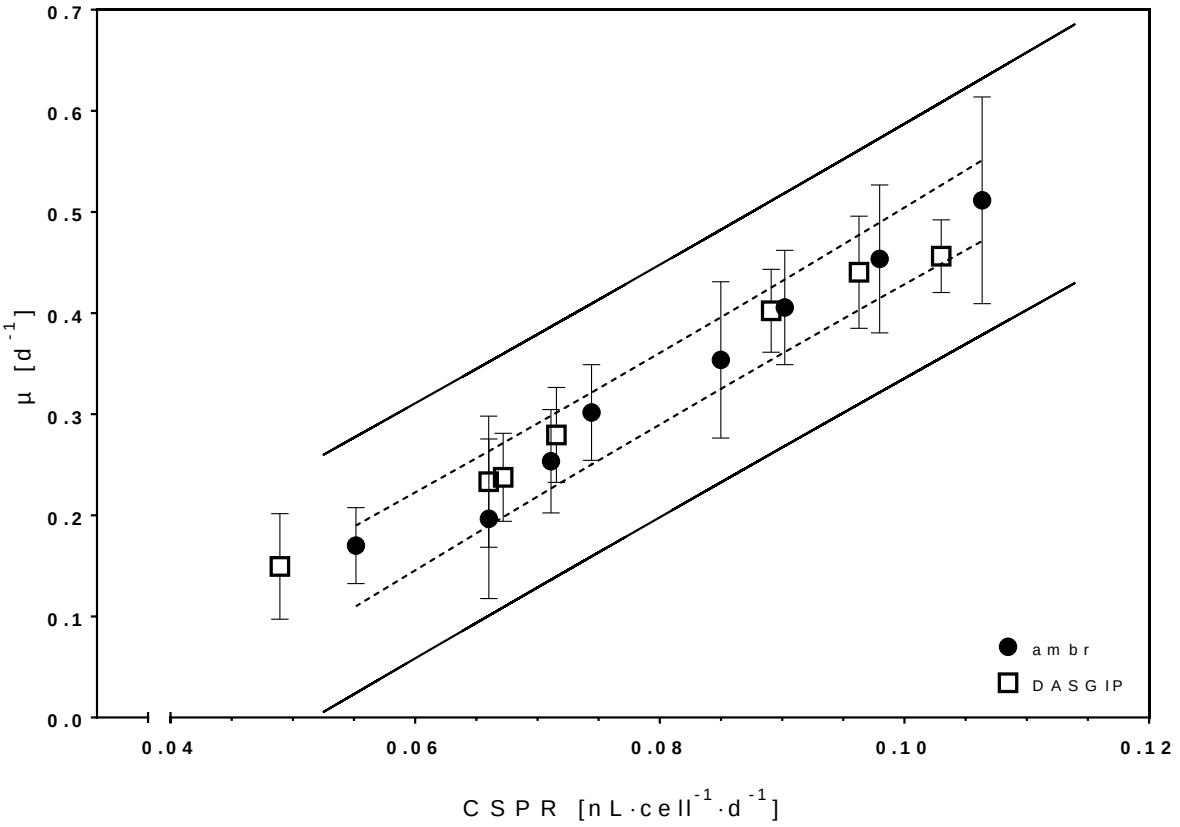

Figure 4-12: Arithmetic mean of μ of ambr™ (filled circles) and DASGIP (clear squares) cultures over CSPR. Error bars are standard deviations of μ (ambr™: N=10; DASGIP: N=9). The 90% CIM is indicated with dotted lines, the 90% CID is shown as a solid line.

In contrast to the similar steady state VCD values, the metabolism of cells cultured in pseudo-continuous mode in the ambr™ system was different compared to the cells from DASGIP continuous cultures. As mentioned in chapter 4.1.1, the ammonium measurements of the DASGIP cultures were unreliable and were excluded from the comparison. Also, the glutamate concentrations were not considered due to the very low concentrations so that no further analysis was considered based on this metabolite.

Nonetheless, a metabolic comparison based on glucose, lactate and glutamine was possible. Interestingly, the continuous cultures of the DASGIP bioreactors showed higher q_{Glc} for all the CSPR tested compared to ambr™ cultures (Figure 4-13 (A)). The same distribution was observed for q_{Lac} (Figure 4-13 (B)). The observed higher q_{Lac} of the DASGIP cultures was associated with the increased glucose consumption as described for hybridoma cells (Miller et al., 1988; Sanfeliu et al., 1997). Neither q_{Glc} nor q_{Lac} were within the 90% CIM so that the cultures were regarded as not similar. However, for q_{Glc} the slopes of the linear regression (not shown) of the ambr™ cultures and the DASGIP cultures were almost identical. The stable offset was roughly 0.5 nM·cell^{-1}·d^{-1}. This signifies that, besides the different glucose consumption and thus different metabolism at similar CSPR, targeting and transferring a specific q_{Glc} set-point with CSPR is possible. The slopes for q_{Lac} on the other hand, were not similar and showed

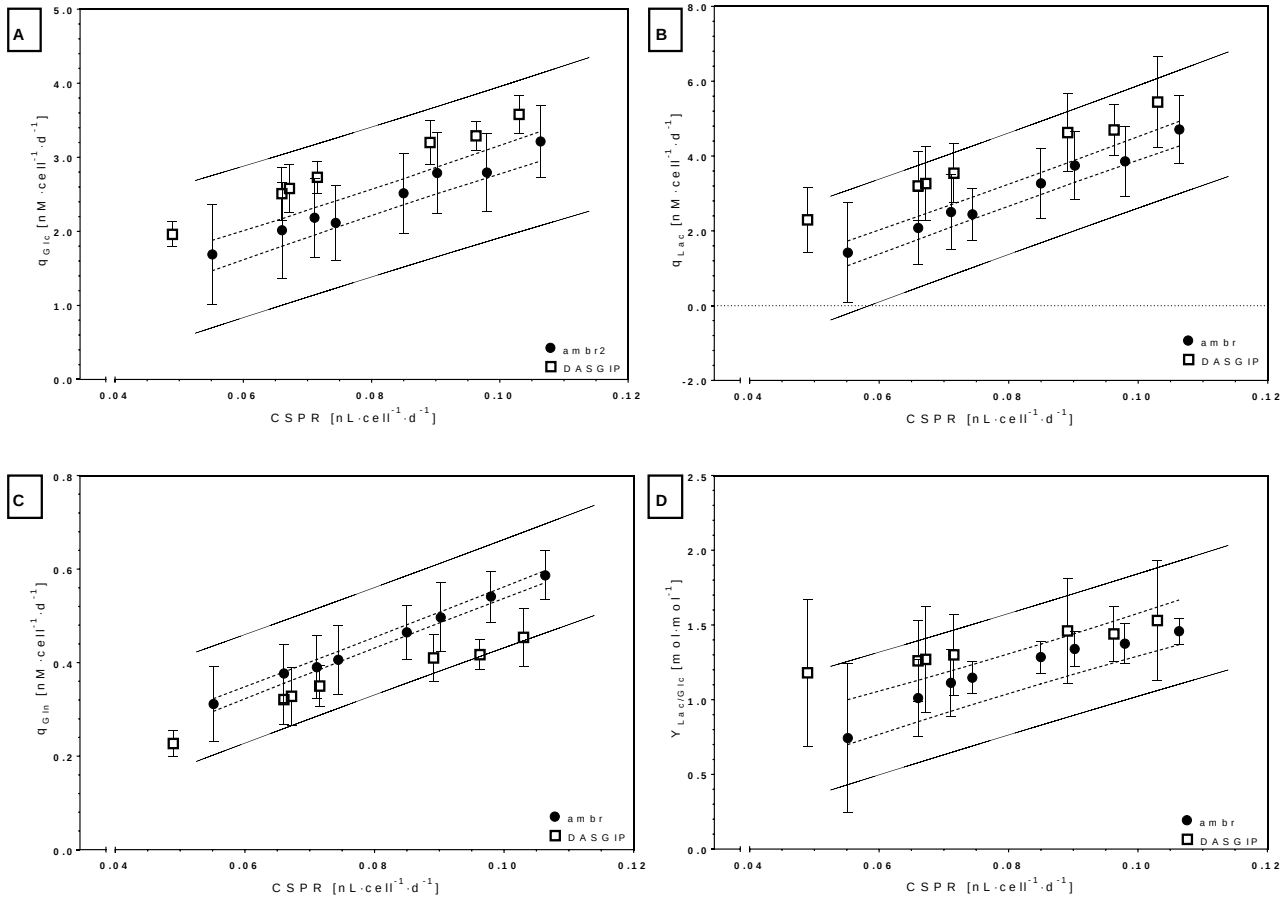

Figure 4-13: Cell specific rates and $y_{Lac/Glc}$ over CSPR for ambr^{TM} (filled circles) and DASGIP (open squares) cultures. A: q_{Glc} against CSPR. B: q_{Lac} against CSPR. C: q_{Gln} against CSPR. D: $y_{Lac/Glc}$ against CSPR. Error bars are standard deviations of μ (ambr^{TM}: N=10; DASGIP: N=9). The 90% CIM is indicated with dotted lines, the 90% CID is shown as a solid line.

that the difference in cell specific lactate production rate between the two systems decreased with increasing CSPR. Here also, the values of the continuous cultivation were not part of the 90% CIM of the pseudo-continuous cultivations. Yet, they fitted into the 90% CID. In overall, this indicates that cultures in ambr^{TM} and DASGIP bioreactors operated at high CSPR and thus high D show a more similar turnover of the main carbon source glucose. This feature also is reflected when plotting the lactate to glucose yield over CSPR (Figure 4-13 (D)). With increasing CSPR, the difference in $y_{Lac/Glc}$ was reduced until at CSPR≥0.089 nL·cell^{-1}·d^{-1} the yield was almost the same around 1.45 mol·mol^{-1}. When observing the $y_{Lac/Glc}$ curve in more detail, it can be assumed that the ambr^{TM} cultures were behaving abnormal at low CSPR, since no linear correlation could be established which actually should be expected (Henry et al., 2008). The low volume addition at low CSPR in the ambr^{TM} might have contributed to the noticeably different behavior. In earlier experiments it was observed that a substantial fraction of the reaction liquid volume evaporated during ambr^{TM} cultivations (Martin Heitmann, personal communication, 28.07.2014). This uninvestigated effect combined with the possible homogeneity issues of the ambr^{TM} bioreactors (Nienow et al., 2013) could have contributed in an integrated way. At a higher volume addition, i.e. higher CSPR, the impact of evaporation is diminished which could explain the more linear trend there.

Thus, when the data points at low CSPR are neglected, also for $y_{Lac/Glc}$ a stable offset between ambr™ and DASGIP cultures was observed.

The distinct metabolism between ambr™ and DASGIP cultures is also obvious when regarding q_{Gln} as a function of CSPR (Figure 4-13 (C)). Here also, a difference between the two culture systems is observed. The DASGIP cultures values did not fit into the 90% CIM and cultures with CSPRs≥0.089 nL·cell^{-1}·d^{-1} were very close to the lower limit of the 90% CID. The slopes of the linear regressions for both data sets are different which demonstrate the divergence between the two systems. It seems that energy generation in DASGIP cultures was shifted more to the consumption of glucose rather than glutamine compared to the cultures of the ambr™ system. The glutamine consumption rates of the DASGIP system at high CSPR do not seem to follow a linear trend. q_{Gln} of the culture with the highest CSPR was calculated from 5 data points instead of 9 which might have led to the lower value. The time point for taking a sample for subsequent analysis might also have contributed to the observed differences and resulted in non-linear trends. The samples of ambr™ cultures were taken by the automated liquid handler each day at the same time point. Here, the harvesting had to be started immediately after the last feed addition because of the tight schedule for controlling 24 cultivations in parallel. The samples of the DASGIP cultures were taken at different time points daily so that sampling after or before feed additions occurred. Consequently, different substrate, metabolite and protein concentration samples might have been taken due to dilution effects. In general, the comparison of metabolic rates showed that differences between the systems exist. A transfer based on CSPR however, is still possible since stable offsets were observed. Additional experiments concerning the sampling procedure should elucidate whether a dilution effect occurred.

The different metabolism also affected the cell specific production rate and VP when both systems are compared based on CSPR as can be seen in Figure 4-14. A general trend to higher VP at higher CSPR for both systems is visible. Yet, the VP of the DASGIP cultures at lower CSPR between 0.048 nL·cell^{-1}·d^{-1} and 0.089 nL·cell·d^{-1} were higher than corresponding cultures of the ambr™ system. At a CSPR of approximately 0.066 nL·cell^{-1}·d^{-1}, the VP of the DASGIP culture was for example 38% higher than for the culture of the ambr™ system. The 90% CIM demonstrated that 3 cultures of the DASGIP system were outside the lower or upper limit. However, as mentioned in chapter 4.1.1, the cultures at a CSPR of 0.067 nL·cell^{-1}·d^{-1} and 0.096 nL·cell·d^{-1} were believed not to depict the normal distribution. Thus, only one culture, which was believed to display a presumably correct pattern, was outside of the CIM. When the two cultures are not considered in the linear regression analysis, the slopes of the DASGIP and ambr™ cultures are almost identical (9.33 and 10.17 respectively). A definite statement was difficult due to the large error bars, which at least partially originated from noisy ELISA measurements. Nonetheless, the slightly higher VP of the DASGIP cultures correlated well with the higher glucose uptake rate previously mentioned which apparently stimulated protein synthesis. The slightly higher protein production is also reflected when comparing q_P of both systems. A similar trend can be seen, where q_P values of the DASGIP cultures were either in the same range or higher as cultures of the ambr™ systems at similar CSPR when the before mentioned cultures are not considered. Higher q_P in bench-top scale can also be derived from data reported in literature (Nienow et al., 2013). However, different scale-up parameters were used. In this work, the range of q_P for the calculated means of both systems was between 1.17 and 0.84 which, considering the noisy ELISA data, is a satisfying result. Moreover, the assumption of a non-growth associated protein production is supported.

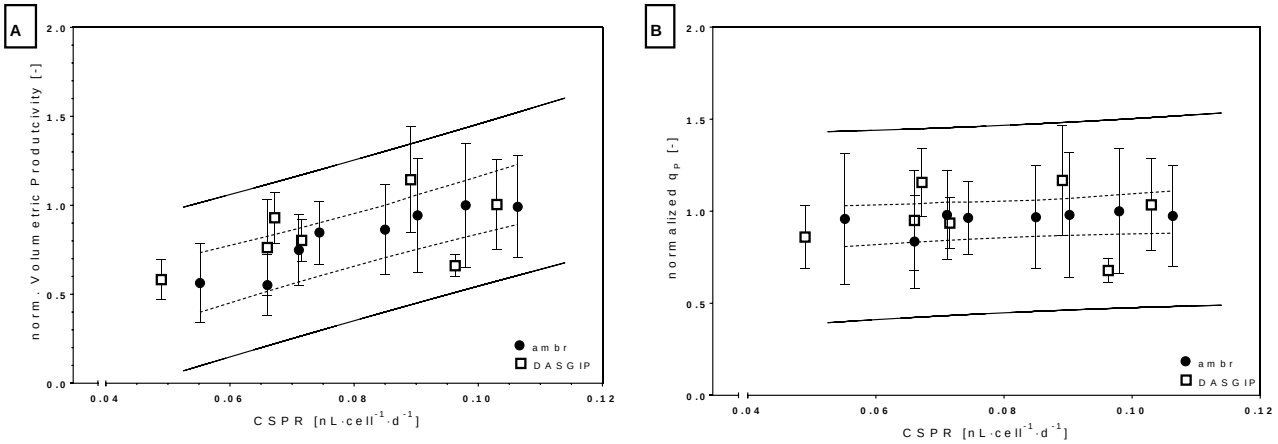

Figure 4-14: VP (A) and q_P (B) against CSPR from ambr™ (filled circles) and DASGIP (open squares) cultures. Error bars are standard deviations of µ (ambr™: N=10; DASGIP: N=9). The 90% CIM is indicated with dotted lines, the 90% CID is shown as a solid line.

As mentioned in chapter 4.1.1, an additional tool to overcome a possible distortion by imprecise VCD measurements might be the use of VBV instead to calculate specific rates. Thereby, the effect of variable cell densities on biomass measurement can be taken into account. The CSPR would then be expressed as a specific perfusion rate (SPR). When comparing VP based on SPR (see Figure 4-15 (A)), the values of the DASGIP cultures seem to correlate better to the corresponding ambr™ data compared to the VP against CSPR graph. The values for q_P on the other hand show, when plotted against SPR (Figure 4-15 (B)), more elevated values for the DASGIP cultures than compared to Figure 4-14. Slightly larger error bars are calculated which demonstrates a decline in resolving power that is mainly due to error propagation. Since no better elucidation can be expected when using VBV instead of VCD, this method

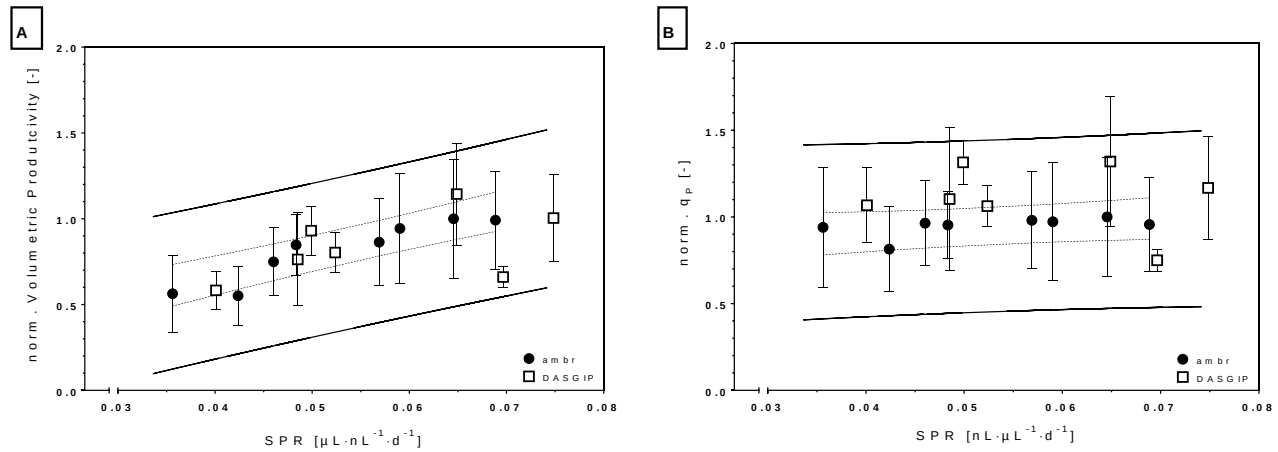

Figure 4-15: Comparison of VP and q_P of DASGIP and ambr™ cultures on basis of SPR. q_P was calculated with VBV. The same symbols were used. Error bars are standard deviations of µ (ambr™: N=10; DASGIP: N=9). The 90% CIM is indicated with dotted lines, the 90% CID is shown as a solid line.

was not further pursued. Yet, it could indicate that specific productivity in DASGIP cultures was elevated in comparison to ambr^{TM} cultures.

In conclusion, differences between ambr^{TM} pseudo-continuous cultures and DASGIP continuous cultures have been identified. Either the scale, the bioreactor system, or the process operation mode resulted in different substrate consumption and metabolite production rates which in turn affected protein synthesis. When the slopes of the linear regression analysis for each culture set were compared, it was shown that transferable and non-transferable culture parameters exist. VP, q_{Glc}, VCD, and μ seem to be directly transferable when appropriate CSPRs are chosen. For VP and q_{Glc}, an offset has to be considered when a process transfer should be performed. The transfer of q_{Gln} and q_{Lac} is a significant issue where CSPR based scaling might not be applicable. The ultimate goal should be the transfer of all CPP which was not possible with this set-up.

Thus, further analysis was necessary to elucidate the impact of process conditions on cell culture performance. As mentioned before, different factors might have influenced the outcome of this comparison. First of all, it was observed that different transition phases of ambr^{TM} and DASGIP cultures lead to different VCD and viability values in the early process stages. Although these parameters were almost identical during steady state, it could not be ruled out that the different start-phases between batch and continuous culture contributed to the observed differences in the late phase of the processes. To investigate this issue, an experiment focusing only on the cellular response in regard to the switch from batch to continuous culture was conducted. Besides the impact of continuous start phases, the effect of the different feeding schemes was explored more in detail. The continuous bleed and hourly feed of the DASGIP cultures compared to the two hour feed interval of the ambr^{TM} cultures also could have had an impact on cell culture performance. The feed every two hours led to higher bolus feeds and thus to higher initial glucose concentrations within an interval. Therefore, further experiments were conducted to explore these possible key determinants for the transfer of process conditions between pseudo-continuous and continuous processes and to explain the observed different metabolism.

4.2.2 Effect of different transition phases between batch and continuous culture on cell culture performance

Based on the comparison of DASGIP and ambr^{TM} cultures at various dilution rates, the transition phase between batch and continuous cultivation was identified as a possible impact factor which could have contributed to the observed different culture performance during steady state. In order to explore the effect of a different transition phase on the outcome of cell cultures, a DoE-like design study using the ambr^{TM} bioreactor system was conducted. Since the cellular response on different conditions during the transition phase was investigated, the chosen bioreactor system and operation mode was presumably trivial for the experiment. Therefore, the ambr^{TM} system was used due to its simpler set-up.

After a 72 hour initial batch phase, the bioreactor cultures were operated in pseudo-continuous mode. The usual procedure of starting the pseudo-continuous cultivation (as described in 3.2.1) was modified for one group of the cultures. These cultures were operated at D=0.5 d^{-1} for the first day after the batch

phase. Then, the dilution rate was lowered every day with $\Delta D=0.1\ d^{-1}$ until the intended set-point, D_{set}, was reached. For cultures with an odd-numbered D, ΔD was $0.05 d^{-1}$ at the last day of reduction. The purpose of this process strategy was to adapt the initially high growth rates after the batch phase by incrementally reducing the dilution rate to the actual process set-point. The aim was to generate a smooth transition where μ would match D more closely than in non-adapted cultures. As a result, the oscillatory behavior of VCD was expected to be less pronounced during the transition phase compared to

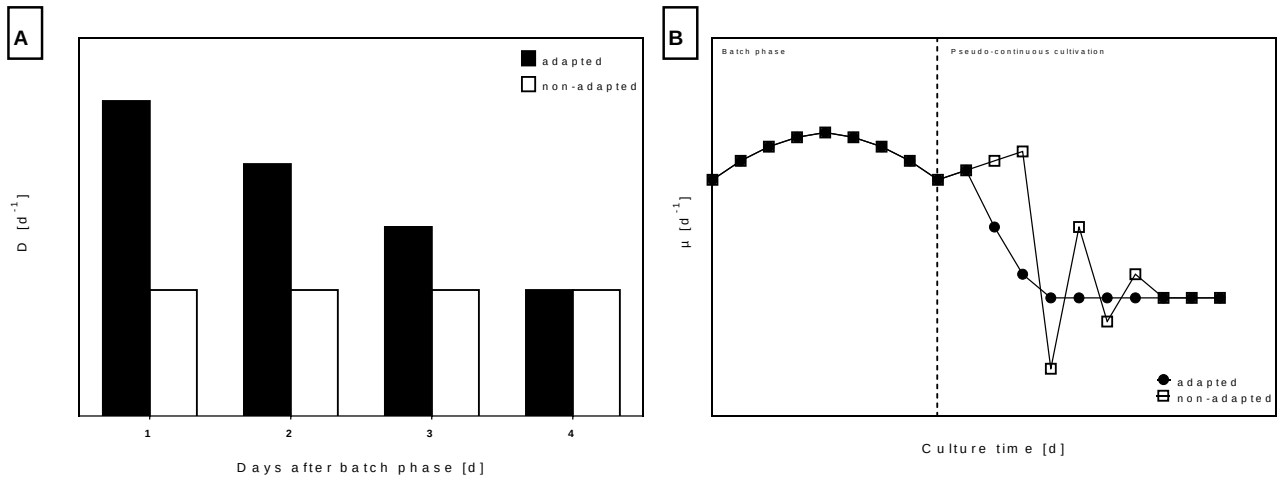

Figure 4-16: A: Strategy for the adaptation of pseudo-continuous cultures. D is lowered step-wise daily after the batch phase for adapted cultures (filled columns) until the desired set-point is reached. For non-adapted cultures (clear columns), D is kept constant. B: Simulated growth data of the assumed time course of μ for adapted (filled circles) and non-adapted cultures (open squares). The dotted line separates batch and continuous phase.

non-adapted cultures. Thus, any difference in the outcome of the cell cultures could be ascribed to this distinct process operation. Ultimately, conclusions could be drawn whether the different conditions during the transition phase between ambr™ and DASGIP cultures of chapter 4.2.1 had had a major impact on the observed distinct culture performance. For both culture groups, the same range of final D_{set} was assigned. The control group was operated as usual where D_{set} was set from the start. All other process parameters were maintained. In Figure 4-16, an illustration of the process strategy for the dilution rate adapted processes is shown.

The VCD during the transition phase was, as expected, quite divergent between adapted and non-adapted cultures. At high dilution rates, the difference between cultures was reduced since here the adaptation phase was shortened. However, the desired lower oscillatory behavior of the adapted cultures was not observed. On the contrary, the adaptation process led to higher VCD peaks and a subsequent decrease until the VCD was in steady state. The non-adapted cultures showed a much smoother transition to the steady state VCD. In Figure 4-17, two exemplary cultures (at $D=0.25\ d^{-1}$) are shown. Immediately after the switch to continuous cultivation mode, both cultures showed almost identical VCD values until day 5. However, the trends are highly different. The non-adapted culture showed a saturation-like time course until day 6 whereas the adapted culture ($D_{adapt}=0.3\ d^{-1}$ at day 6) demonstrated an almost exponential increase in VCD. The former then displayed the already described oscillatory behavior. The VCD of the adapted culture, on the other hand, increased further up to day 7 ($D=0.25\ d^{-1}$) and then declined almost linearly before at day 10 steady state was reached. Stable VCD

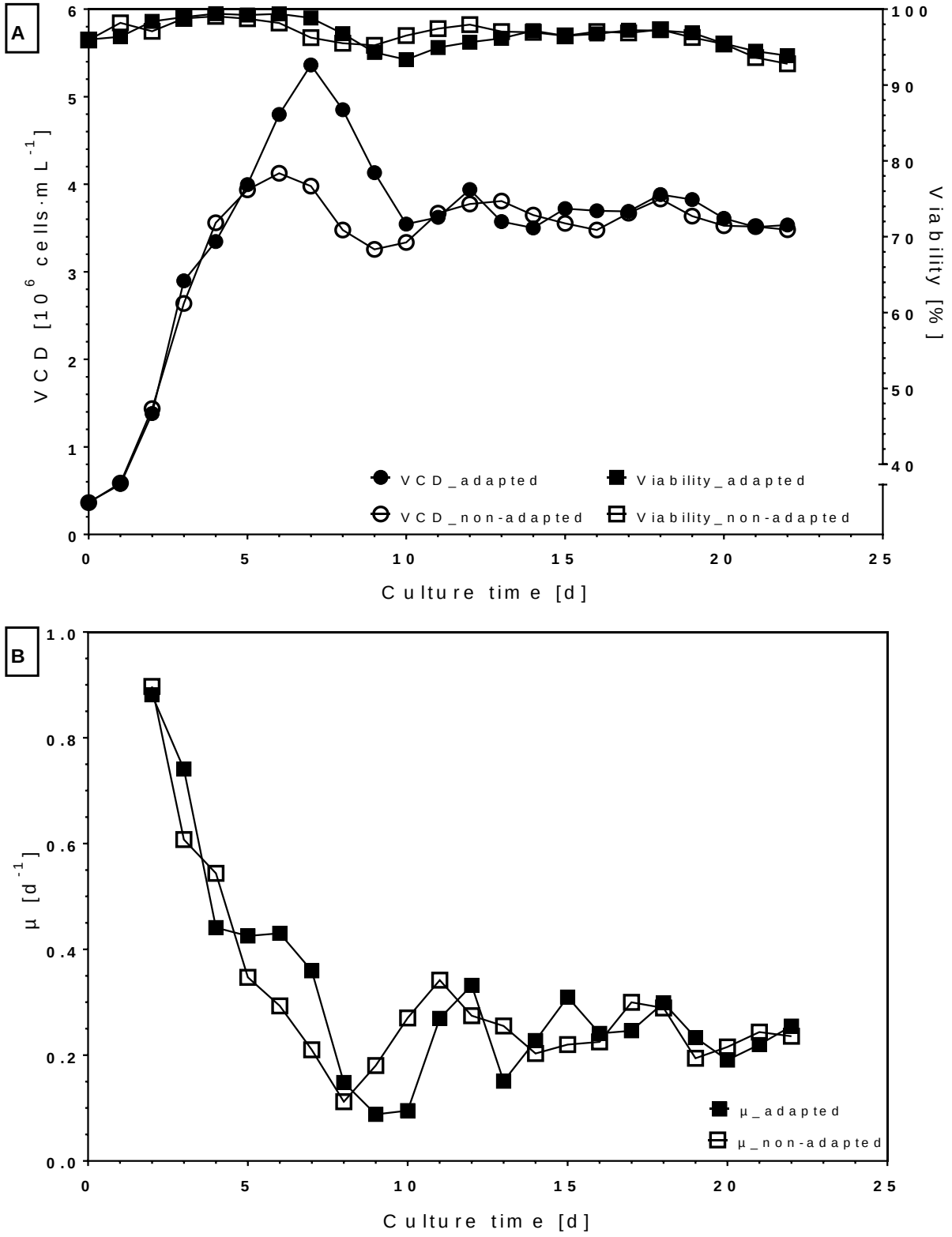

Figure 4-17: A: Time course of VCD (circles) and viability (squares) over time of adapted (filled symbols) and non-adapted (clear symbols) cultures. B: Time course of μ of adapted (filled squares) and non-adapted cultures (clear squares). Cultures were operated at D=0.25 d^{-1}.

conditions were reached by the two cultures simultaneously. The adapted culture showed a very abrupt transition from rapidly declining VCD to stable values. The peak in VCD was not surprising since the higher D in the beginning allowed for a higher μ. Yet, the magnitude and duration of this elevated VCD was unexpected. Apparently, the high μ was maintained at a constant value until day 6. Here, a μ of 0.43 d^{-1} was calculated at a prevailing D=0.3 d^{-1}. The characteristics of μ bore resemblance to the observed μ in chapter 4.2.1 of the DASGIP cultures and the following different adaptation to D_{set} compared to the ambr™ cultures of the same chapter. The trend of μ indicates that the adapted cultures were not readjusting in the same speed as the incremental decrease. After a small decrease in μ at day 7, the growth rate decreased to 0.1 d^{-1} until day 10 and showed an oscillation around the μ of the non-adapted cultures thereafter. After day 15, the growth rate of the adapted culture exhibited a comparable behavior to the μ from the non-adapted cultures. Thus, after day 7 the bigger offset between set μ (via D) and actual μ led to a sudden decrease in μ and VCD. Similar characteristics were displayed at other dilution rates. Both groups eventually reached the same steady state values which is congruent with the cultures used for the comparison in 4.2.1. Although the primary goal, namely a smoother transition, was not accomplished, the different shifts from batch to continuous culture can be useful to verify or contradict their impact on cell culture performance in general. In addition, the adapted cultures showed a comparable trend during the transition phase as DASGIP continuous cultures in chapter 4.2.1.

The overview of steady state VCD at different D revealed no direct impact of the transition phase on VCD (Figure 4-18 (A)). Both cultures showed the previously observed plateau at high D and a linear correlation between D=0.15 d^{-1} and D=0.35 d^{-1}. This is in accordance with chapter 4.2.1. Consequently, the achieved growth rates, when compared by the corresponding CSPR of the cultures (Figure 4-18 (B)), showed no deviation between adapted and non-adapted cultures. The 90% CIM of μ of the non-adapted cultures comprised almost all of the growth rates of the adapted cultures. Only the adapted culture at CSPR=0.103 nL·cell·d^{-1} was slightly outside the CIM. However, the non-similarity of this culture might have originated from measurement inaccuracies as indicated by the large error bars. Thus, the μ values during steady state were regarded as identical for the two culture groups.

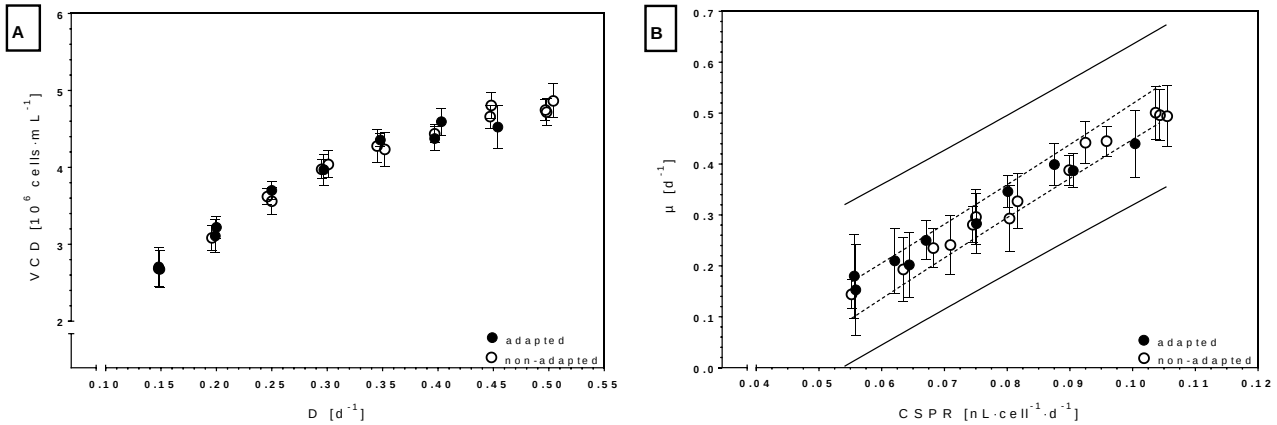

Figure 4-18: A: Steady state VCD arithmetic mean values against D for adapted (filled circles) and non-adapted (clear circles). Error bars show standard deviations (N=7). B: Steady state arithmetic mean μ values against CSPR. The dashed lines show the 90% CIM, the solid lines show the 90% CID of non-adapted cultures. The symbols and the error bars indicate the same as in (A).

Similar observations were made when metabolic rates were compared (Figure 4-19). The cell specific glucose consumption rate and specific lactate production rate showed almost no difference between adapted and non-adapted cultures at corresponding CSPR. The 90% CIM included all of the mean values so that both culture groups were regarded as similar. This is supported by the slopes of the linear regression analysis. Here, the slopes of q_{Glc} and q_{Lac} were in very close proximity with 26.5 (q_{Glc} non-adapted) and 25.6 (q_{Glc} adapted), respectively, and 56.7 (q_{Lac} non-adapted) and 59.2 (q_{Lac} adapted), respectively. Although the q_{Gln} data points of the adapted cultures were not fully included in the 90% CIM of the non-adapted cultures and the slopes of the linear regression indicate a difference between adapted and non-adapted cultures, a conclusive determination was difficult. Adapted cultures at CSPR≤0.067 $nL \cdot cell^{-1} \cdot d^{-1}$ showed slightly elevated q_{Gln} compared to non-adapted cultures. Consequently, it could be assumed that cultures, which experienced a longer adaption phase and thus more distinct μ values during the transition to continuous cultivation, exhibited a different metabolism. However, the large error bars for both cultures and the very narrow 90% CIM put the displayed differences into perspective which therefore could also derive from inaccurate measurements. Additionally, the cell specific glutamine consumption rate was different from the ambr™ cultures in 4.2.1. However, the similar slope of the linear regression analysis of the non-adapted control culture and the 1st ambr™ experiment (chapter 4.2.1, data not shown) implies a systematic error caused by the measurement system. Due to the long time between experiments, different reagent batches for metabolite analysis were used which could explain the observed offset. Regarding the cell specific rate of ammonium, which is mainly produced during glutaminolysis, the assumption of possible differences in the glutamine metabolism between adapted and non-adapted cultures is partially supported. Also here, elevated q_{Amm} could be observed at low CSPR. Nonetheless, the same large error bars and narrow 90% CIM at least showed that the differences were marginal. Similar to q_{Gln}, q_{Amm} was lower than in the 1st ambr™ cultivation but showed the same trend. The question whether this originated from a bias of the measurement system or by other unidentified causes could not be answered. The trends of the two rates however, suggest that no significant metabolic change occurred. Even the cell specific glutamate rate, which was beforehand considered to be non-reliable due to the strongly fluctuating raw data, showed a similar distribution for both culture groups. The slopes of the linear regression were almost identical (-972 for non-adapted and -976 for adapted cultures). Conclusively, the metabolic analysis revealed no significant difference between the culture groups.

In this context, congruent metabolic rates were also observed to some extent during the comparison of DASGIP and ambr™ cultures. There however, VP and q_P showed a slightly different behavior when compared based on CSPR.

The trend of VP of adapted and non-adapted cultures displayed in both cases the already described trend of higher VP at higher CSPR (Figure 4-20 (A)). For lower CSPR values and thus cultures which were impacted the most by the adjusted transition phase, a slightly lower VP for adapted cultures was observed. Yet, at higher CSPR and thus almost the same transition phase, the VP of adapted cultures was

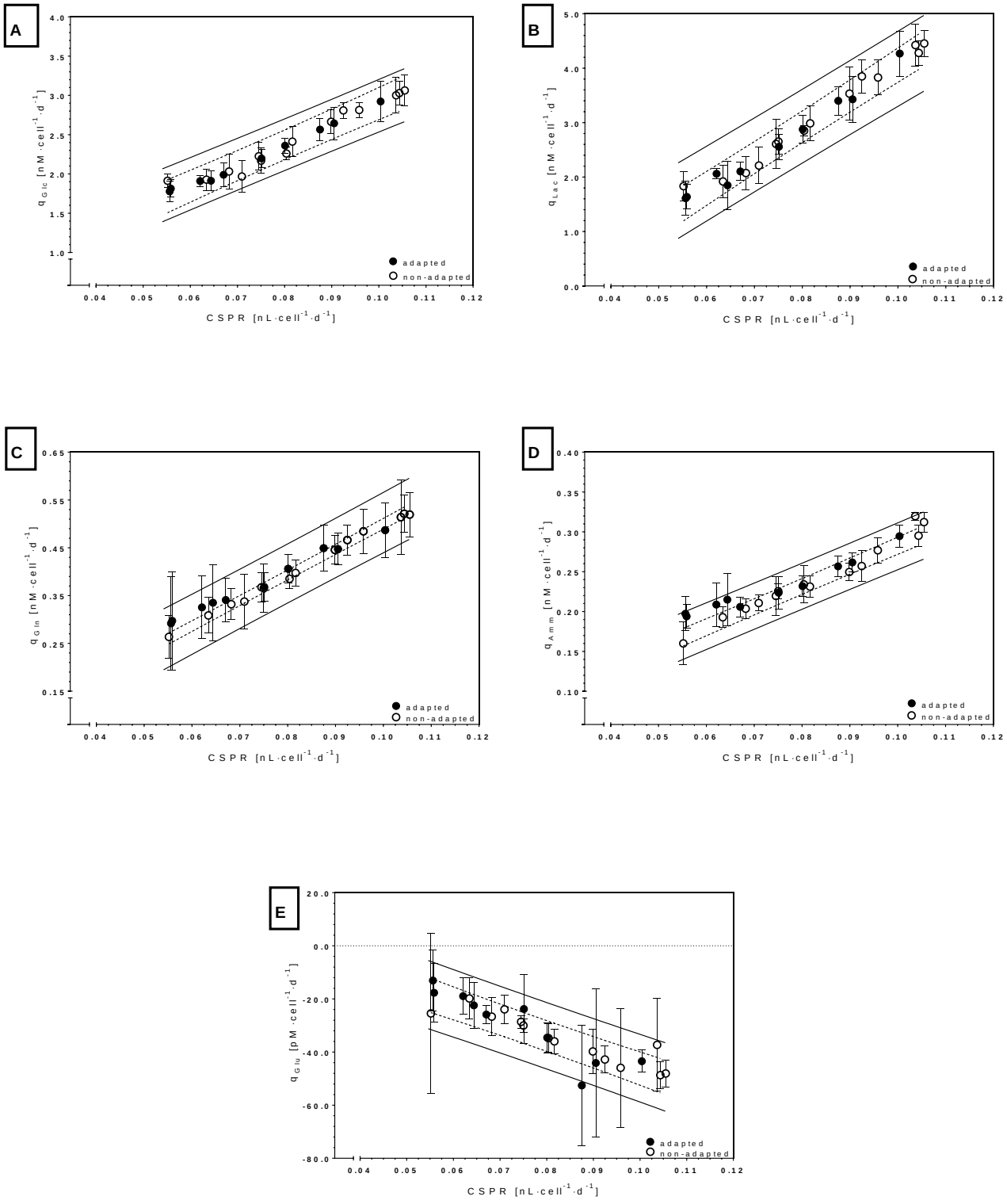

Figure 4-19: Metabolic rates against CSPR for adapted (filled circles) and non-adapted cultures (clear circles). A: q_{Glc}; B: q_{Lac}; C: q_{Gln}; D: q_{Amm}; E q_{Glu}. Error bars show standard deviations (N=7). The dashed lines show the 90% CIM, the solid lines show the 90% CID of non-adapted cultures.

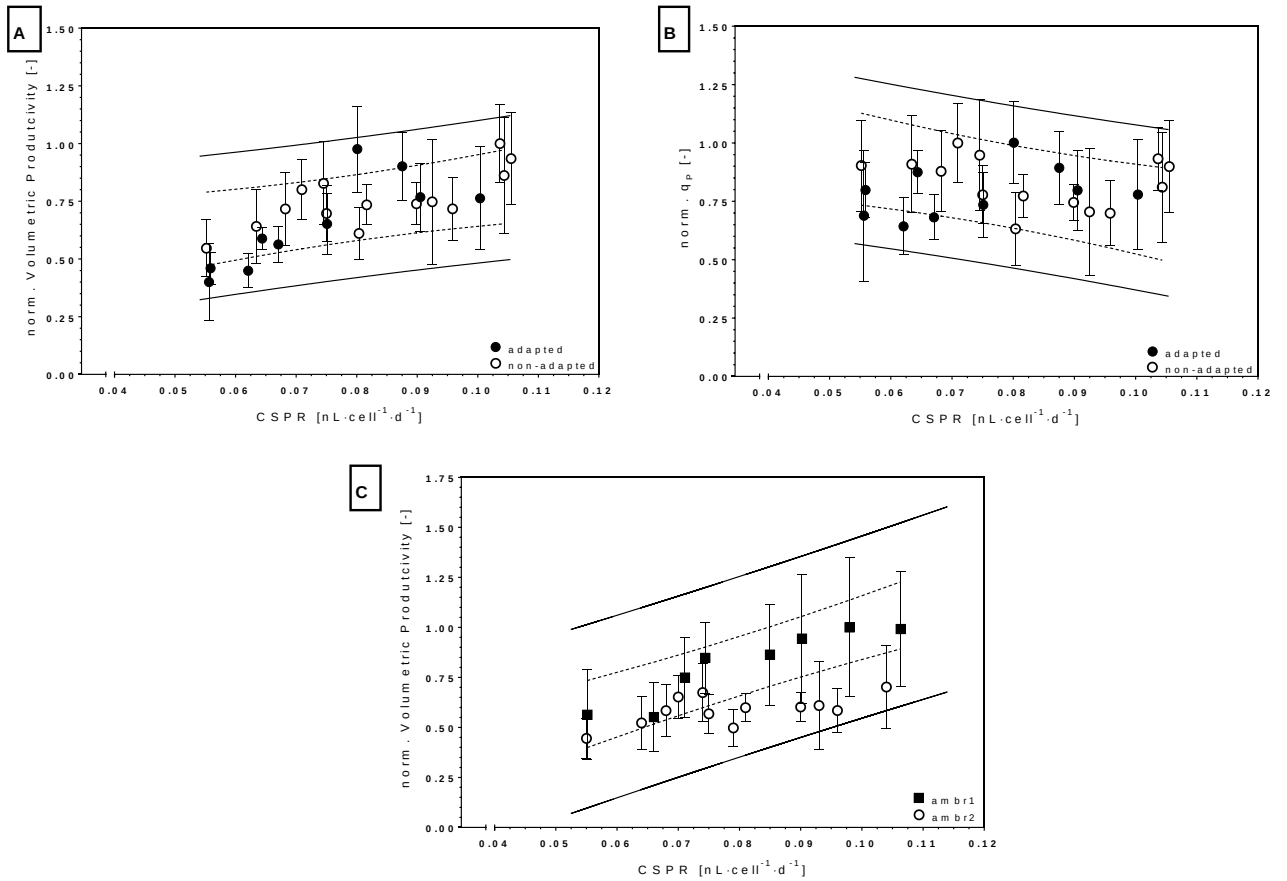

Figure 4-20: A: Normalized VP against CSPR of adapted (filled circles) and non-adapted cultures (clear circles). B: Normalized q_P against CSPR of adapted (filled circles) and non-adapted cultures (clear circles). Error bars show standard deviations (N=7). The dashed lines show the 90% CIM, the solid lines show the 90% CID of non-adapted cultures. C: Normalized VP against CSPR of non-adapted cultures from the first (chapter 4.2.1) (filled squares) and the non-adapted (clear circles) ambr™ experiment. Error bars are standard deviations of VP (1st ambr™: N=7; 2nd ambr™: N=7). The 90% CIM calculated from the 1st ambr™ experiment is indicated with dotted lines, the 90% CID is shown as a solid line.

higher than the non-adapted cultures at corresponding CSPR. Most of the data points were included in the 90% CIM, whereas all lay within the 90% CID. The fluctuations within the non-adapted culture group showed the unsteady VP measurements over CSPR, so that no significant difference based on this data set could be concluded. On the other hand, the VP data of the non-adapted ambr™ control culture did not reflect the distribution observed during the 1st ambr™ cultivation of chapter 4.2.1 (Figure 4-20 (C)). The large error bars of this experiment, the experiment in 4.2.1, as well as various reports of the highly reproducibility of ambr™ cultivations including recombinant protein related data, indicate that rather the reproducibility of the ELISA results was an issue. The samples for ELISA measurements had been diluted 10-fold for subsequent analysis. The slope of the sigmoidal calibration curve in the expected concentration range was very shallow so that fluctuations were likely.

Also, the CSPR based comparison of q_P (Figure 4-20 (B)) showed a similar distribution for adapted and non-adapted cultures. Again, a non-growth associated protein production could be observed, whereas adapted cultures showed lower q_P at low CSPR and higher q_P at high CSPR compared to non-adapted

cultures. Hence, the adapted cultures, which were comparable to DASGIP cultures in terms of higher μ during the transition phase, did show that no major influence of different transitions phases on VP or q_p can be expected.

In conclusion, VP and q_P showed variations between adapted and non-adapted cultures. The differences could not be attributed to the distinct transition phases but could have been impacted by the analysis method. Substrate consumption rates, metabolite production rates and recombinant protein related data showed only minor disparities between adapted and non-adapted cultures which also could have originated from measurement inaccuracy. The assumption that no metabolic shift was initiated is supported by acceleratostat experiments, i.e. a continuous culture where the dilution rate is changed gradually at a constant acceleration. Thereby, μ is adapted to the changing environment faster than in conventional chemostat experiments. Comparison to classical continuous culture, where the dilution rate was changed incrementally, showed that the same glucose consumption and lactate consumption rates were achieved (Bjerre-Nielsen et al., 2007). Thus, no different metabolism between adapted and non-adapted cultures was assumed which in turn suggested that the differences between DASGIP and ambr™ cultures were not affected by the different transition phases.

4.2.3 Effect of the feeding strategy on cell culture performance

Besides the different transition phases during the switch between batch and continuous or pseudo-continuous cultivation, the different feeding strategy was regarded as a possible impact factor that could have influenced the outcome of the DASGIP and ambr™ cultures. In a simulated approximation of continuous culture by semi-continuous culture, Westgate and Emery (1989) proposed that differences between continuous and semi-continuous cultures originated from feed concentration, replacement rate and time between replacements. The definition of a semi-continuous process in this paper was different from the pseudo-continuous process applied in the ambr™ system. There, a fixed volume of cell culture is replaced with an equal volume of fresh medium at fixed times. Nonetheless, some considerations of their model for the approximation of continuous culture can also be transferred to the pseudo-continuous cultures of this work. Technically, pseudo-continuous culture consists of a series of short repeated batch fermentations where a new batch is started after substrate is fed via a fixed inflow of fresh medium. The cultivation period between feeding intervals could be considered as a batch operation. During these feeding intervals, the cells convert substrates into cell mass, recombinant protein and metabolites. Thus, varying the feeding interval could result in different final substrate concentrations due to concentration dependent consumption (Miller et al., 1989). Small interval lengths between replacements were found to mimic continuous cultures (Westgate and Emery, 1989). Regarding the experiments of this project and the proposed impact factors for approximation of continuous cultures, the feed concentration was identical for both culture systems. The replacement rate (similar to D) was also tested in the same range.

Thus, most interesting for this project was to study the effect of the time between replacements reported in literature, which is identical to the feeding interval as introduced in 3.2.1. In the DASGIP cultures an hourly feed was used, whereas for ambr™ cultures a feed every second hour had been implemented. This difference might have contributed to the observed deviations. Simultaneously to the ambr™ cultures that were compared to the DASGIP cultures in chapter 4.2.1, 16 cultivations including

two groups with different feeding intervals were run to study this effect. Since the culture supplied with fresh medium every second hour was compared to the DASGIP cultures, this group was regarded as a reference and the 90% CIM and 90% CID were calculated for these cultures.

In Table 4-4, an overview of the process conditions of the corresponding feeding interval groups is shown.

Table 4-4: Outline of the planned experiments for the study of the effect of feeding intervals.

Culture group	Feeding interval	Number of cultures	Dilution rate range (Δ=0.05 d^{-1})
1	Every hour	8	0.15 d^{-1} – 0.5 d^{-1}
2	Every 2nd hour	8	0.15 d^{-1} – 0.5 d^{-1}
3	Every 4th hour	8	0.15 d^{-1} – 0.5 d^{-1}

Culture group 1 was supplied with medium every hour, group 2 every 2nd hour, and group 3 every 4th hour. The time between volume reductions was maintained at 24 hours. Agitation, pH, and temperature set-points were as described in chapter 2.6. Culture group 2 is identical to the ambr^{TM} cultures used for the comparison in chapter 4.2.1. During the experiment it was noticed that culture group 1 was not pH controlled due to the internal programming of the liquid handler of the ambr^{TM} system where base addition is only possible if the concerning bioreactors are not accessed by the LH within 30 minutes. Because of the high feeding frequency, this criterion could not be met. Thus, the pH of group 1 was maintained only by the addition of fresh medium at around 6.96±0.06 and was approximately 0.1 pH units below the controlled cultures.

The comparison of VCD based on the D set-points (Figure 4-21 (A)) demonstrates distinct characteristics between the pH-controlled (group 2 and group 3) and non-controlled cultures (group 1). The VCD of group 1 was elevated for all D tested, whereas group 2 and group 3 showed only minor variations. The saturation-like trend was similar for all culture groups. Hence, based on the similarities of VCD data of culture group 2 and group 3, the difference between the latter and culture group 1 was rather assigned to the influence of lower pH on cell density than the effect of different feeding intervals. Cells of culture group 1 were smaller than cells of the pH-controlled cultures which affected the VCD measurement as already mentioned in chapter 4.2.1. Here, the aggregation rate for all cultures was similar, so that the computation of the average cell diameter was not affected by this parameter. Figure 4-21 (C) and (D) display the average cell diameter and aggregation rate of the different culture groups. Due to the smaller AVC, an assessment of the biomass was conducted. When plotting biomass as VBV against D the differences between the groups are diminished (Figure 4-21 (B)). Thus, further investigation whether possible differences were also observed for VBV based calculated rates was necessary. Due to the slightly

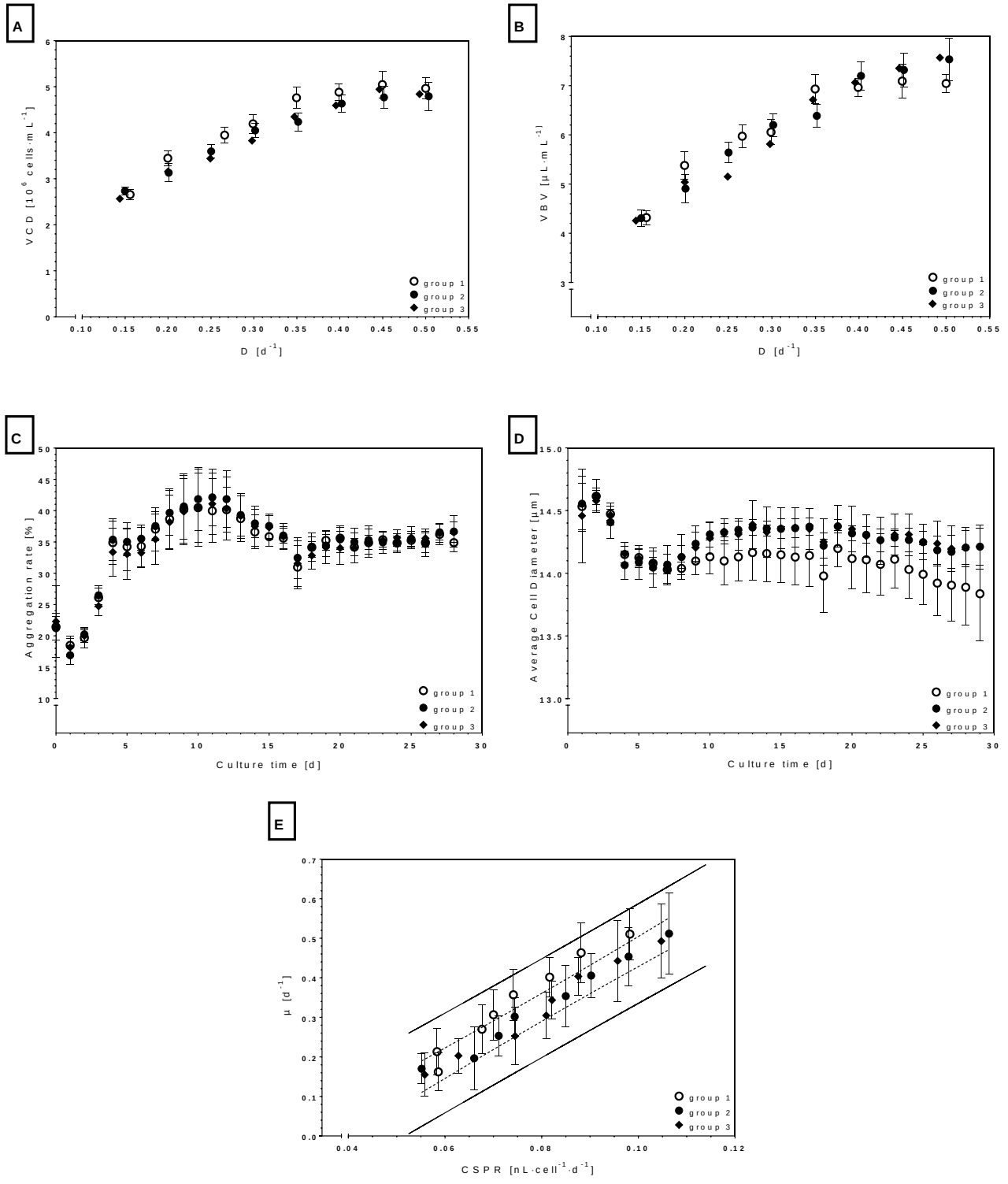

Figure 4-21: A: Averaged steady state VCD against D for different feed intervals. B: Averaged steady state VBV against D for different feed intervals. C: Averaged aggregation rates of all cultures of each group. D: Mean of average cell diameter of all cultures of each group. E: Averaged steady state µ state against CSPR for different feed intervals. Symbols: culture group 1=clear circles, culture group 2=filled circles, culture group 3=filled diamonds. For (A), (B), and (E) the error bars show standard deviations (N=10). Dashed lines in (E) symbolize the 90% CIM, straight lines the 90% CID of group 2. Error bars in (C) and (D) are standard deviations of all discrete values within the culture groups (N=8).

elevated VCD of culture group 1, higher growth rates were calculated in comparison to group 2 and group 3 at corresponding CSPR. At CSPR≥0.070 nL·cell^{-1}·d^{-1}, the μ values of group 1 were outside the 90% CIM of group 2. Culture group 2 and group 3 demonstrated a very similar trend of μ which supports the assumption that not different feeding intervals but pH influenced cell culture parameters.

pH is widely described as an important culture parameter that affects metabolism and productivity of mammalian cells (Miller et al., 1988; McDowell and Papoutsakis, 1998; Trummer et al., 2006b). The examination of the cell specific metabolic rates supported the assumption that the observed disparities derived from the lower culture pH. Although the rates and CSPR were calculated with VCD values, a substantial heterogeneity is visible in Figure 4-22. The cell specific rates for glucose consumption and lactate production showed different characteristics for all calculated CSPR. Since the VCD measurements (Figure 4-21 (A)) showed a stable offset, the different characteristics were not impacted by the definition of biomass (i.e. VCD or VBV). Consequently, differences were also observed for VBV based calculated specific metabolic rates (e.g. q_{GLc}: Appendix 2). The cell specific glucose consumption rate (Figure 4-22 (A)) of group 1 was considerably lower than q_{Glc} for group 2 and group 3, which is consistent with literature where lower culture pH has been reported to lower the glucose consumption of CHO cells (Trummer et al., 2006a). The data points of the two pH-controlled groups were considered not to be significantly different because group 3 was fitting in the 90% CIM of group 2. The difference between group 1 and the other two groups was greater at higher CSPR where group 1 did not fit within the 90% CID. This diverging trend might be attributed to the slightly lower pH values that were measured at higher CSPR for group 1 (not shown). The lower glucose consumption of group 1 is reflected by the lower lactate production specified by q_{Lac} against CSPR (Figure 4-22 (B)). Here also, group 2 and group 3 showed a similar distribution and similar values. Data points of group 3 were within the 90% CIM and thus were considered not significantly different. Interestingly, group 1 also showed a lower lactate to glucose yield (Figure 4-22 (C)) which was, however, showing the same trend as the yields of group 2 and group 3. When the similarity of group 2 and group 3 is taken into account, an effect of the feeding interval on the hitherto analyzed culture parameters were unlikely.

The consumption of glutamine was very similar for all culture groups. However, marginally higher q_{Gln} (Figure 4-22 (D)) were calculated for group 1 and group 3 whose data points resided at the upper 90% CIM limit. The higher q_{Gln} also affected q_{Amm} (Figure 4-22 (E)) which was also higher for group 1. Thus, the more efficient glucose metabolism was accompanied by a more inefficient utilization of glutamine. This is also displayed in the higher ammonium to glutamine yield (Figure 4-22 (F)). The comparison of the VBV based q_{Gln} against SPR, however, did not support the assumption of elevated q_{Gln} for group 1. On the other hand VBV based q_{Amm} was also higher for group 1 (see Appendix 3). Yet, also group 3 showed different VCD based q_{Amm}. Considering the similar metabolic rates and the significant error bars, the q_{Amm} data had to be critically questioned.

The different metabolism of pH-controlled and non-controlled cultures was also reflected in the course of VP and q_P against CSPR (Figure 4-23). Culture group 2 and group 3 exhibited similar VP values for the CSPR range tested. Only the data point at CSPR=0.082 nL·cell·d^{-1} of group 3 was outside the 90% CIM. Thus, it was concluded that an extension of the feeding interval from 2 to 4 hours did not influence the productivity. Culture group 1 on the other hand, showed either similar values as group 2 and group 3 or

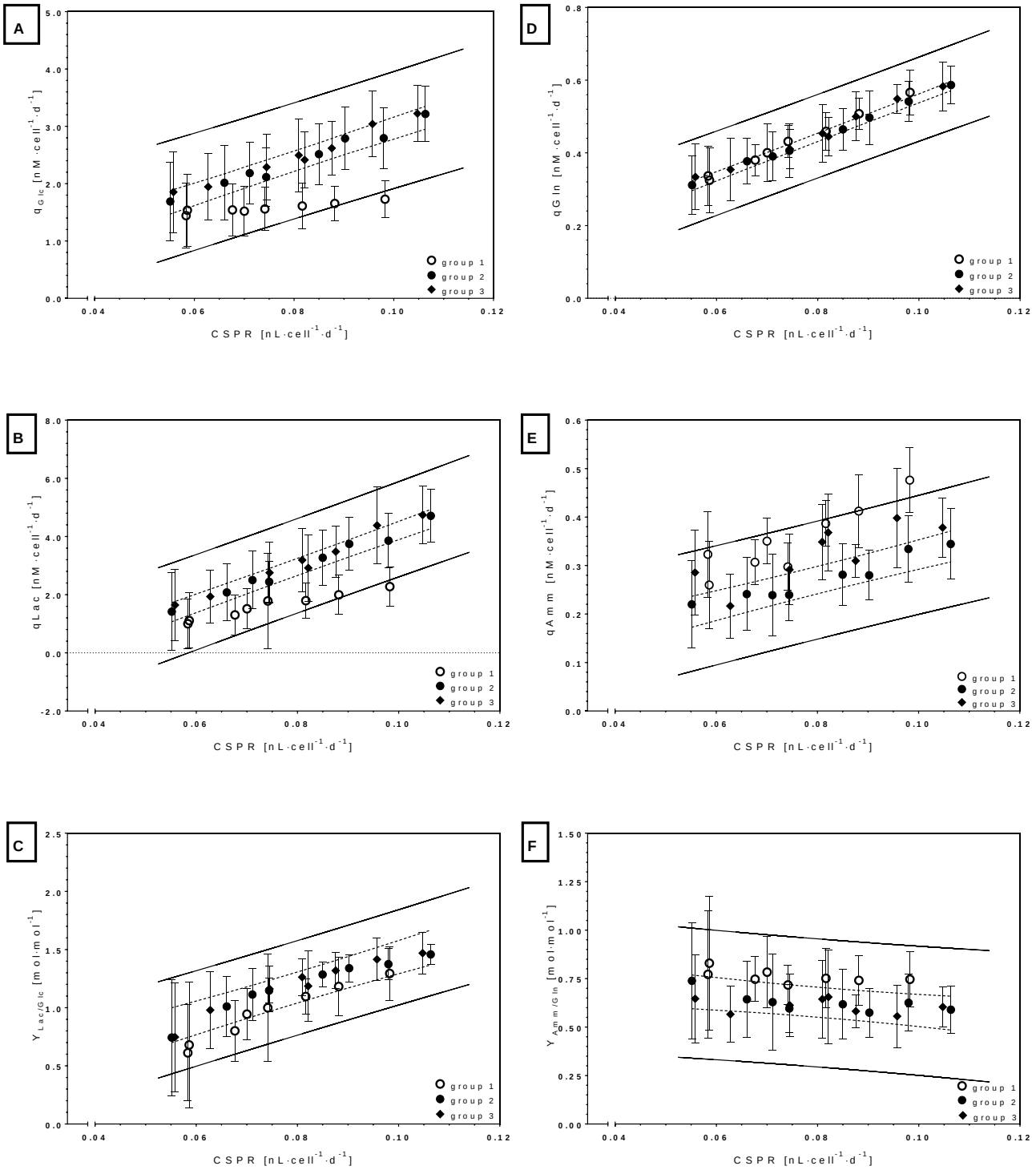

Figure 4-22: Averaged metabolic specific rates of steady state against CSPR of culture group 1 (clear circles), group 2 (filled circles) and group 3 (filled diamonds). A: q_{Glc} against CSPR; B: q_{Lac} against CSPR; C: $y_{Lac/Glc}$ against CSPR; D: qGln against CSPR; E q_{Amm} against CSPR, F $y_{Amm/Gln}$ against CSPR. Error bars are standard deviations of the averaged values (N=10). Dashed lines are the 90% CIMs, solid lines the 90% CIDs of culture group 2.

elevated VP. Three data points were above the upper 90% CIM whereas another value was close to the upper border.

The impact of pH, i.e. lower pH leading to higher VP, is also described in literature (Trummer et al., 2006 a, Trummer et al., 2006 b). Regarding the cell specific protein production rate, this relationship is not reflected but group 1 shows a more similar distribution to group 2 and group 3. This is plausible since q_P is calculated by dividing VP and VCD. Thus, the elevated VP and higher VCD of group 1 were neutralized. The 90% CIM in this case is not significant due to the large error bars. Yet, the similar spread of q_P values demonstrates again the non-growth associated protein production. Thus, the comparable q_P illustrates that VP is proportional to VCD, which can also be derived from equation 2-n in chapter 2.5.1. However, it could be argued that the calculation of q_P with VBV instead of VCD would allow a different interpretation of effects of different feeding intervals (see Figure 4-21 (B)). As mentioned before, the differences between the culture groups are less concise when plotting VBV against D. Thus, with a VBV based calculation of cell specific rates a different distribution of the data points of each culture group was observed. Unfortunately, the evaluation of q_P against SPR (not shown) did not contribute to any clarification and was not pursued because of the high influence of error propagation and the resulting large error bars on the results. Yet, it emphasizes that the choice which biomass definition is employed for the determination of specific rates is of crucial importance when a comparison of cell cultures is conducted.

In conclusion, the results of this experiment imply that cells exhibited a different metabolism based on different pH conditions rather than different feeding intervals. Culture group 2 and group 3 (controlled pH) demonstrated very similar trends for all rates and VCDs tested whereas culture group 1 (uncontrolled pH) showed a deviant distribution. The lower pH of culture group 1 affected mainly the cell size and glucose and glutamine metabolism. Cells of group 1 showed a smaller average cell diameter which resulted in higher VCD recorded. The apparently decoupled protein synthesis from the metabolism might be an artefact from the different VCD measurements between groups 2 and 3 and group 1. Nonetheless, an effect of the different feeding strategies of the cultures compared in chapter 4.2.1 could not be confirmed.

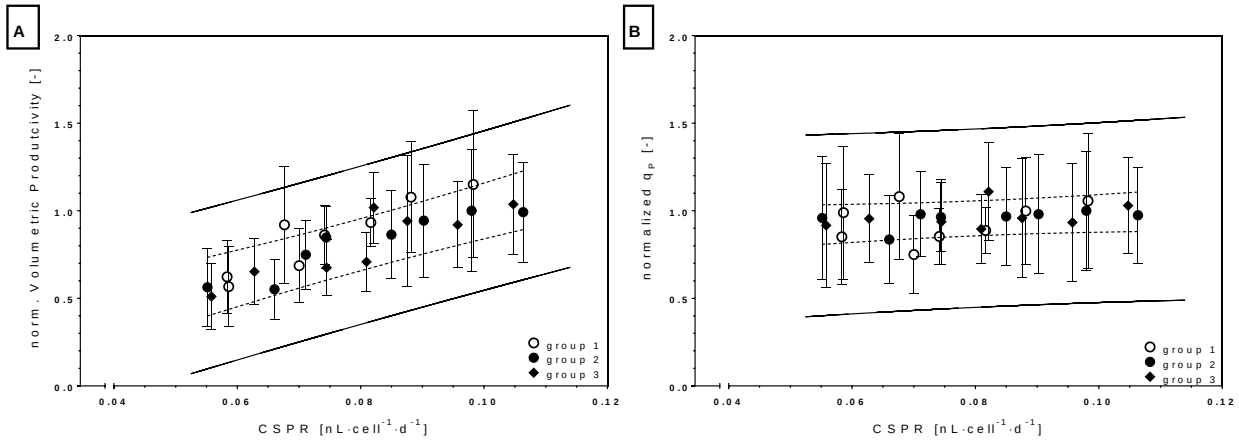

Figure 4-23: Normalized averaged VP (A) and normalized averaged q_P (B) in steady state against CSPR of culture group 1 (clear circles), group 2 (filled circles) and group 3 (filled diamonds). Error bars are standard deviations of the averaged value range (N=10). Dashed lines symbolize the 90% CIM, solid lines the 90% CID of group 2.

4.2.4 Effect of pCO_2 and pH on cell culture performance

Due to the non-affirmative assumptions –different transition phases and different feeding intervals would result in distinct cell culture performance – further differences between the compared DASGIP continuous cultures and ambr™ pseudo-continuous cultures were evaluated.

After a thorough investigation of various culture parameters, a difference in culture pCO_2 between DASGIP and ambr™ cultures was identified. The dissolved carbon dioxide in DASGIP cultures was between 60 mmHg and 85 mmHg whereas cultures with a higher D exhibited higher pCO_2 levels. In contrast, pCO_2 of ambr™ cultures only showed values between 23 mmHg and 30 mmHg. pCO_2 levels between 40-50 mmHg are considered to be optimal (Godía and Cairó, 2006) which implies that both cultures were not meeting these conditions. The differences arose mainly because of the enhanced stripping present in the ambr™ bioreactors due to the additional oxygen flow next to the constant basic gas flow (Nienow et al., 2013). The additional oxygen flow was as high as 0.08 ccm and thus almost as high as the basic gas flow. Moreover, after evaluating the algorithms of the DASGIP gas mixing module, it was discovered that a constant CO_2 gas flow was set to 5% of the total gas flow by factory settings which were believed not to be activated. Thus, CO_2 was not only produced by cells but also supplied by the bioreactor system. The constant addition of CO_2, however, was not maintained because it interfered with the pH control. Therefore, CO_2 was added sporadic as a step-function. Many studies were conducted in order to investigate the effect of pCO_2 on cell culture (Kimura and Miller, 1996; deZengotita et al., 1998; Zanghi et al., 1999; Tagaki et al., 2000 Schmelzer et al., 2001; deZengotita et al., 2002a; deZengotita et al., 2002b; Zhu et al., 2005) but all studies focused on elevated pCO_2 levels (above 100 mmHg) which normally occur in production scale and fed-batch operation modes. Since neither the ambr™ nor the DASGIP cultures were in the optimal physiological range or the range studied in literature, an additional experiment was conducted to evaluate the impact of different pCO_2 levels on cell culture performance. The DASGIP system offered the best possibility to accurately maintain the pCO_2 values because of the gas mix algorithm with a basic constant gas flow which ensured a constant stripping. Moreover, the effect of different pH-set points was investigated in order to verify the assumptions made in chapter 4.2.3. Also, slight differences in the pH operating point between the compared cultures of chapter 4.2.1 were observed. The experimental outline of this experiment is presented in Table 4-5.

Table 4-5: Planned experiments for the evaluation of pH and pCO_2 effects on cell culture performance. The grey highlighted culture was not used for comparison due to technical difficulties during cultivation.

Culture	Group	pH set-point	Gas flow (ccm)	Dilution rate	pCO_2 [mmHg]
1	a	6.9±0.05	3.00	0.25	55
2	a	6.9±0.05	4.14	0.25	59
3	a	6.9±0.05	10.0	0.25	73
4	b	7.1±0.05	3.00	0.25	52
5	b	7.1±0.05	4.14	0.25	70
6	b	7.1±0.05	10.0	0.25	74

Culture group a and group b served the evaluation of pH and pCO_2 effects on cell culture performance. The gas flow rates were chosen based on the previous DASGIP cultures. The gas flow of 3 ccm was selected in order to allow higher pCO_2 levels than in the first DASGIP experiments. Even lower flow rates were not possible owing to technical restrictions. The gas flow of 4.14 ccm was used for control cultures since this rate was already applied for the DASGIP cultures in chapter 4.2.1. 10 ccm reflected a vvm-based scaling of ambr™ gas flow rates and should result in lower pCO_2 values. pH set-points of all previous ambr™ and DASGIP cultures were covered and pCO_2 ranges were varied in comparison to control DASGIP cultures.

When culture group a and group b are compared (Figure 4-24), different effects of pCO_2 and pH on various cell culture parameters can be observed. The reported decrease in q_{Glc} at elevated pCO_2 (deZengotita et al., 1998) is only observable for culture group a. At 52 mmHg pCO_2, the glucose consumption was 33% higher than at 73 mmHg. The q_{Glc} values of group b showed almost no difference at different pCO_2 values. A slightly decreasing trend for higher pCO_2 might be visible but was not significant as indicated by the error bars. Thus, the lower glucose consumption could be an integrated effect of pH and pCO_2. Since osmolality within the culture groups was comparable, any contribution of this parameter could be ruled out. The comparison of cultures with the same pCO_2 but different pH (e.g. culture 3 and culture 6) demonstrated that higher pH alone is accompanied by an increase in q_{Glc}. Although the osmolality was higher in culture 6, a contributing effect has been rejected because the osmolality range of these cultures between 305 $mOsm \cdot kg^{-1}$ and 345 $mOsm \cdot kg^{-1}$ was reported not to affect CHO cells significantly (Kurano et al., 1990; deZengotita et al., 1998). The same relationship as for q_{Glc} has been observed when comparing q_{Lac} of the two cultures. No difference in glutamine consumption rate could be observed at different pCO_2 or pH values (data not shown). In the case of varying pH values, this is not surprising since the cultures in chapter 4.2.3 showed only little deviation in q_{Gln}. For the comparison of ambr™ and DASGIP cultures this implied that lower q_{Gln} did not originate from the different process conditions, i.e. pCO_2 levels, but either from the process operation mode or the different physical bioreactor characteristics.

Regarding the unanswered differences of chapter 4.2.1 and the assumptions of 4.2.3, conclusions from the generated data can be drawn. The metabolic rates supported the assumption made in chapter 4.2.3, where the lower q_{Glc} and q_{Lac} was ascribed to lower pH rather than the feeding intervals. Considering the comparison of ambr™ and DASGIP cultures, the metabolic rates of the experiment in the current chapter only provided ambiguous results. No correlation between elevated pCO_2 and higher q_{Glc} could be found at the corresponding culture pH. Thus, the higher glucose consumption of the DASGIP cultures must have originated elsewhere. However, the pCO_2 range tested during this experiment was much tighter than the differences between ambr™ and DASGIP cultivations in chapter 4.2.1. Another experiment in ambr™ bioreactors at high pCO_2 levels might provide further insights.

The comparison of VP and q_P on basis of CSPR showed that pCO_2 alone had an effect on cell cultures. At higher pCO_2, a lower volumetric productivity and lower q_P was calculated for both culture group a and group b. The large error bars, which were again caused by noisy ELISA measurements, might question the significance of the trend of lower VP and q_P at higher pCO_2. However, the observed trend is consistent with the few reports concerning the effect of pCO_2 on productivity of mammalian cells in literature (Kimura and Miller 1996; Ma et al., 2006). The higher VP at lower pCO_2 contradicts any influence of this

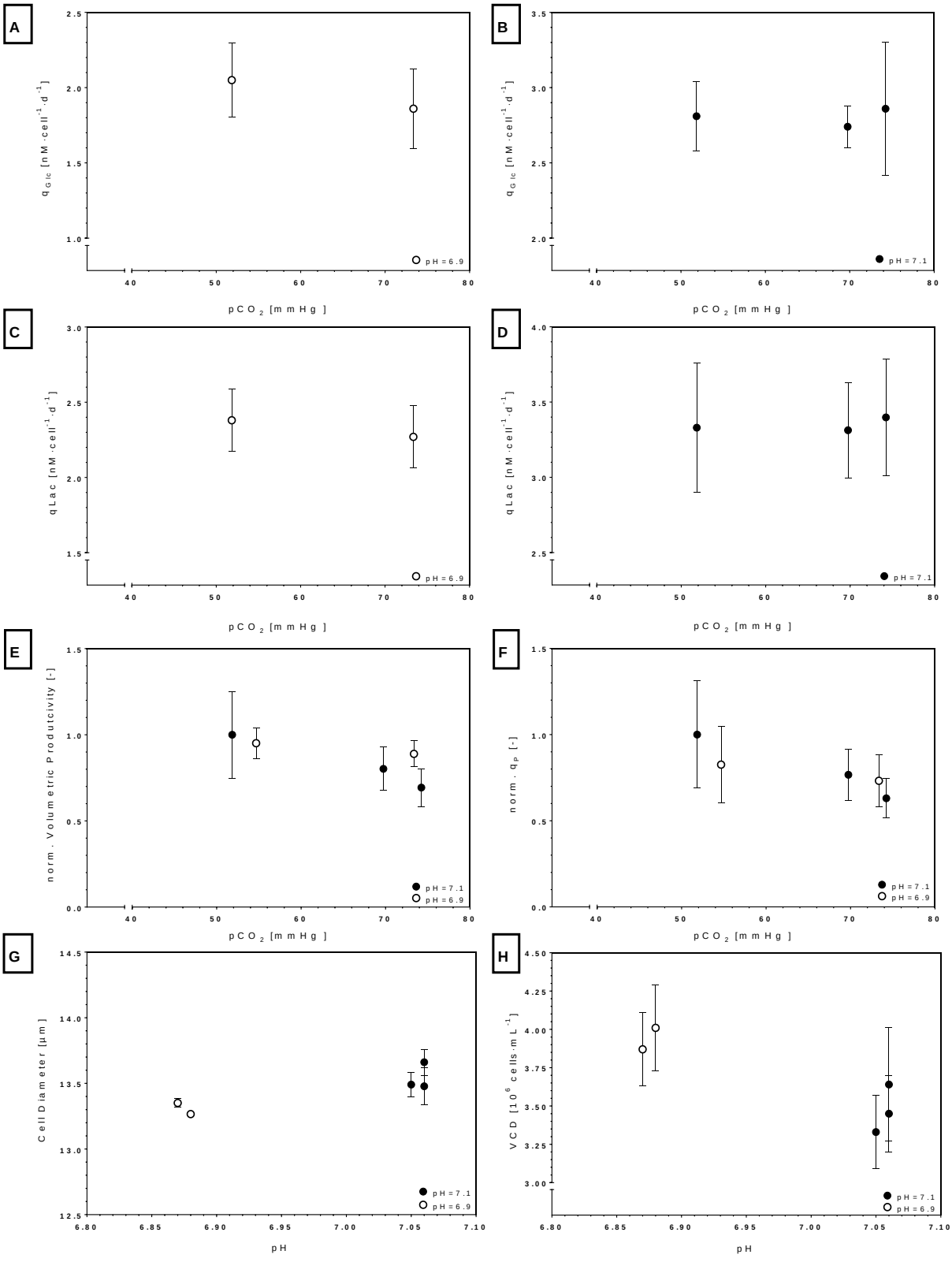

Figure 4-24: Comparison of steady state values of culture group a (clear circles) and group b (filled circles). Error bars are standard deviations of averaged values. Averaged q_{Glc} against pCO_2 of culture group a (A) and group b (B) (N=8). Averaged q_{Lac} against pCO_2 of culture group a (C) and group b (D) (N=8). (E): Averaged normalized VP against pCO_2 (N=8). F: Averaged normalized q_P against pCO_2 (N=8). G: Mean of averaged cell diameter against pH (N=8). H: Averaged VCD against pH (N=8). Substrate and metabolite concentrations were measured with the Bioprofile 100+.

parameter on the observed higher VP of the DASGIP cultures in chapter 4.2.1. It rather indicates that even higher VP would have been generated when the same pCO_2 levels in ambr™ and DASGIP cultures would have been achieved. Yet, the sampling technique for the determination of pCO_2 values in the ambr™ shed doubt on the accuracy of the results. Firstly, the ambr™ bioreactor was opened by the automated liquid handler for the removal of sample material. Here already, CO_2 could evaporate. And secondly, the sample was transferred via a pipette to a conventional Cedex cup which exhibits a large surface area so that further evaporation could occur. The time between opening the bioreactor and the actual measurement was around 30-45 seconds. Thus, a too low pCO_2 might have been measured.

The different pH on the other hand did not have any significant effect on q_P and VP which is not confirming the slightly higher VP for cells cultured at a lower pH described in chapter 4.2.3. Thus, it supports the assumption that cells maintain their specific productivity albeit different uptake and production rates of substrates and metabolites.

Additionally, the effect of pH on VCD was evaluated. Higher VCD and lower AVC was observed for cultures at pH=6.9 compared to cultures at pH=7.1. Thus, the primary effect recorded in the experiments of chapter 4.2.3, i.e. higher VCD and lower cell diameter at lower pH, were verified. This result supports the assumptions, that varying the feeding intervals was not the cause for the observed differences in chapter 4.2.3 but the different pH.

4.2.5 Conclusions drawn from the comparison of ambr™ pseudo-continuous and DASGIP continuous cultures

In conclusion, differences in cell culture performance between ambr™ and DASGIP cultivations were identified and the different aspects were evaluated.

The generated data was error-prone to a large extent due to the used measurement systems which distorted the results. Additionally, the choice which definition of biomass, in this case VCD or VBV, was used to calculate cell specific rates allowed a different angle for the interpretation of cell culture performance between the cultures. For the determination of differences or similarities between culture systems it is thus of crucial importance to include both and possible other biomass definitions into the calculation and evaluation of CPP.

Another critical measurement method was the used ELISA for the quantification of the recombinant product concentration. The large fluctuations between measurements resulted in large standard deviations so that a clear and significant interpretation of possible differences of protein related data was restrained. Yet, the averaged data and their trends suggest a general reproducibility of these parameters between the systems.

The experiments of chapter 4.2.2 - 4.2.4 provided additional information about the origins of the differences in cell culture performance of the ambr™ and DASGIP cultures. Based on supplementary ambr™ cultivations, an impact of different transition phases between batch and continuous cultures and different feeding strategies was ruled out. Especially the similar outcome of pH controlled cultures when different feeding intervals were applied, suggest that the disparities were not caused by the operation

mode but rather by the bioreactor system. Analysis of the effect of pCO_2 demonstrated that the VP of DASGIP cultures can actually be expected to be higher due to the detrimental effects of pCO_2 on VP. Results from other research groups at Novo Nordisk also implied lower VP in ambr™ cultures. A cause for this discrepancy might be found additionally in the heterogeneous mass transfer of ambr™ bioreactors (Nienow et al., 2013).

Although the culture parameters were not transferable with their face values, similar trends were examined. Metabolic rates were different to some extent but showed higher substrate consumption and metabolite production at higher CSPR for both culture systems. VP and q_P were similar for the culture systems tested whereas DASGIP cultures showed slightly elevated VP which is probably connected to the slightly higher VCD recorded. However, the effect of pCO_2 on cell culture performance has to be considered which might have concealed further differences. Regarding the stable offsets of CPP achieved in the different culture systems, a transfer between ambr™ pseudo-continuous cultures and DASGIP continuous cultures based on CSPR is possible.

4.3 Applicability of transferring process conditions from pseudo-continuous and continuous to an ATF-perfusion cultivation

The observed interdependencies and possible impact factors of chapter 4.2, such as pCO_2, were taken into account for the transfer of CPP to a cell culture in perfusion mode with ATF-system in 5 L scale. Most of the cultures run with the ambr™ and DASGIP system were operated at D=0.25 d^{-1} so that these cultures provided the broadest basis for comparison. In steady state, the dilution rate of pseudo-continuous and continuous cultures is equal to μ which was selected as the primary set-point variable for the transfer of CPP because it can be easily implemented via the bleed rate in perfusion processes. Thus, D_{Bleed}=0.25 d^{-1} was set and a final dilution rate with D=1.5 d^{-1} via the additional harvest rate was targeted. In order to compare the ATF-perfusion steady state values to ambr™ and DASGIP cultures, steady state was assumed 10 days after the start of the cell bleed. Thereby, the culture time between the latest change in operation conditions and the assumed steady state was standardized for all cultures. Hence, steady state was assumed for ATF-perfusion after 17 culture days as opposed to 14 culture days in the other systems. After day 6, the samples for ATF-perfusion VCD measurements were diluted 1:2 in PBS since the maximum cell density range of the Cedex system was reached. A basic constant air flow was implemented and adjusted in order to reach pCO_2 levels comparable to DASGIP cultures. The final air flow was 60 ccm and was thus higher than the scaled gas flow (see chapter 2.6). Based on the results of chapter 4.2.4, pCO_2 control was considered to be more important than presumably adequate k_La-based scaling. The results of this ATF-perfusion were compared to the cultures of chapter 4.2.1.

The direct comparison of VCD of the three systems is not feasible due to the dramatically higher VCD measured in ATF-perfusion and provides a good example why other parameters have to be consulted for contrasting cultures operated at different modes. Yet, combined with viability measurements the description of VCD allowed a general assessment of the behavior of this particular cell culture. In Figure 4-25, the trends of both parameters over time are displayed. VCD measurements were showing similar characteristics as in pseudo-continuous and continuous cultivations after the start of the cell bleed rate (see chapter 4.2.1 in Figure 4-10). After an exponential increase during the batch phase until day 3, the ramped harvest rate was started and VCD increased further until day 6. During the ramp, the viability decreased in a linear fashion which is consistent with cultures in continuous culture mode. After the start of the cell bleed, the VCD began to increase with a lower slope in a linear fashion. Both behaviors, the increase in VCD and the decline in viability, were also observed after the start of continuous operation in DASGIP continuous cultures. The different start phase after the batch cultivation was not considered to be influencing the final steady state values since the results of chapter 4.2.2 implied no distinct culture performance after different start phases in pseudo-continuous culture. Although not directly comparable to the start phase of continuous cultures, the ATF-perfusion start phase is basically a prolonged transition phase between batch and continuous culture with cell retention. The VCD showed a maximum at day 10 with 24.8·10^6 cells·mL^{-1} and then declined to 19.2·10^6 cells·mL^{-1} at day 14. Thereafter, the VCD started to oscillate as in the other systems and reached a stable steady state of in average 22.0·10^6 cells·mL^{-1} after

culture day 16. Hence, steady state values of all three systems could be compared from 10 days after the start of the cell bleed onwards. The viability was also constant during this time range with around 89.4% which is much lower than for the ambr™ or DASGIP systems that were around 93% during steady state. A reason for this is the dilution performed prior to the analysis with the Cedex. A series of dilution ranges tested showed that lower VCD and viability was measured when higher dilutions were used. Undiluted samples showed viabilities at around 94% but were not routinely executed since these Cedex measurements were time consuming (30 minutes per measurement) and might have been inaccurate. This indicates that the true VCD and viability values were higher than their apparent values. For the calculation of specific rates, the results of the 1:2 diluted samples were used since only these were within the measurement range of the Cedex.

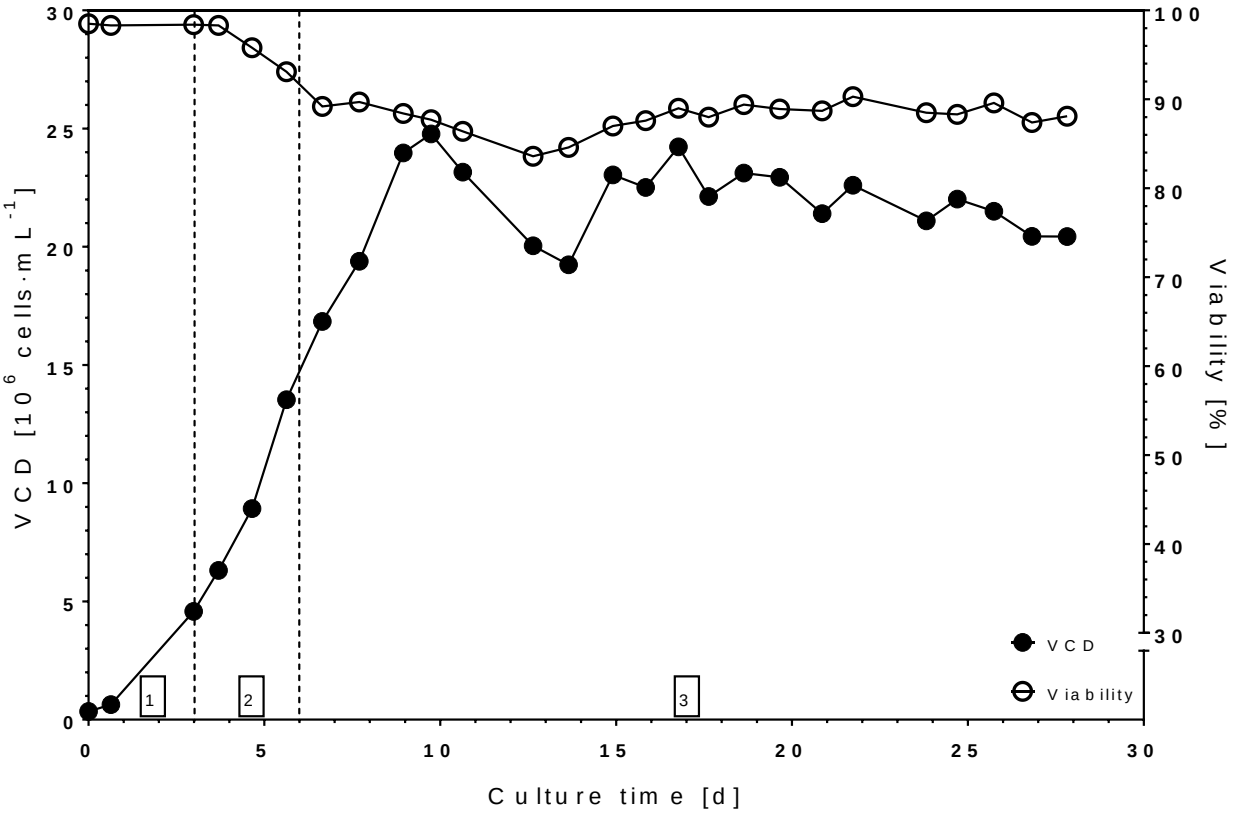

Figure 4-25: VCD (filled circles) and viability (clear circles) over time of an ATF-perfusion cultivation. The dashed line show different phases of the cultivation: (1): batch phase; (2): ramped harvest rate; (3): constant harvest and bleed rate.

The comparison of the main set-point variable μ based on CSPR demonstrated that ATF-perfusion is very well reflected by continuous and pseudo-continuous cultures (Figure 4-26). The μ of the perfusion culture was within the 90% CIM of the ambr™ culture. Error bars of the ATF-culture were very similar to the DASGIP cultures at corresponding CSPR which reflects correlative variations in VCD during steady state. The same percentage difference between two subsequent VCD measurements would produce the same difference in μ. In conclusion, the transfer of the process operation variable μ is feasible with CSPR based

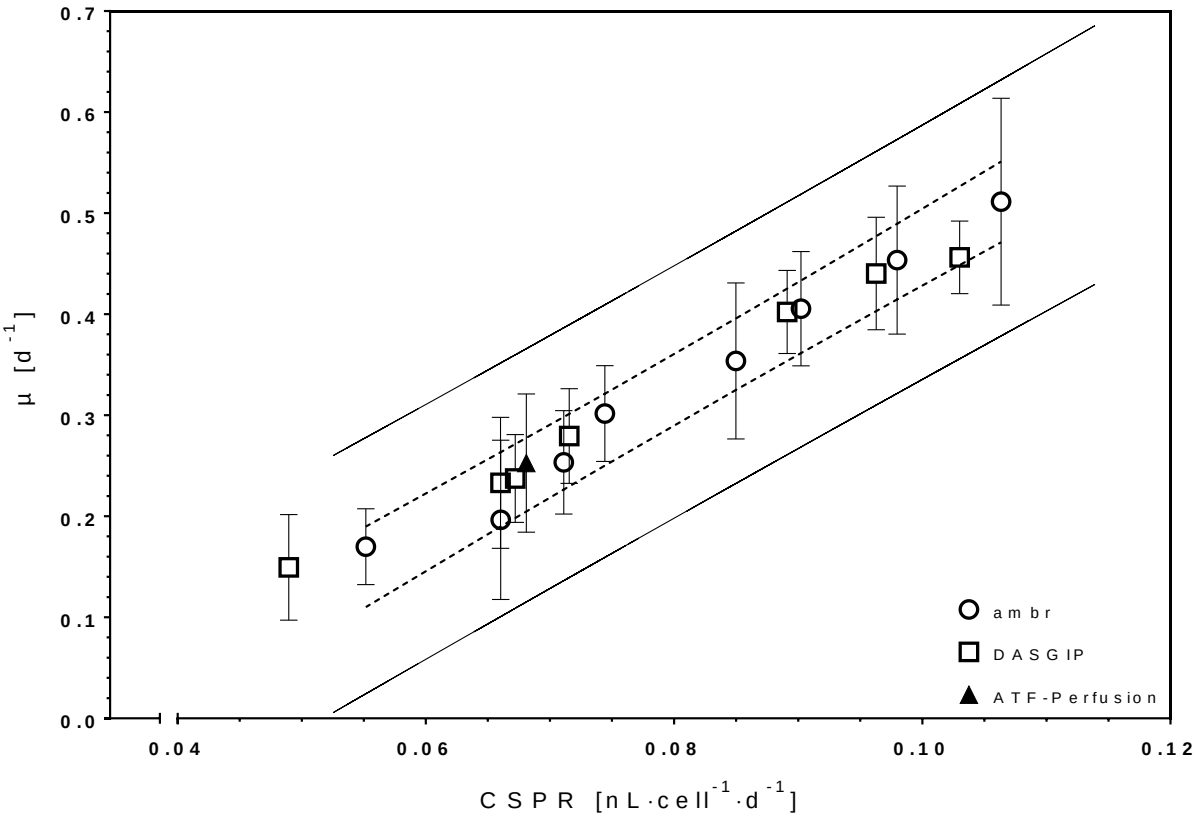

Figure 4-26: Averaged μ of steady state values against CSPR for ambr™ pseudo-continuous (clear circles), DASGIP continuous (clear squares) and ATF-perfusion (filled triangle) cultivations. Error bars indicate standard deviations for the averaged values (ambr™: N=10; DASGIP: N=9; ATF-perfusion: N=10). The dashed lines show the 90% CIM, the solid lines the 90% CID of the ambr™ cultures.

scaling. However, as already indicated in chapter 4.2, differences were to be expected for cell specific substrate consumption and metabolite production rates (Figure 4-27).

Indeed, the calculated glucose consumption rate of the ATF-perfusion was not reflecting the values obtained in pseudo-continuous cultures. Although marginally higher with q_{Glc}=2.85 nM·cell^{-1}·d^{-1}, the glucose consumption rate of the perfusion culture rather resembled the q_{Glc} of the DASGIP cultures. However, when calculating the 90% CIM of DASGIP cultures (not shown), q_{Glc} of the ATF-culture was not residing within those CI limits. Several causes might have contributed to this examination. Based on the discrepancy of q_{Glc} between ambr™ and DASGIP cultures, the higher glucose consumption rate observed in ATF-perfusion culture is partially coherent. Since the geometrical characteristics of the bioreactor, operation mode, and scale were more similar for DASGIP and ATF-perfusion and more disparate between ambr™ and ATF-perfusion, it could be assumed that culture performance is more similar in bench-top bioreactors. Therefore, the fact that the ATF-perfusion q_{Glc} was not included in the 90% CIM of the DASGIP culture might be attributed to the possible lower apparent VCD measurement. With a higher VCD the glucose consumption per cell and day would have been lower and probably fit within the 90% CIM of the DASGIP culture.

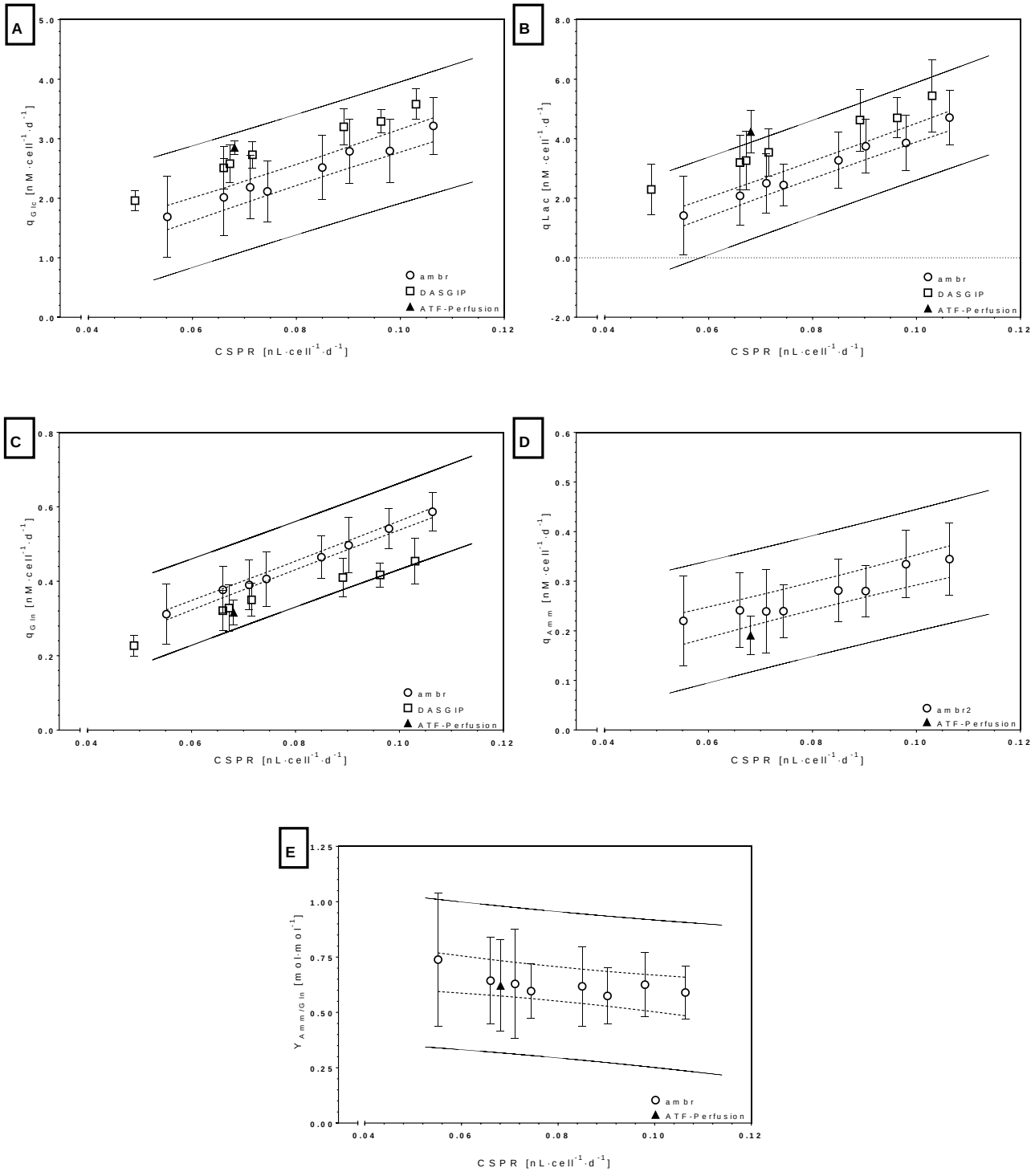

Figure 4-27: Comparison of steady state cell specific metabolic rates of ambr™ pseudo-continuous (clear circles), DASGIP continuous (clear squares), and ATF-perfusion (filled triangles) cultures. Dashed lines indicate the 90% CIM, solid lines the 90% CID of ambr™ cultures. Error bars show the standard deviations of the averaged values (ambr™: N=10; DASGIP: N=9; ATF-perfusion: N=10). A: Averaged q_{Glc} against CSPR. B: Averaged q_{Lac} against CSPR. C: Averaged q_{Gln} against CSPR. D: Averaged q_{Amm} against CSPR. E: Averaged $y_{Amm/Gln}$ against CSPR.

The bigger similarity between ATF-perfusion and DASGIP cultures is reproduced when regarding the lactate production rate. q_{Lac} of the ATF-perfusion was also higher than in ambr™ and DASGIP cultures at corresponding CSPR. However, the difference between ATF-perfusion and DASGIP in terms of q_{Lac} was more significant than for q_{Glc}. Here as well, the possibly lower apparent VCD contributed to the higher q_{Lac} values of the ATF-perfusion. Moreover, the measurement accuracy of lactate was less consistent which is displayed by the larger error bars. They in turn indicate that lactate production in DASGIP and ATF-perfusion cultures was not substantially different. Yet, the value of the ATF-perfusion was not included in the 90% CID of the ambr™ which raises the question of the transferability of q_{Lac} between pseudo-continuous and perfusion cultures. Nevertheless, the earlier mentioned heterogeneities of mass transfer in the ambr™ might have misrepresented the metabolic rates. The same relations can be derived for the comparison of q_{Gln} where ATF-perfusion and DASGIP cultures showed a larger resemblance. For the comparison of ammonium production rate and $y_{Amm/Gln}$, the DASGIP culture results were not included due to the already explained unreliable ammonium measurements for these cultivations. Interestingly, q_{Amm} of the ATF-perfusion resided, though not within, close to the lower 90% CIM of the ambr™ system. Accordingly, the glutamine to lactate yield was within the 90% CIM of the ambr™ system. Based on the similarity of q_{Glc}, q_{Lac}, and q_{Gln} between ATF-perfusion and DASGIP cultures, it is suggested that also ammonium production and $y_{Amm/Gln}$ values would have been congruent. However, this has to be investigated in an additional experiment.

The comparison of metabolic rates showed that a difference between pseudo-continuous cultures, continuous, and perfusion cultures exists whereas the latter are more coinciding. Further experiments of ATF-perfusion over a wider range of CSPR cultures would be needed to verify this assumption. Nonetheless, due to the similarity of ATF-perfusion and DASGIP cultures and the already observed transferability between ambr™ and DASGIP cultures in chapter 4.2.1 a CSPR based scaling of CPP - though not with their face values - is generally applicable.

Based on the findings of the metabolic rates and the results of chapter 4.2 it could be assumed that the recombinant protein related data would be similar for all culture systems. Surprisingly, the q_P of the ATF-perfusion was considerably lower than in ambr™ and DASGIP cultures. It was residing outside the 90% CIM of the ambr™ system and was approximately 33% and 53% lower than in ambr™ and DASGIP cultures, respectively, at corresponding CSPR (Figure 4-28 (A)). This outcome could not be explained based on the observed growth and metabolic characteristics.

For the ATF-perfusion a higher pCO_2 (80 mmHg) was recorded than in corresponding cultures at the same CSPR in ambr™ (23 mmHg) and DASGIP (70 mmHg) cultures. This probably contributed to the lower q_P measured when considering the results from chapter 4.2.4 which indicated a higher q_P at lower pCO_2. Still, the higher pCO_2 cannot be considered as the main driving force for the observed disparity. The low error bars also indicate more stable ELISA results than for the other culture systems but at the same time question the results achieved for ambr™ and DASGIP cultures. A subsequent reanalysis of the protein samples with a changed dilution factor for the ELISA measurement showed that the dilution factor used for protein analysis in this work was too low since the slope of the calibration curve was very shallow at these concentrations using a sigmoidal curve fit. Thus, higher dilution factors, which would allow protein concentration measurement in a steeper part of the calibration curve, would have reflected

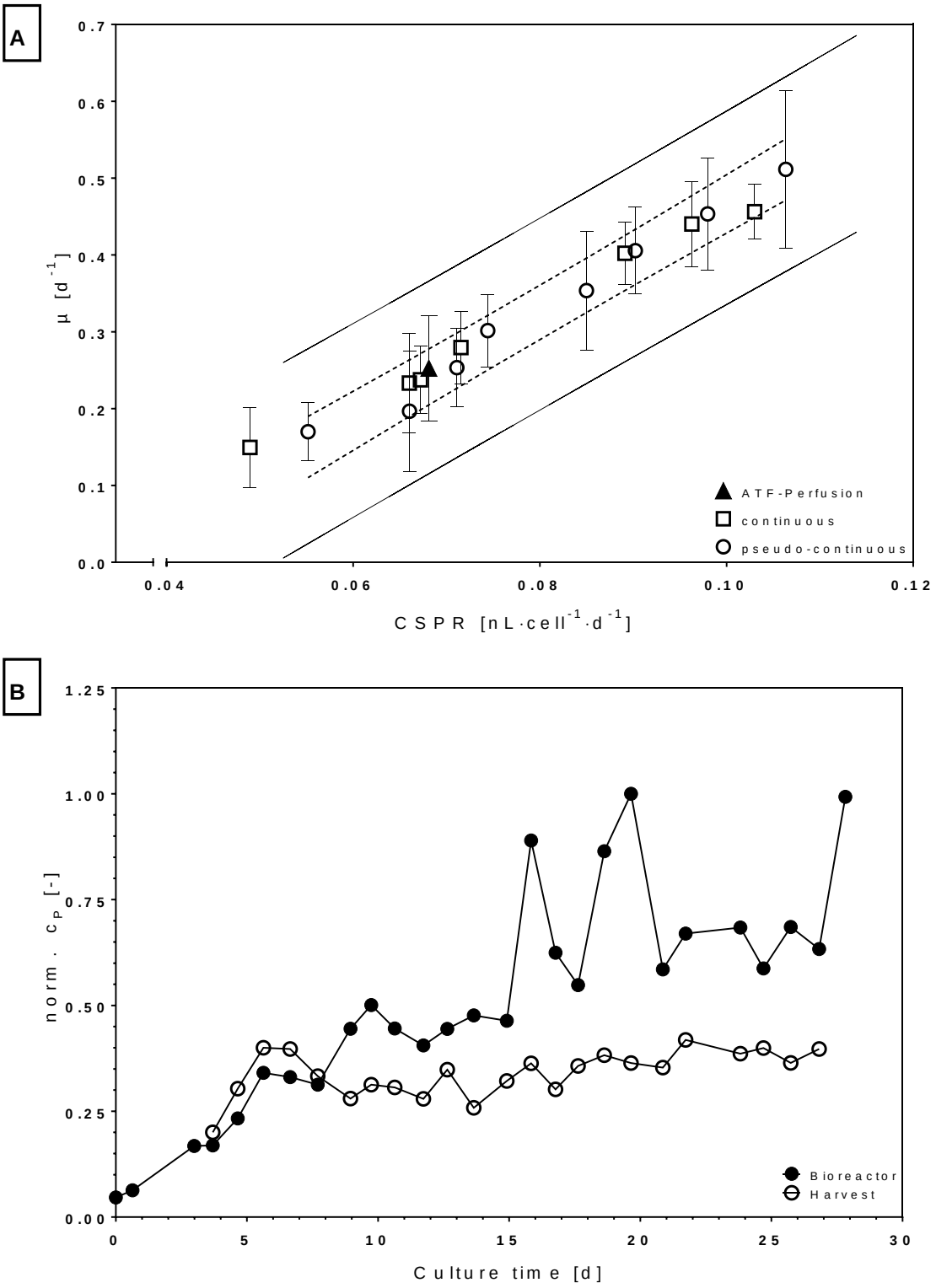

Figure 4-28: A: Averaged q_P against CSPR of ambr™ pseudo-continuous (clear circles), DASGIP continuous (clear squares), and ATF-perfusion (filled triangles) cultures. Dashed lines indicate the 90% CIM, solid lines the 90% CID of ambr™ cultures. Error bars show the standard deviations of the averaged values (ambr™: N=10; DASGIP: N=9; ATF-perfusion: N=10). B: Time course of the normalized recombinant product concentration of sample taken from the bioreactor (filled circles) and from the harvest stream (clear circles). The analysis with a low dilution factor is shown.

the true value in a more accurate way. Yet also here, large fluctuations in triplicate measurements were recorded.

Another aspect which probably contributed to the observed lower q_P was the fact that the transmission of protein through the ATF-membrane was impaired (Figure 4-28 (B)). The averaged transmission rate, i.e. the percentage difference between measured protein concentration in the bioreactor and the harvest stream, was around 56% during steady state and indicates that the expressed recombinant protein was retained by the hollow fiber module. It is questionable whether the retained proteins were transported back into the bioreactor and thus led to an apparent higher protein concentration in the bioreactor, disintegrated, or remained in the ATF-module. Lower retention efficiency has been observed at low viability. Preliminary experiments showed that at below 90% viability the transmission was significantly reduced (data not shown). However, when assuming that the protein concentration in the bioreactor was reflecting the actual protein amount expressed in the system, the calculated normalized q_P was 0.97 and thus would fit within the 90 %CIM. Probably all of these factors played a role and might have had an integrated effect on recombinant protein related data. Due to the numerous assumptions, the results concerning q_P and VP therefore have to be handled carefully.

5 Conclusion and Outlook

A considerable objective in process development is mimicry of sophisticated cell culture processes by easy-to-control alternatives. Step-wise simplification of perfusion processes offer the possibility to select production clones and design robust processes in a perfusion-related environment in a less time- and work-consuming manner. Characteristic process set-points achieved in this way have to be transferred from the simpler to the more complex bioreactor set-ups and process modes. In this work, a scale-up and transfer of process conditions from 15 mL pseudo-continuous culture to 1 L continuous culture and finally 5 L ATF-perfusion culture based on appropriate scaling parameters was evaluated. Distinct differences in cell culture performance between the respective bioreactor systems and cultivation methods were identified and evaluated.

The transfer of the process operating points, such as the growth rate of cells, is resulting in the same CSPR for all bioreactor systems used. Thus, during steady state, the same amount of cells can be supported by the same volume of medium. Therefore, CSPR has been proven to be a suitable scaling parameter for the reproduction of growth characteristics in simpler small-scale equipment. Comparison of cell specific metabolic rates revealed, however, that DASGIP continuous cultures and ATF-perfusion cultures showed higher cell specific glucose consumption and lactate production rate at various CSPR compared to the ambr™ pseudo-continuous system. Cell specific glutamine consumption on the other hand was higher for ambr™ cultures. Although different rates between ambr™ and bench-top bioreactor systems were observed, similar trends with stable off-sets were recorded. The cell specific protein production rate was not reflected by the cell specific metabolic rates. DASGIP continuous cultures and ambr™ pseudo-continuous cultures showed similar q_P over a wide range of CSPR whereas the cell specific protein production rate of the ATF-perfusion was only around 30-50% of q_P of the other systems. Reasons for this behavior were numerous.

a) The measurement principle of determining biomass played a crucial role for the comparability of culture parameters based on specific perfusion rates. Differences in cell diameter have significant influences on VCD measurements, whereas the actual biomass might be unaffected. In some cases, the comparison based on VBV derived rates showed a more homogenous distribution between cultures. It is a question of principle what measure of biomass to use for comparison since both exhibit advantages and disadvantages. In this work, VCD was chosen for further comparison because more literature sources are available and error propagation was not as dominant as for VBV based calculations. Other methods of determining biomass, i.e. a biomass sensor based on capacitance or the determination of the packed cell volume, might provide additional insight, but were not investigated in this work. Nonetheless, the two different biomass measures used in this work showed that comparison based on specific perfusion rates demands an accurate determination of biomass and to question its informative value.

b) The determination of recombinant protein related data was impeded due to very noisy ELISA results. Protein samples were measured using a broad calibration range which contributed to the large deviation between measurements.

c) It was suggested that differences originated from the bioreactor system and general process conditions rather than from the operation mode. The investigation of different feed addition – the crucial difference between pseudo-continuous and continuous cultures – was conducted in ambr™ bioreactors and resulted in a similar outcome. Different mass transfer characteristics of ambr™ bioreactors compared to conventional bench-top bioreactors were reported in literature (Nienow et al, 2013) and supported the assumption. Additionally, divergent transition phases between batch and continuous mode resulted in similar cell culture performance in ambr™ pseudo-continuous cultures. This indicates that different start phases, such as in the beginning of the ATF-perfusion, do not have a have a major impact on steady state behavior.

d) Different pCO_2 levels contributed to the observed differences in q_P between the culture systems. An additional experiment for the investigation of pCO_2 effects on CHO cells at the same dilution rate in DASGIP continuous cultures indicated distinct recombinant protein related trends. Increased pCO_2 levels, as in the ATF-perfusion and the DASGIP continuous cultures, led to lower q_P. Thus, at a similar pCO_2, it could be assumed that ambr™ cultures would have shown lower q_P compared to DASGIP and ATF-perfusion cultures, which in turn would reflect the higher cell specific glucose consumption rate of the latter. An assessment of the influence of pCO_2 on cell culture performance in the other bioreactor system would be needed to verify this assumption.

e) In the case of the ATF-perfusion a partial retention of protein by the hollow-fiber membrane module was detected. Hence, the calculated q_P might not have reflected the true value.

f) The time point of harvesting, i.e. taking a sample, was different between the three culture systems. Whereas for the ambr™ fixed interval between sampling was programmed, the time between harvests for the other systems was fluctuating. Thus, especially for the DASGIP culture different concentrations of substrate, metabolites and protein might have been measured because of dilution effects exerted by the hourly feed.

In conclusion, growth behavior could be adequately scaled using CSPR. The observed differences in cell specific metabolic rates and cell specific protein production rate only partially originated from the different bioreactor systems and operation modes but were also impacted to a great extent by general process conditions and measurement inaccuracy. Although these rates differed between the bioreactor systems, stable off-sets and similar trends were observed. It can therefore be concluded that it is feasible to utilize CSPR as a scaling parameter for scale-down models of CHO cell perfusion processes.

Additional experiments are needed to verify assumptions that differences between bench-top bioreactor systems and ambr™ cultures originate from the physical bioreactor characteristics rather than from the operation mode. Here, a pseudo-continuous cultivation in DASGIP bioreactors would address the question. Along with the traditional scale-up techniques that focus on k_La-based scaling, special care should be taken concerning pCO_2 control. Online pCO_2 sensors are available and pCO_2 controlled processes could be designed. In this context, pCO_2 ranges comparable to the ambr™ cultures of this project should be investigated in order to examine the effects of very low pCO_2 on cell culture performance. Moreover, an improved protein quantification method would allow a more exact determination of protein concentration and thus clarification of the effects of different bioreactor systems, scales and operation modes on recombinant protein production.

The results of this work indicate that cell culture processes could be transferred from pseudo-continuous over continuous to ATF-perfusion cultures using CSPR as a scaling factor. Initial growth and stability characteristics could then be evaluated in ambr™ pseudo-continuous cultures since a high number of experiments can be conducted in this system. Metabolism assessment could be executed in DASGIP systems. Rates for substrate uptake and metabolite production between DASGIP continuous cultures and ATF-perfusion cultures were very similar at corresponding CSPRs. Thus, a transfer of the observed metabolic and growth conditions to ATF-perfusion cultures should be easily possible with the culture systems investigated.

The investigation of minimum CSPR in order to achieve fed-batch-like titers following the "push-to-low" approach (Konstantinov et al., 2006) should be facilitated when using simpler fully-instrumented small-scale cultures such as the ambr™ and DASGIP systems to approximate the final perfusion process and would allow a more systematic approach. The effects of CSPR on cell metabolism can be predicted in the simple systems, thus saving resources.

6 Appendix

6.1 Additional figures

Appendix 1: Lactate concentration and VCD over culture time of DASGIP continuous culture 1 of chapter 4.1. Lactate concentrations were measured with the BioProfile 100+.

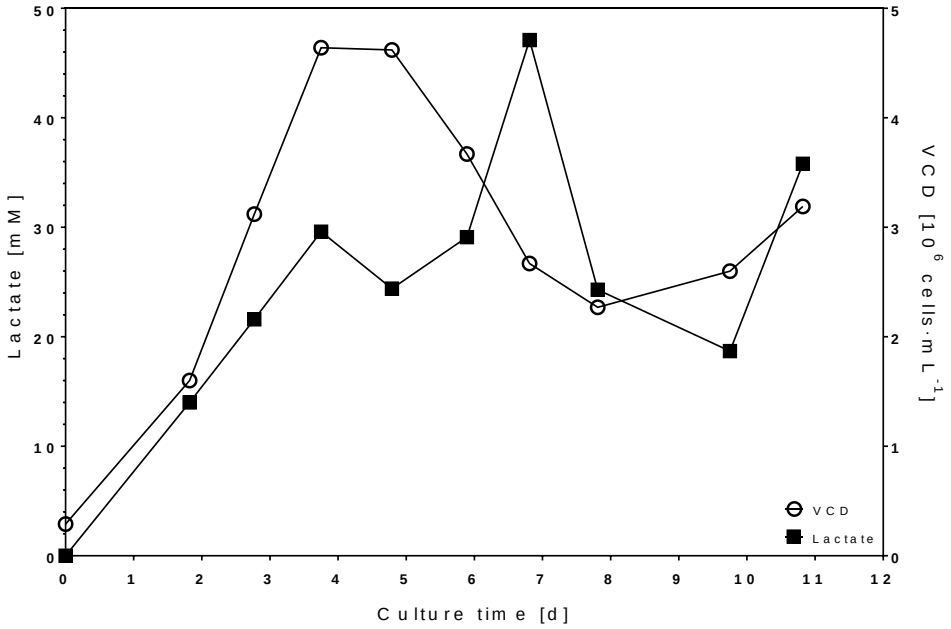

Appendix 2: q_{Glc} calculated against SPR from cultures in chapter 4.2.3. The rate was calculated with VBV. Symbols are the same as in chapter 4.2.3.

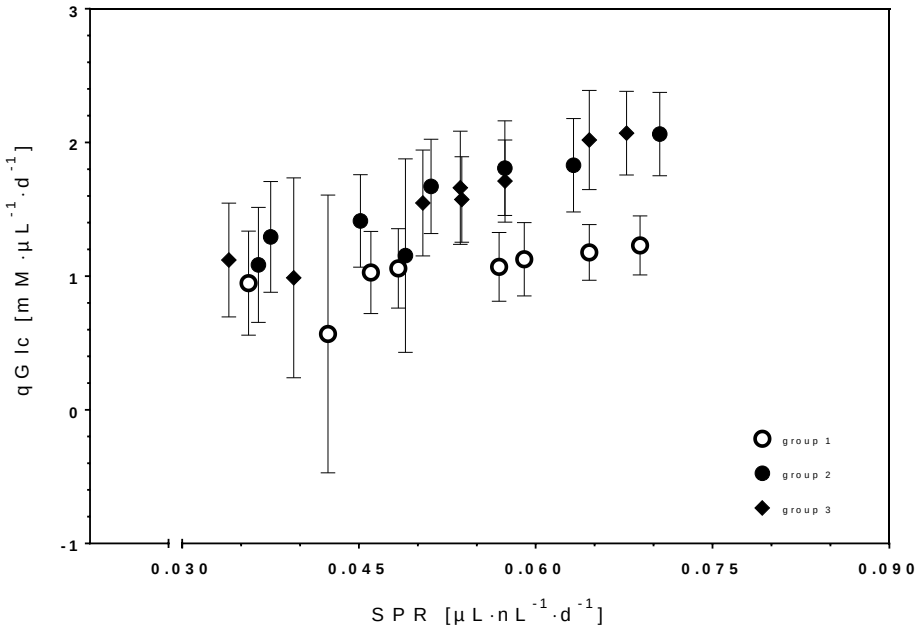

Appendix 3: q_{Gln} (A) and q_{Amm} (B) against SPR from cultures in chapter 4.2.3. Both rates were calculated with VBV. Symbols are the same as in chapter 4.2.3.

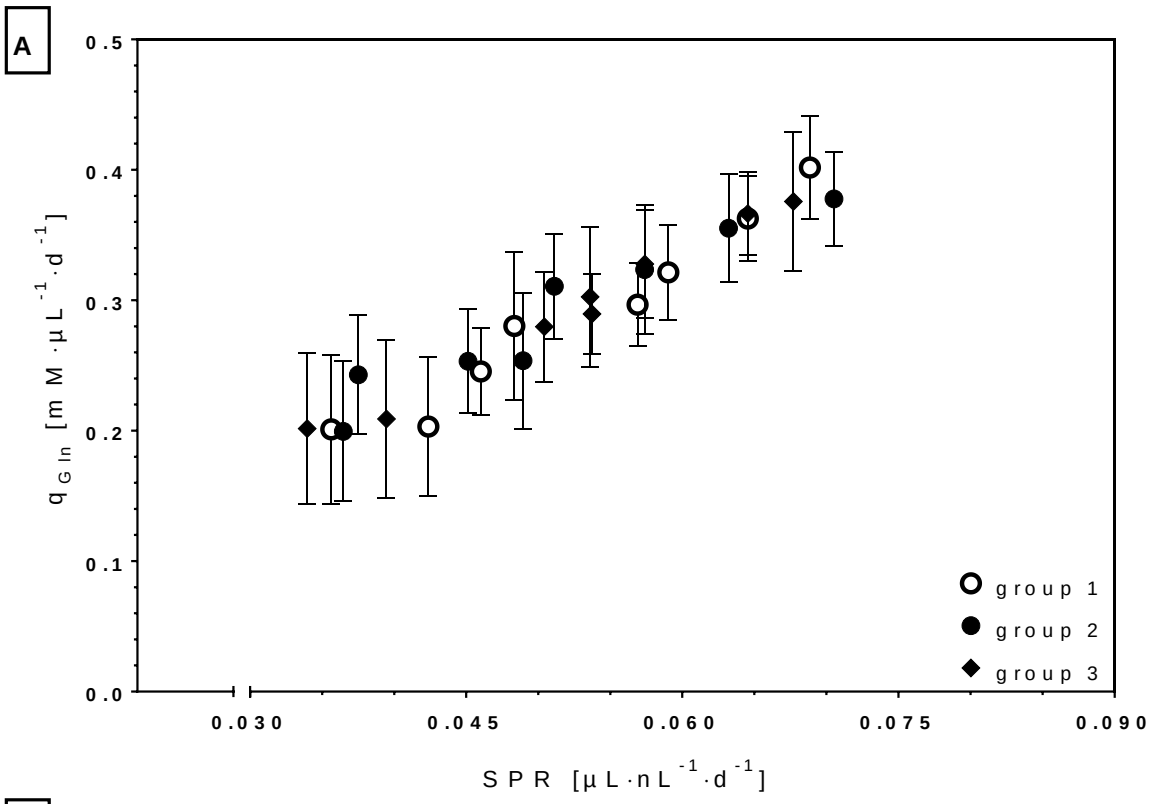

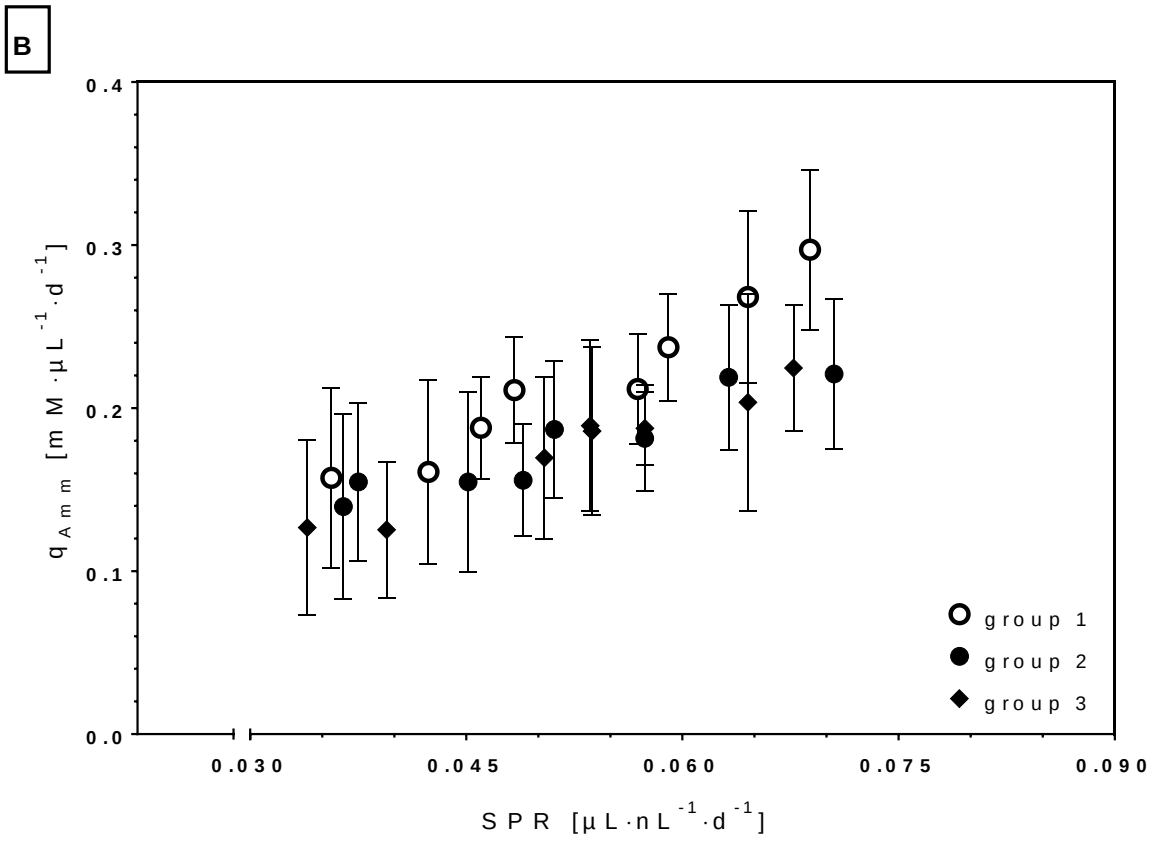

6.2 List of Abbreviations

°C	Degrees Celsius
µ	Growth rate
µg	Microgram
µL	Microliter
µm	Micrometer
ABC	Streptavidin-biotin-peroxidase complex
Acetyl CoA	Acetyl coenzyme A
ambr™	Advanced Microscale Bioreactor
ATF	Alternating tangential flow
ATP	Adenosine triphosphate
A_V	Cross sectional area of a vessel
AVC	Average cell diameter
BHK	Baby hamster kidney
ccm	Cubic centimeter
CHO	Chinese hamster ovary
CI	Confidence Interval
CID	Confidence Interval of all data points
CIM	Confidence Interval of the arithmetic means
cm^2	square centimeter
CO_2	Carbon dioxide
c_{PL}	Product concentration in the bioreactor
CPP	Critical process parameter
c_{SL}	Substrate concentration in the bioreactor
CSPR	Cell specific perfusion rate
$CSPR_{min}$	Minimal cell specific perfusion rate
c_{SR}	Substrate concentration in the reservoir
c_{XL}	Cell concentration in the bioreactor
D	Dilution rate
d	day
D_{adapt}	Dilution rate during adaptation phase
D_{Bleed}	Dilution rate when only the bleed rate is considered
D_{crit}	Critical dilution rate
D_i	Impeller diameter
DMSO	Dimethyl sulfoxide
DO	Dissolved oxygen
DoE	Design of Experiments
D_{set}	Dilution rate set-point
ELISA	Enzyme-Linked Immunosorbent Assay

F_{AF}	Antifoam flow rate
F_B	Base flow rate
F_{Bleed}	Bleed flow rate
FDA	Food and drug administration
F_{feed}	Feed flow rate
F_G	Volumetric gas flow rate
$F_{Harvest}$	Harvest flow rate
F_{Hinit}	Initial harvest flow rate
F_{Hset}	Harvest flow rate set-point
F_{in}	Volumetric input flow rate
F_{out}	Volumetric output flow rate
g	Gravitational acceleration
H_2O	Hydrogen oxide
ISE	Ion selective electrodes
K	Constant
k_La	Volumetric mass transfer coefficient
L	Liter
LAF	Laminar down flow
LH	Liquid handler
M	Molar concentration
min	Minute
$CSPR_{min}$	Minimal CSPR
mL	Milliliter
mmHg	Millimeter of mercury
$mOSm \cdot kg^{-1}$	Milliosmol per kilogram
m_{XL}	Cell mass
N	Stirrer Speed
n	number of feeds per hour
NAD^+	Oxidized nicotinamide adenine dinucleotide
NADH	Reduced nicotinamide adenine dinucleotide
nL	Nanoliter
nM	Nanomolar
N_P	Power number
O_2	Oxygen
OTR	Oxygen transfer rate
P	Gassed power input
PAG	Phosphate activated glutaminase
PAT	Process Analytical Technology
PBS	Phosphate buffered saline
pCO_2	Partial pressure of carbon dioxide
pO_2	Partial Pressure of oxygen

q_{Amm}	Cell specific ammonia production rate
QbD	Quality by Design
q_{Glc}	Cell specific glucose consumption rate
q_{Gln}	Cell specific glutamine consumption rate
q_{Glu}	Cell specific glutamate consumption or production rate
q_{Lac}	Cell specific lactate production rate
q_P	Cell specific protein production rate
R&D	Research & Development
R^2	Coefficient of determination
rpm	Rounds per minute
SPR	Specific Perfusion Rate
STR	Stirred tank Reactor
TCA	Tricarboxylic Acid Cycle
TMB	3,3',5,5'-Tetramethylbenzidine
USD	U.S. dollar
VBV	Viable biomass volume
VCD	Viable cell density
V_L	Liquid volume
VP	Volumetric Productivity
VPI	Volumetric Power Input
v_s	Superficial gas velocity
vvm	Volume per volume per minute
$W \cdot m^{-3}$	Watt per cubic meter
$y_{Amm/Gln}$	Yield of ammonia to glutamine
$y_{Lac/Glc}$	Yield of Lactate to Glucose
α	Constant
β	Constant
ρ	Density of liquid

6.3 Table of figures

6.4 List of tables

6.5 References

Adamson, R. (1994). Design and operation of a recombinant mammalian cell manufacturing process for rFVIII. *Annals of Hematology, 68*(3), S9-S14. doi:10.1007/BF01774523

Altamirano, C., Illanes, A., Casablancas, A., Gómez, X., Cairó, J. J., & Gódia, C. (2001). Analysis of CHO cells metabolic redistribution in a glutamate-based defined medium in continuous culture. *Biotechnol Progress, 17*(6), 1032-1041.

Altamirano, C., Berrios, J., Vergara, M., & Becerra, S. (2013). Advances in improving mammalian cells metabolism for recombinant protein production. *Electronic Journal of Biotechnology, 16*, 10-10.

Aunins, J. G., & Henzler, H. (2008). Aeration in cell culture bioreactors. *Biotechnology* (pp. 219-281) Wiley-VCH Verlag GmbH.

Bailey, L. A., Hatton, D., Field, R., & Dickson, A. J. (2012). Determination of chinese hamster ovary cell line stability and recombinant antibody expression during long-term culture. *Biotechnology and Bioengineering, 109*(8), 2093-2103.

Banik, G. G., & Heath, C. A. (1995a). Hybridoma growth and antibody production as a function of cell density and specific growth rate in perfusion culture. *Biotechnology and Bioengineering, 48*(3), 289-300. doi:10.1002/bit.260480315 [doi]

Banik, G. G., & Heath, C. A. (1995b). Partial and total cell retention in a filtration-based homogeneous perfusion reactor. *Biotechnology Progress, 11*(5), 584-588. doi:10.1021/bp00035a013 [doi]

Banik, G., Todd, P., & Kompala, D. (1996). Foreign protein expression from S phase specific promoters in continuous cultures of recombinant CHO cells. *Cytotechnology, 22*(1-3), 179-184. doi:10.1007/BF00353937

Berrios, J., Altamirano, C., Osses, N., & Gonzalez, R. (2011). Continuous CHO cell cultures with improved recombinant protein productivity by using mannose as carbon source: Metabolic analysis and scale-up simulation. *Chemical Engineering Science, 66*(11), 2431-2439.

Boedeker, B. G. D. (2013). Recombinant factor VIII (kogenate®) for the treatment of hemophilia A: The first and only world-wide licensed recombinant protein produced in high-throughput perfusion culture. *Modern biopharmaceuticals* (pp. 429-443) Wiley-VCH Verlag GmbH & Co. KGaA.

Borys, M. C., Linzer, D. I., & Papoutsakis, E. T. (1993). Culture pH affects expression rates and glycosylation of recombinant mouse placental lactogen proteins by chinese hamster ovary (CHO) cells. *Biotechnology (Nature Publishing Company), 11*(6), 720-724.

Buchs, J. (2001). Introduction to advantages and problems of shaken cultures. *Biochemical Engineering Journal, 7*(2), 91-98. doi:S1369703X00001066 [pii]

Carpio, M., & Patel, S. (2012). Evaluation and characterisation of the advanced microscale bioreactor (ambr) system for use in antibody cell line development. *Poster presented at the XIIIth Cell Culture Engineering, Scottsdale, Arizona*

Casipit, C.L., Burky, J., Townsend, R., Traul, D.L., Sar, N., Stathis, P., Mulkerrin, M (2012). Advanced microscale bioreactor, ambr, for the rapid screening of biopharmaceutical producing cell lines. *Poster presented at the XIIIth Cell Culture Engineering, Scottsdale, Arizona*

Castilho, L. R., & Medronho, R. A. (2002). Cell retention devices for suspended-cell perfusion cultures. *Advances in Biochemical Engineering/Biotechnology, 74*, 129-169.

Chisti, Y. (1993). Animal cell culture in stirred bioreactors: Observations on scale-up. *Bioprocess Engineering, 9*(5), 191-196. doi:10.1007/BF00369402

Chotteau, V., Björling, T., Boork, S., Drapeau, D. (2001). Development of a large scale process for the production of recombinant truncated factor VIII in CHO cells under cell growth arrest conditions. *Animal cell technology: From target to market* (pp. 287-292) Springer Netherlands.

Clincke, M., Mölleryd, C., Zhang, Y., Lindskog, E., Walsh, K., & Chotteau, V. (2013). Very high density of CHO cells in perfusion by ATF or TFF in WAVE bioreactor:. part I. effect of the cell density on the process. *Biotechnol Progress, 29*(3), 754-767.

Cruz, H. J., Freitas, C. M., Alves, P. M., Moreira, J. L., & Carrondo, M. J. T. (2000). Effects of ammonium and lactate on growth, metabolism, and productivity of BHK cells. *Enzyme and Microbial Technology, 27*(1), 43-52.

Dalm, M. C., Cuijten, S. M., van Grunsven, W. M., Tramper, J., & Martens, D. E. (2004). Effect of feed and bleed rate on hybridoma cells in an acoustic perfusion bioreactor: Part I. cell density, viability, and cell-cycle distribution. *Biotechnology and Bioengineering, 88*(5), 547-557. doi:10.1002/bit.20287 [doi]

deZengotita, V., Kimura, R., & Miller, W. (1998). Effects of CO2 and osmolality on hybridoma cells: Growth, metabolism and monoclonal antibody production. *Cytotechnology, 28*(1-3), 213-227. doi:10.1023/A:1008010605287

deZengotita, V. M., Abston, L. R., Schmelzer, A. E., Shaw, S., & Miller, W. M. (2002a). Selected amino acids protect hybridoma and CHO cells from elevated carbon dioxide and osmolality. *Biotechnology and Bioengineering, 78*(7), 741-752.

deZengotita, V. M., Schmelzer, A. E., & Miller, W. M. (2002b). Characterization of hybridoma cell responses to elevated pCO2 and osmolality: Intracellular pH, cell size, apoptosis, and metabolism. *Biotechnology and Bioengineering, 77*(4), 369-380.

Dowd, J. E., Jubb, A., Kwok, K. E., & Piret, J. M. (2003). Optimization and control of perfusion cultures using a viable cell probe and cell specific perfusion rates. *Cytotechnology, 42*(1), 35-45. doi:10.1023/A:1026192228471 [doi]

Europa, A. F., Gambhir, A., Fu, P., & Hu, W. (2000). Multiple steady states with distinct cellular metabolism in continuous culture of mammalian cells. *Biotechnology and Bioengineering, 67*(1), 25-34.

Fernandez, D., Femenia, J., Cheung, D., Nadeau, I., Tescione, L., Monroe, B., Gorfien, S. (2009). Scale-down perfusion process for recombinant protein expression. *Animal cell technology: Basic & applied aspects* (pp. 59-65) Springer Netherlands.

Follstad, B. D., Balcarcel, R. R., Stephanopoulos, G., & Wang, D. I. C. (1999). Metabolic flux analysis of hybridoma continuous culture steady state multiplicity. *Biotechnology and Bioengineering, 63*(6), 675-683.

Franchini, M. (2010). Plasma-derived versus recombinant factor VIII concentrates for the treatment of haemophilia A: Recombinant is better. *Blood Transfusion = Transfusione Del Sangue, 8*(4), 292-296. doi:10.2450/2010.0067-10 [doi]

Garber, K. (2006). Energy deregulation: Licensing tumors to grow. *Science (New York, N.Y.), 312*(5777), 1158-1159. doi:312/5777/1158 [pii]

Gódia, F., & Cairó, J. J. (2006). Cell metabolism. In S. S. Ozturk, & W. S. Hu (Eds.), *Cell culture technology for pharmaceutical and cell-based therapies* (pp. 81) Taylor & Francis.

Gramer, M. J., & Goochee, C. F. (1993). Glycosidase activities in chinese hamster ovary cell lysate and cell culture supernatant. *Biotechnology Progress, 9*(4), 366-373. doi:10.1021/bp00022a003 [doi]

Gringeri, A. (2011). Factor VIII safety: Plasma-derived versus recombinant products. *Blood Transfusion = Trasfusione Del Sangue, 9*(4), 366-370. doi:10.2450/2011.0092-10 [doi]

Heath, C., & Kiss, R. (2007). Cell culture process development: Advances in process engineering. *Biotechnol Progress, 23*(1), 46-51.

Heitmann, M. (2013). Scale-down tools for evaluation of perfusion cultivations. *Poster presented at the XIVth Cell Culture Engineering, Quebec City, Canada*

Henry, O., Kwok, E., & Piret, J. M. (2008). Simpler noninstrumented batch and semicontinuous cultures provide mammalian cell kinetic data comparable to continuous and perfusion cultures. *Biotechnology Progress, 24*(4), 921-931. doi:10.1002/btpr.17 [doi]

Hewitt, C. J., & Nienow, A. W. (2007). The scale-up of microbial batch and fed-batch fermentation processes. *Advances in Applied Microbiology, 62*, 105-135. doi:S0065-2164(07)62005-X [pii]

Hiller, G. W., Aeschlimann, A. D., Clark, D. S., & Blanch, H. W. (1991). A kinetic analysis of hybridoma growth and metabolism in continuous suspension culture on serum-free medium. *Biotechnology and Bioengineering, 38*(7), 733-741.

Hiller, G. W., Clark, D. S., & Blanch, H. W. (1993). Cell retention-chemostat studies of hybridoma cells-analysis of hybridoma growth and metabolism in continuous suspension culture in serum-free medium. *Biotechnology and Bioengineering, 42*(2), 185-195.

Holmberg, A., Blomstergren, A., Nord, O., Lukacs, M., Lundeberg, J., & Uhlén, M. (2005). The biotin-streptavidin interaction can be reversibly broken using water at elevated temperatures. *Electrophoresis, 26*(3), 501-510.

Hsu, W. T., Aulakh, R. P., Traul, D. L., & Yuk, I. H. (2012). Advanced microscale bioreactor system: A representative scale-down model for bench-top bioreactors. *Cytotechnology, 64*(6), 667-678. doi:10.1007/s10616-012-9446-1 [doi]

Hubbard, D. W. (1987). Scaleup strategies for bioreactors containing non-newtonian broths. *Annals of the New York Academy of Sciences, 506*(1), 600-606. doi:10.1111/j.1749-6632.1987.tb23854.x

Kadouri, A. & Spier, R. E. (1997). Some myths and messages concerning the batch and continuous culture of animal cells. *Cytotechnology, 24*(2), 89-98. doi:10.1023/A:1007932614011 [doi]

Kiehl, T. R., Shen, D., Khattak, S. F., Jian Li, Z., & Sharfstein, S. T. (2011). Observations of cell size dynamics under osmotic stress. *Cytometry : The Journal of the Society for Analytical Cytology, 79A*(7), 560-569.

Kim, N. S., & Lee, G. M. (2002). Response of recombinant chinese hamster ovary cells to hyperosmotic pressure: Effect of bcl-2 overexpression. *Journal of Biotechnology, 95*(3), 237-248.

Kompala, D. S., & Ozturk, S. S. (2006). Optimization of high cell density perfusion bioreactors. In S. S. Ozturk, & W. S. Hu (Eds.), *Cell culture technology for pharmaceutical and cell-based therapies* (pp. 387) Taylor & Francis.

Konstantinov, K., Goudar, C., Ng, M., Meneses, R., Thrift, J., Chuppa, S., Naveh, D. (2006). The "push-to-low" approach for optimization of high-density perfusion cultures of animal cells. *Advances in Biochemical Engineering/Biotechnology, 101*, 75-98.

Koplove, H. M. (1994). Cell culture and purification process: Purity and safety testing.*68*(3), S15-S20.

Kurano, N., Leist, C., Messi, F., Kurano, S., & Fiechter, A. (1990). Growth behavior of chinese hamster ovary cells in a compact loop bioreactor: 1. effects of physical and chemical environments. *Journal of Biotechnology, 15*(1-2), 101-111. doi:0168-1656(90)90054-F [pii]

Lodish H, Berk A, Zipursky SL, et al. (2000). Oxidation of Glucose and Fatty Acids to CO2. In *Molecular Cell Biology*. Section 16.1. 4th edition. New York: W.H. Freeman; Available from: http://www.ncbi.nlm.nih.gov/books/NBK21624/

Louis, K., & Siegel, A. (2011). Cell viability analysis using trypan blue: Manual and automated methods. *Mammalian cell viability* (pp. 7-12) Humana Press.

Lai, T., Yang, Y., & Ng, S. K. (2013). Advances in mammalian cell line development technologies for recombinant protein production. *Pharmaceuticals (Basel, Switzerland), 6*(5), 579-603. doi:10.3390/ph6050579 [doi]

Langheinrich, C., & Nienow, A. W. (1999). Control of pH in large-scale, free suspension animal cell bioreactors: Alkali addition and pH excursions. *Biotechnology and Bioengineering, 66*(3), 171-179.

Lao, M., & Toth, D. (1997). Effects of ammonium and lactate on growth and metabolism of a recombinant chinese hamster ovary cell culture. *Biotechnol Progress, 13*(5), 688-691.

Lara, A. R., Galindo, E., Ramirez, O. T., & Palomares, L. A. (2006). Living with heterogeneities in bioreactors: Understanding the effects of environmental gradients on cells. *Molecular Biotechnology, 34*(3), 355-381. doi:MB:34:3:355 [pii]

Lee, M. S., & Lee, G. M. (2001). Effect of hypoosmotic pressure on cell growth and antibody production in recombinant Chinese hamster ovary cell culture. *Cytotechnology*, *36*(1-3), 61–69. doi:10.1023/A:1014032701800

Lee, M. G. and Koo, J. 2010. Osmolarity Effects, Chinese Hamster Ovary Cell Culture. *Encyclopedia of Industrial Biotechnology. 1–8*

Leno, M., Merten, O. W., & Hache, J. (1992). Kinetic analysis of hybridoma growth and monoclonal antibody production in semicontinuous culture. *Biotechnology and Bioengineering, 39*(6), 596-606. doi:10.1002/bit.260390603 [doi]

Link, T., Backstrom, M., Graham, R., Essers, R., Zorner, K., Gatgens, J., Noll, T. (2004). Bioprocess development for the production of a recombinant MUC1 fusion protein expressed by CHO-K1 cells in protein-free medium. *Journal of Biotechnology, 110*(1), 51-62. doi:10.1016/j.jbiotec.2003.12.008 [doi]

Lu, M., Zhou, L., Stanley, W. C., Cabrera, M. E., Saidel, G. M., & Yu, X. (2008). Role of the Malate-Aspartate Shuttle on the Metabolic Response to Myocardial Ischemia. *Journal of Theoretical Biology*, *254*(2), 466–475. doi:10.1016/j.jtbi.2008.05.033

Ludlam, C. A., Lowe, G. D., & Mayne, E. E. (1995). A pharmacokinetic study of an ion-exchange solvent-detergent-treated high-purity factor VIII concentrate. Haemophilia directors for Scotland and Northern Ireland. *Transfusion Medicine (Oxford, England), 5*(4), 289-292.

Ma, M., Mollet, M., & Chalmers, J. J. (2006). Aeration, mixing and hydrodynamics in bioreactors. In S. S. Ozturk, & W. S. Hu (Eds.), *Cell culture technology for pharmaceutical and cell-based therapies* (pp. 225) Taylor & Francis.

Marques, M. P. C., Cabral, J. M. S., & Fernandes, P. (2010). Bioprocess scale-up: Quest for the parameters to be used as criterion to move from microreactors to lab-scale. *Journal of Chemical Technology and Biotechnology (Oxford, Oxfordshire : 1986), 85*(9), 1184-1198.

Martens, D. E., de Gooijer, C. D., van der Velden-de Groot, C. A., Beuvery, E. C., & Tramper, J. (1993). Effect of dilution rate on growth, productivity, cell cycle and size, and shear sensitivity of a hybridoma cell in a continuous culture. *Biotechnology and Bioengineering, 41*(4), 429-439. doi:10.1002/bit.260410406 [doi]

Marx, N. (2012). *Charakterisierung und Vergleich zweier Hochzelldichte-Perfusionskultivierungen mit Pattensedimenter und ATF-system.* Bachelor's thesis, University of Applied Sciences Bielefeld, Fachbereich Ingenieurwissenschaften und Mathematik.

McDowell, C. L., & Papoutsakis, E. T. (1998). Decreasing extracellular pH increases CD13 receptor surface content and alters the metabolism of HL60 cells cultured in stirred tank bioreactors. *Biotechnol Progress, 14*(4), 567-572.

Miller, W. M., Blanch, H. W., & Wilke, C. R. (1988). A kinetic analysis of hybridoma growth and metabolism in batch and continuous suspension culture: Effect of nutrient concentration, dilution rate, and pH. *Biotechnology and Bioengineering, 32*(8), 947-965. doi:10.1002/bit.260320803 [doi]

Miller, W. M., Wilke, C. R., & Blanch, H. W. (1989). Transient responses of hybridoma cells to nutrient additions in continuous culture: I. glucose pulse and step changes. *Biotechnology and Bioengineering, 33*(4), 477-486.

Moreno-Sanchez, R., Rodriguez-Enriquez, S., Marin-Hernandez, A., Saavedra, E. (2007). Energy metabolism in tumor cells. *The FEBS Journal, 274*(6), 1393-1418. doi:EJB5686 [pii]

Narang, A. (1998). The steady states of microbial growth on mixtures of substitutable substrates in a chemostat. *Journal of Theoretical Biology, 190*(3), 241-261.

Nielsen, R., & Wilson, G. (2007). Comparison of cultivations of CHO cell line in chemostat and acceleratostat experiments. *Cell technology for cell products* (pp. 609-609) Springer Netherlands.

Nienow, A. W., Langheinrich, C., Stevenson, N. C., Emery, A. N., Clayton, T. M., & Slater, N. K. (1996). Homogenisation and oxygen transfer rates in large agitated and sparged animal cell bioreactors: Some implications for growth and production. *Cytotechnology, 22*(1-3), 87-94. doi:10.1007/BF00353927 [doi]

Nienow, A. W., Rielly, C. D., Brosnan, K., Bargh, N., Lee, K., Coopman, K., & Hewitt, C. J. (2013). The physical characterisation of a microscale parallel bioreactor platform with an industrial CHO cell line expressing an IgG4. *Biochemical Engineering Journal, 76*(0), 25-36.

Osman, J. J., Birch, J., & Varley, J. (2001). The response of GS-NS0 myeloma cells to pH shifts and pH perturbations. *Biotechnology and Bioengineering, 75*(1), 63-73. doi:10.1002/bit.1165 [pii]

Ozturk, S. S., & Palsson, B. O. (1991). Effect of medium osmolarity on hybridoma growth, metabolism, and antibody production. *Biotechnology and Bioengineering, 37*(10), 989-993.

Ozturk, S. S., & Palsson, B. O. (1991). Growth, metabolic, and antibody production kinetics of hybridoma cell culture: 2. effects of serum concentration, dissolved oxygen concentration, and medium pH in a batch reactor. *Biotechnol Progress, 7*(6), 481-494.

Ozturk, S. S., Riley, M. R., & Palsson, B. O. (1992). Effects of ammonium and lactate on hybridoma growth, metabolism, and antibody production. *Biotechnology and Bioengineering, 39*(4), 418-431. doi:10.1002/bit.260390408 [doi]

Ozturk, S. S. (1994). Optimization and scale-up of high density cell culture bioreactors. *Advances in bioprocess engineering* (pp. 133-139) Springer Netherlands.

Ozturk, S. (1996). Engineering challenges in high density cell culture systems. *Cytotechnology, 22*(1-3), 3-16. doi:10.1007/BF00353919

Ozturk, S. S., Thrift, J. C., Blackie, J. D. and Naveh, D. (1997), Real-time monitoring and control of glucose and lactate concentrations in a mammalian cell perfusion reactor. *Biotechnol. Bioeng., 53: 372–378.* doi: 10.1002/(SICI)1097-0290(19970220)53:4<372::AID-BIT3>3.0.CO;2-K

Reitzer, L. J., Wice, B. M., & Kennell, D. (1979). Evidence that glutamine, not sugar, is the major energy source for cultured HeLa cells. *The Journal of Biological Chemistry, 254*(8), 2669-2676.

Reuveny, S., Velez, D., Macmillan, J. D., & Miller, L. (1986a). Factors affecting cell growth and monoclonal antibody production in stirred reactors. *Journal of Immunological Methods, 86*(1), 53-59.

Reuveny, S., Velez, D., Miller, L., & Macmillan, J. D. (1986b). Comparison of cell propagation methods for their effect on monoclonal antibody yield in fermentors. *Journal of Immunological Methods, 86*(1), 61-69.

Rita, H., & Ekholm, P. (2007). Showing similarity of results given by two methods: A commentary. *Environmental Pollution, 145*(2), 383-386. doi: http://dx.doi.org/10.1016/j.envpol.2006.08.007

Robin, J. (2013). Case study: Challenges and learning in implementing ATF perfusion process. Presented at the *ECI conference on Integrated Continuous Biomanufacturing, Castelldefels, Spain.* Retrieved from http://www.engconf.org/staging/wp-content/uploads/2013/12/jarno_ICB-13AQ-Monday.pdf. Accessed: 02.01.2015

Sanfeliu, A., Paredes, C., Cairó, J. J., & Gódia, F. (1997). Identification of key patterns in the metabolism of hybridoma cells in culture. *Enzyme and Microbial Technology, 21*(6), 421-428.

Sarkadi, B., Attisano, L., Grinstein, S., Buchwald, M., & Rothstein, A. (1984). Volume regulation of chinese hamster ovary cells in anisoosmotic media. *Biochimica Et Biophysica Acta (BBA) - Biomembranes, 774*(2), 159-168.

Schmelzer, A., Miller, W., deZengotita, V., & Abston, L. (2001). Environmental effects on cell physiology and metabolism: Response to elevated pC02. In E. Lindner-Olsson, N. Chatzissavidou & E. Lüllau (Eds.), (pp. 121-128) Springer Netherlands. doi:10.1007/978-94-010-0369-8_27

Schmidt, F. R. (2005). Optimization and scale up of industrial fermentation processes. *Applied Microbiology and Biotechnology, 68*(4), 425-435. doi:10.1007/s00253-005-0003-0 [doi]

Severinghaus, J. W. (2004). First electrodes for blood Po2 and Pco2 determination. *Journal of Applied Physiology, 97*(5), 1599-1600. doi:10.1152/classicessays.00021.2004

Takagi, M., Hayashi, H., & Yoshida, T. (2000). The effect of osmolarity on metabolism and morphology in adhesion and suspension chinese hamster ovary cells producing tissue plasminogen activator. *Cytotechnology, 32*(3), 171-179. doi:10.1023/A:1008171921282 [doi]

Trummer, E., Fauland, K., Seidinger, S., Schriebl, K., Lattenmayer, C., Kunert, R., Muller, D. (2006a). Process parameter shifting: Part I. effect of DOT, pH, and temperature on the performance of epo-fc

expressing CHO cells cultivated in controlled batch bioreactors. *Biotechnology and Bioengineering, 94*(6), 1033-1044. doi:10.1002/bit.21013 [doi]

Trummer, E., Fauland, K., Seidinger, S., Schriebl, K., Lattenmayer, C. K.,R., Vorauer-Uhl, K., Müller, D. (2006b). Process parameter shifting: Part II. biphasic cultivation: A tool for enhancing the volumetric productivity of batch processes using epo-fc expressing CHO cells. *Biotechnology and Bioengineering, 94*(6), 1045-1052.

Van't Riet, K. (1979). Review of measuring methods and results in nonviscous gas-liquid mass transfer in stirred vessels. *Ind.Eng.Chem.Proc.Des.Dev., 18*(3), 357-364.

Varley, J., & Birch, J. (1999). Reactor design for large scale suspension animal cell culture. *Cytotechnology*, *29*(3), 177–205. doi:10.1023/A:1008008021481

Vehar, G. A., Keyt, B., Eaton, D., Rodriguez, H., O'Brien, D. P., Rotblat, F., Capon, D. J. (1984). Structure of human factor VIII. *Nature, 312*(5992), 337-342.

Verkman, A. S., van Hoek, A. N., Ma, T., Frigeri, A., Skach, W. R., Mitra, A., Farinas, J. (1996). Water transport across mammalian cell membranes. *The American Journal of Physiology, 270*(1 Pt 1), C12-30.

Werner, R. G., Walz, F., Noé, W., & Konrad, A. (1992). Safety and economic aspects of continuous mammalian cell culture. *Journal of Biotechnology, 22*(1), 51-68.

Westgate, P. J., & Emery, A. H. (1990). Approximation of continuous fermentation by semicontinuous cultures. *Biotechnology and Bioengineering, 35*(5), 437-453. doi:10.1002/bit.260350502 [doi]

White, G. C., McMillan, C. W., Kingdon, H. S., & Shoemaker, C. B. (1989). Use of recombinant antihemophilic factor in the treatment of two patients with classic hemophilia. *N Engl J Med, 320*(3), 166-170.

www.pipelinereview.com (accessed 16th of April 2014). *TOP 30 Biologics*. Retrieved from https://www.pipelinereview.com/free-downloads/TOP-30_Biologics_2011_RDPN_Special_April_2012.pdf.

Yang, J., Angelillo, Y., Chaudhry, M., Goldenberg, C., & Goldenberg, D. M. (2000). Achievement of high cell density and high antibody productivity by a controlled-fed perfusion bioreactor process. *Biotechnology and Bioengineering, 69*(1), 74-82.

Yoon, S. K., Choi, S. L., Song, J. Y., & Lee, G. M. (2005). Effect of culture pH on erythropoietin production by chinese hamster ovary cells grown in suspension at 32.5 and 37.0Â°C. *Biotechnology and Bioengineering, 89*(3), 345-356.

Zanghi, J. A., Schmelzer, A. E., Mendoza, T. P., Knop, R. H., Miller, W. M. (1999). Bicarbonate concentration and osmolality are key determinants in the inhibition of CHO cell polysialylation under elevated pCO2 or pH. *Biotechnology and Bioengineering, 65*(2), 182-191.

Zeng, A. P., & Bi, J. X. (2006). Cell culture kinetics and modeling. In S. S. Ozturk, & W. S. Hu (Eds.), *Cell culture technology for pharmaceutical and cell-based therapies* (pp. 299) Taylor & Francis.

Zeng, A. P., Deckwer, W. D., & Hu, W. S. (1998). Determinants and rate laws of growth and death of hybridoma cells in continuous culture. *Biotechnology and Bioengineering, 57*(6), 642-654. doi:10.1002/(SICI)1097-0290(19980320)57:6<642::AID-BIT2>3.0.CO;2-L [pii]

Zeng, A. P., & Deckwer, W. D. (1999). Model simulation and analysis of perfusion culture of mammalian cells at high cell density. *Biotechnology Progress, 15*(3), 373-382. doi:10.1021/bp990040a [doi]; bp990040a [pii]

Zhou, Y., Shingu, T., Feng, L., Chen, Z., Ogasawara, M., Huang, P. (2011). Metabolic alterations in highly tumorigenic glioblastoma cells: Preference for hypoxia and high dependency on glycolysis. *The Journal of Biological Chemistry, 286*(37), 32843-32853. doi:10.1074/jbc.M111.260935 [doi]

Zhu, J. (2012). Mammalian cell protein expression for biopharmaceutical production. *Biotechnology Advances, 30*(5), 1158-1170.

Zhu, M. M., Goyal, A., Rank, D. L., Gupta, S. K., Vanden Boom, T., & Lee, S. S. (2005). Effects of elevated pCO2 and osmolality on growth of CHO cells and production of antibody-fusion protein B1: A case study. *Biotechnology Progress, 21*(1), 70-77. doi:10.1021/bp049815s [doi]

Zupke, C., Ulibarri, D., J. Wendling, J (2012). Evaluation of the ambr microreactor system. *Poster presented at the XIIIth Cell Culture Engineering, Scottsdale, Arizona*

Declaration

I hereby, declare that I wrote the present thesis independently and that I did no use any other sources and resources than those indicated therein. This thesis has not been submitted in this or any other form at another institution.

_____ _____

Place, Date Signature